COPY NO. 207

[redacted]

CLASSIFICATION CHANGE

To Unclassified
By authority of T.D. 72-59
Changed by Olenis L. ... Date 1/19/72
... Control Station, NASA
Scientific and Technical Information Facility

NACA

NACA PRESENTATION
at

INDUSTRY-GOVERNMENT MEETING

ON

ENGINE-INLET DUCT COMPATIBILITY

I.N. 9365

Wright-Patterson Field
Dayton, Ohio

AUG 15 1955

June 14, 15, and 16, 1955

To
NASA Hqs. let. to All NASA Centers
dtd. 11/14/62 TTN/cu
12/7/62

NACA PRESENTATION
at
INDUSTRY-GOVERNMENT MEETING
ON
ENGINE-INLET DUCT COMPATIBILITY

Wright-Patterson Field
Dayton, Ohio

June 14, 15, and 16, 1955

INTRODUCTION

On June 14-16, 1955, the Air Force and the Bureau of Aeronautics sponsored a government-industry meeting on the compatibility of engines and inlet ducts; the meeting was held at Wright Aeronautical Development Center. Attendees were members of the military services and representatives of engine and aircraft manufacturers.

Papers were delivered by participants from the services, from NACA, and from industry. The papers presented by NACA were based on panel discussions given at Lewis Flight Propulsion Laboratory Feb. 3, 1955, for members of the military services. They deal with stall and surge in turbojet engines.

The NACA papers are presented here so that you may have them for reference. This presentation supplements material contained in NACA reports.

National Advisory Committee
for Aeronautics

CONTENTS

CONFEREES

Name	Affiliation
Abernathy, L. X.	Bureau of Aeronautics, Wash., D.C.
Accorsi, F.	WCLP-WADC, Dayton, O.
Alford, J. S.	General Electric, Lockland, O.
Ammann, Dr. R. M.	WCR-WADC, Dayton, O.
Anderson, H. L.	WCLS-WADC, Dayton, O.
Appold, Col. N. C.	WCLP-WADC, Dayton, O.
Archey, Jesse P.	Grumman, Bethpage, L. I.
Atkinson, A. S.	Bureau of Aeronautics, Wash., D.C.
Baird, Cap't. A. L.	Bureau of Aeronautics, Wash., D.C.
Barrett, J. G.	WCLP-WADC, Dayton, O.
Bartlett, Lt. Col. T. E.	WCLG-WADC, Dayton, O.
Beach, W. C.	North American, Columbus, O.
Beck, Dr. N. J.	Douglas Aircraft, Long Beach, Calif.
Bell, E. D.	WCS-WADC, Dayton, O.
Bellamy, C. W.	North American, Downey, Calif.
Benneche, R. A.	Bureau of Aeronautics, Wash., D. C.
Benser, W. A.	NACA-Lewis
Beriniati, V. J.	Bureau of Aeronautics, Wash. D. C.
Blatz, W. J.	McDonnell Aircraft, St. Louis, Mo.
Blom, T.	WCD-WADC, Dayton, Ohio
Blum, Col. E. F.	AFDRD-USAF, Wash, D.C.
Bosse, P. C.	WCLP-WADC, Dayton, O.
Boyer, R. P.	Arnold Engineering, Tullahoma, Tenn.
Brown, H. S.	WCL-WADC, Dayton, O.
Brown, L. E.	Wright Aeronautical, Wood-Ridge, N.J.
Brown, R. B.	Boeing Aircraft, Seattle, Wash.
Buchner, R.	WCLP-WADC, Dayton, O.
Buehl, F. W.	Radioplane Co., Van Nuys, Calif.
Bullock, R. O.	NACA-Lewis
Cahill, J. F.	Lockheed Aircraft, Marietta, Ga.
Calhoun, J. T.	Beech Aircraft, Wichita, Kansas
Callan, Cap't. E. J.	WCR-WADC, Dayton, O.
Cesaro, R. S.	NACA-Washington
Chandler, Cmdr. R. S.	Bureau of Aeronautics, Wash., D. C.
Chapman, G. E.	Allison-G.M., Indianapolis, Ind.
Childs, J. H.	NACA-Lewis
Christensen, R. G.	Boeing Aircraft, Seattle, Wash.

Name	Affiliation
Chwedden, R. T.	Radioplane Co., Van Nuys, Calif.
Cole, R. W.	Curtiss-Wright, Wood-Ridge, N.J.
Collins, Cmdr. T.W. Jr.	Office of Sec. of Defense, Wash., D.C.
Collins, W.	Continental Aviation, Detroit, Mich.
Coyle, J. B.	WCLP-WADC, Dayton, O.
Creel, R. L.	Bureau of Aeronautics, Wash., D. C.
Dailey, Lt. W. A.	WCLP-WADC, Dayton, O.
Downey, D. J.	Boeing Aircraft, Seattle, Wash.
Drell, H.	Lockheed, Burbank, Calif.
DuBois, Maj. J.M.	USAF, Lewis Lab.
Elder, D. L.	Douglas Aircraft, Long Beach, Calif.
Elliott, R. D.	Ryan Aero., San Diego, Calif.
Ervin, B. H.	Rheem Mfg., Downey, Calif.
Faught, H. F.	Westinghouse, Kansis City, Mo.
Fenley, Maj. R. A.	Eglin Airforce Base, Fla.
Fishow, M.	Bureau of Aeronautics, Wash., D. C.
Fitzhugh, Lt. Cmdr. M. M.	Bureau of Aeronautics, Wash., D. C.
Fleming, W. A.	NACA-Lewis
Forry, J. E.	Office of Sec. of Defense, Wash., D.C.
Friedman, R.	NACA-Lewis
Friend, C. F.	Lockheed, Marietta, Ga.
Gabriel, D. S.	NACA-Lewis
Gardner, Maj. A. J.	WCLP-WADC, Dayton, O.
Garner, C. M.	WCLP-WADC, Dayton, O.
Garrett, R. S.	WCLB-WADC, Dayton, O.
Gavin, J. E.	Pratt & Whitney, E. Hartford, Conn.
Gershon, I.	WCLP-WADC, Dayton, O.
Gienche, Lt. Col. E. J.	WCLP-WADC, Dayton, O.
Goodrich, Capt. J. W.	WCR-WADC, Dayton, O.
Gorman, Cmdr. B.	BAGR-CD-WADC, Dayton, O.
Graig, W.	WCS-WADC, Dayton, O.
Gray, W. A.	Glenn L. Martin Co., Baltimore, Md.
Greene, G.	WCLP-WADC, Dayton, O.
Hackler, M. G.	Cessna - Wichita, Kansas
Hallett, R. W.	Douglas - El Segundo, Calif.
Hargis, C. B.	WSCLS-WADC, Dayton, O.

Name	Affiliation
Harris, F.	WCR-WADC, Dayton, O.
Hasinger, S.	WCR-WADC, Dayton, O.
Haugen, Brig. Gen. V. R.	WSCL-WADC, Dayton, O.
Hawkens, Lt. Co. E. A.	WSCL-WADC, Dayton, O.
Heilig, L. F.	Northrop Aircraft, Hawthorne, Calif.
Heissenbuttel, Maj. W.	WCS-WADC, Dayton, O.
Hensley, R. V.	Fairchild, Farmingdale, L. I., N.Y.
Higginbotham, R. R.	Republic, Farmingdale, L. I., N.Y.
Hixson, E. W.	WCLP-WADC, Dayton, O.
Hoffman, R. E.	WCLP-WADC, Dayton, O.
Hood, J. H.	Consolidated-Vultee, San Diego, Calif.
Hopkins, Lt. Cmdr., W.A.	BAGR-CD-WADC, Dayton, Ohio
Horn, E. W.	WCLP-WADC, Dayton, O.
Hunter, Lt. R.	WSCR-WADC, Dayton, O.
Jackes, A. M.	Bell Aircraft, Niagara Falls, N.Y.
Johnson, C. G.	WCS-WADC - Dayton, O.
Johnson, E.	WCR-WADC, Dayton, O.
Johnson, Maj. F. D.	WCS-WADC, Dayton, O.
Jones, Maj. K. L.	WCLP-WADC, Dayton, O.
Jordon, L. R.	Douglas Aircraft, Santa Monica, Calif.
Kassner, R. R.	AVCO, Stratford, Conn.
Kelly, T. J.	Grumman, Bethpage, L. I., N.Y.
Kopplin, C. H.	Pratt & Whitney, E. Hartford, Conn.
Kotcher, E.	WCL-WADC, Dayton, O.
Kuhns, R. M.	Consolidated-Vultee, San Diego, Calif.
Lawson, M. O.	WCR-WADC, Dayton, O.
Lefler, E. D.	WCLS-WADC, Dayton, O.
Levine, Lt. P.	WCR-WADC, Dayton, O.
Litton, R. S.	WCLP-WADC, Dayton, O.
Long, C. M.	Boeing, Wichita, Kansas
Lovett, C. E.	WCLP-WADC, Dayton, Ohio
Lundin, B. T.	NACA-Lewis
Luskin, H.	Douglas Aircraft, Santa Monica, Calif.
Manganiello, E. J.	NACA-Lewis
Mann, Maj. R. A.	WCS-WADC, Dayton, O.
Manson, S. S.	NACA-Lewis
Maravel, J.	Republic Av., Farmingdale, L.I., N.Y.

Name	Affiliation
Matz, Lt. R. J.	Arnold Eng., Tullahoma, Tenn.
Maurer, R. J.	Bureau of Aeronautics, Wash., D.C.
McFadden, H. M.	Boeing Aircraft, Wichita, Kans.
McKee, Col. D. D.	WCLS-WADC, Dayton, O.
Melrose, G. B.	Bell Aircraft, Niagara Falls, N.Y.
Meyer, A. J.	NACA-Lewis
Miller, R. T.	Bureau of Aeronautics, Wash., D.C.
Mitchell, E. H.	Pratt & Whitney, Dayton, O.
Mobley, Lt. F. F.	WCLS-WADC, Dayton, O.
Monts, L. F.	Beech Aircraft, Wichita, Kans.
Morris, M. L.	Wright Aero., Wood-Ridge, N. J.
Moses, J. J.	Ryan Aero., San Diego, Calif.
Murphy, H. T.	Bureau of Aeronautics, Indianapolis
Nay, H. O.	Douglas, El Segundo, Calif.
Neitzel, R. E.	General Electric, Lockland, O.
Nicks, O. W.	North American, Downey, Calif.
Nolan, D. J.	Allison, Indianapolis, Ind.
Nordli, R. L.	WCLP-WADC, Dayton, O.
Norton, R. P.	Boeing Aircraft, Wichita, Kansas
Olds, R. H.	U.S. Naval Sta., China Lake, Calif.
Orazio, F. D.	WCLS-WADC, Dayton, O.
Outman, H. V. Jr.	McDonnell Aircraft, St. Louis, Mo.
Pappas, C. E.	Republic Avia., Farmingdale, L.I., N.Y.
Parker, D. E.	General Electric, Lockland, O.
Patella, F.	WCLP-WADC, Dayton, O.
Pettitt, J.	WCLP-WADC, Dayton, O.
Piercy, T. G.	NACA-Lewis
Pierie, Lt. W. R.	SCLP-WADC, Dayton, O.
Pinnes, R. W.	Bureau of Aeronautics, Wash., D. C.
Porter, R. F.	WCLS-WADC, Dayton, O.
Powell, Cmdr. L. C.	Bureau of Aeronautics, Wash., D. C.
Pratt, P. W.	Pratt & Whitney, E. Hartford, Conn.
Rall, Lt. F. T.	WCLS-WADC, Dayton, O.
Rapp, G. C.	General Electric, Lockland, O.
Rea, M. E.	WCLP-WADC, Dayton, O.
Robbins, Lt. Col. H. W.	RDTDP-ARDC, Baltimore, Md.
Rock, E. A.	Boeing Aircraft, Wichita, Kansas

Name	Affiliation
Rodean, H. C.	Chance-Vought, Dallas, Texas
Rodert, L. A.	NACA-Lewis
Rogerson, D. B.	North American, Los Angeles, Calif.
Rosenthal, S. H.	G. E., West Lynn, Mass.
Rossow, P.	Republic Avia., Farmingdale, L.I., N.Y.
Roy, R. E.	WSCLP-WADC, Dayton, O.
Ruhfel, R. E.	Fairchild, Farmingdale, L.I., N.Y.
Ryan, C. E.	WSCLP-WADC, Dayton, O.
Sadler, C. E.	McDonnell Aircraft, St. Louis, Mo.
Samara, Dr. D. G.	WCR-WADC, Dayton, O.
Scalia, M. E.	Glenn L. Martin Co., Baltimore, Md.
Scarborough, R.	Glenn L. Martin Co., Baltimore, Md.
Schlachman, B.	Naval Gun Factory, Wash., D.C.
Schloemer, P. G.	WSCLP-WADC, Dayton, O.
Schmidt, J. F.	WCL-WADC, Dayton, O.
Schubert, F. E.	WCLP-WADC, Dayton, O.
Schumacher, H. E.	WCLP-WADC, Dayton, O.
Schwartz, W.	WCS-WADC, Dayton, O.
Schwoerer, F.	Westinghouse, Kansas City, Mo.
Sea, A. L.	WCS-WADC, Dayton, O.
Shafer, R.	Bureau of Aeronautics, Wash., D.C.
Shows, H. R.	WCL-WADC, Dayton, O.
Silvern, D.	Continental Avia., Detroit, Mich.
Silverstein, A.	NACA-Lewis
Simpson, E. C.	WCLP-WADC, Dayton, O.
Simpson, G. R.	U.S. N.T. Sta., Trenton, N. J.
Smith, A. E.	Pratt & Whitney, E. Hartford, Conn.
Smith, C. B.	Pratt & Whitney, E. Hartford, Conn.
Smith, H. H.	WCLB-WADC, Dayton, O.
Smith, Cmdr. J. H. Jr.	Bureau of Aeronautics, Wash., D.C.
Sorgen, C. C.	Office of Sec. of Defense, Wash., D.C.
Stein, W. S.	AVCO Mfg., Stratford, Conn.
Stobaugh, Lt. W. K.	WCLP-WADC, Dayton, O.
Sulkin, M. A.	North American, Los Angeles, Calif.
Tate, Lt. S. E.	WCLB-WADC, Dayton, O.
Telerico, J. A.	U.S. Naval Training St., Trenton, N.J.
Thornburg, V. E.	Pratt & Whitney, E. Hartford, Conn.
Towle, H. C.	Republic Avia., Farmingdale, L.I., N.Y.
Trent, W. C.	Chance-Vought, Dallas, Texas

Name	Affiliation
VanderPutten, H.	North American, Columbus, O.
Von Ohain, Dr. H.	WCR-WADC, Dayton, O.
Wainwright, T. W.	Beech Aircraft, Wichita, Kansas
Warner, C. F.	Bureau of Ordnance, Wash., D. C.
Washington, Cmdr. T. Jr.	Bureau of Aeronautics, Wash., D. C.
Watson, J. O.	Bureau of Ordnance, Wash., D. C.
Welch, W. W.	North American, Columbus, O.
Westra, L.	Continental Avia., Detroit, Mich.
Wheeler, W. L.	North American, Columbus, O.
Wiard, W. D.	WCLS-WADC, Dayton, O.
Wieben, H. C.	Glenn L. Martin Co., Baltimore, Md.
Woeste, W. J.	WSCLP-WADC, Dayton, O.
Wright, F.	WSCLP-WADC, Dayton, O.
Wyatt, D. D,	NACA-Lewis
Yost, J. H.	Bell Aircraft, Niagara Falls, N.Y.
Zahrt, K. W.	WCR-WADC, Dayton, O.
Ziegler, D.	WCS-WADC, Dayton, O.
Zimmerman, Lt. Cmdr., C.A.	Bureau of Ordnance, Wash., D. C.
Zimmerman, G. A.	WCLP-WADC, Dayton, O.

I

STALL AND SURGE IN TURBOJET ENGINES

by
D. S. Gabriel, E. W. Conrad, H. B. Finger, R. W. Graham

I - STALL AND SURGE IN TURBOJET ENGINES

By D. S. Gabriel, E. W. Conrad, H. B. Finger
and R. W. Graham

Compressor stall limits the useful operating range of turbojet engines. In order to achieve maximum performance, modern engines must operate very close to the stall limits at some operating conditions. Consequently, avoiding compressor stall has become one of the most pressing operational problems. The purpose of this paper is to explain the basic reasons for the existence of stall and to describe some of the effects of stall limits on the operation of modern engines.

Stall and surge originate in the compressor. The compressor, of course, is comprised of rows of airfoils. If the angle of attack of a wing or airfoil is increased sufficiently the flow over the airfoil will separate, the lift will no longer increase as angle of attack is increased, and the airfoil is said to be stalled. Stall in compressors is associated with the same separation phenomena that occur in wings.

Figure 1 shows this stall in a compressor cascade. The blades in a compressor are arranged in rows or cascades as illustrated in the figure. At low angles of attack the flow over the blades is smooth and lift is developed. If the angle of attack is increased sufficiently stall will occur in the cascade. Usually in a cascade when stall starts, because of some local variation in flow or blade missetting, stall occurs in only a small portion of the cascade rather than over the whole cascade at once. For simplicity, the stalled or separated flow is indicated by the lightly shaded area in figure 1, as occurring in only one blade passage, although in an actual cascade it may cover several blades. The direction of flow approaching the cascade is indicated by the arrows. The separation of flow in the stalled passage reduces the flow area and thus dams up the flow between the blades. The damming up, indicated by the heavily shaded area, causes the flow to be partly diverted around the stalled passage. The diversion of flow changes the direction of the flow approaching the blades. As shown by the arrows, the flow directions change so that compared to the original angle of attack, the angle of attack on the stalled blades is decreased and the angle of attack on the next blade is increased. The reduction in angle of attack on the stalled blade results in unstalling of the blade and the increase in angle of attack on the next blade results in stalling of that blade. By this process the stalled region actually advances from one blade to the next or is propagated across the cascade.

As shown in figure 2, when the cascade is wrapped around a disk, it becomes a compressor rotating row, or a single-stage compressor, and propagating stall in the cascade becomes rotating stall in the single-stage compressor. By the method of propagation discussed in connection

with figure 1, the stall zones rotate around the compressor. Experiments with many compressors have shown that the stall zones rotate at about half the compressor rotating speed. If a hot-wire anemometer is installed in the compressor, which is stationary with respect to the compressor casing, it will pick up a trace of the flow as a function of time, as shown on the right of figure 2. Each time one of the stalled zones passes the instrument there is a reduction in flow and pressure. The flow, therefore, varies cyclically. There can be many kinds of rotating stall zones. They may vary in number from one to eight, may be concentrated at the tip of the blades, or may extend from hub to tip. The configuration that occurs depends on the compressor design and how it is operated.

Rotating stall occurs only at high angles of attack. Of course, at lower angles of attack the flow over the blades of the single-stage compressor is smooth and the compressor develops lift, or in other words, produces a pressure ratio without stall. Figure 3 shows the performance of a single-stage compressor in a plot of compressor pressure ratio which is proportional to the lift developed by the blades against the ratio of the volume flow of air through the compressor to the rotating speed of the compressor which is inversely proportional to the angle of attack. The lower the value of the volume flow to speed ratio the higher the angle of attack. In a compressor test rig the angle of attack may be changed in the single-stage compressor by throttling the compressor outlet, thereby reducing the volume flow and increasing the angle of attack, or the angle of attack may be changed by varying the speed of rotation. If the flow through the compressor is throttled, or the angle of attack is increased, the lift or pressure ratio developed by the compressor increases up to the point where the rotating stall previously described, occurs. If the flow is further reduced or the angle of attack is further increased, the pressure ratio developed by the stage falls off. Rotating stall occurs throughout the entire stalled range of compressor operation. Generally the number of rotating stall zones or the size of the zones increases as the compressor is operated further and further into stall. In some stages the change in pressure ratio may be discontinuous in the stall region.

Similar stall phenomena occur in the multistage compressor. In figure 4 a sketch of a multistage compressor is shown. Each stage in the compressor is designed to accept the flow from the previous stage and to produce a certain pressure ratio. The annular flow area and the blade angles are set so that at the design point the flow through the compressor will be smooth and the compressor will operate with good efficiency. As the air progresses through the compressor, when it is operating at the design point, the pressure and the density of the air increase so that it is necessary to reduce the annular flow area in the successive stages of the compressor. The operating points of typical inlet and outlet stages are illustrated in the stage characteristic maps

on the bottom of the slide. Generally, the compressor is designed so that the operating point of all stages at the design condition is considerably removed from the stall.

Of course, the compressor must operate at speeds both higher and lower than the design speed. At these off-design speeds the flow areas and blade settings for the fixed-geometry compressor become mismatched, which leads to stall problems.

If the speed is reduced appreciably below the design speed, the pressure ratio developed by the rear stages of the compressor falls off with the result that to get the air flow through the compressor the velocities in the back end of the compressor are greatly increased. The flow actually becomes choked in the back stages of the compressor, which blocks the flow so that the air flow through the compressor is actually reduced. This reduction in flow forces the operating point of the front stages of the compressor to move toward the stall limit. If speed is reduced sufficiently, the inlet stages stall and rotating stall occurs in the compressor. As will be discussed in a subsequent paper, this problem can be alleviated by variable-geometry devices, such as bleed or variable guide vanes; but this discussion will be limited to fixed-geometry compressors.

If the compressor is operated at speeds appreciably higher than the design speed, the density in the rear stages of the compressor is increased and the velocities are decreased. These changes in density and velocity result in the operating point of the back stages of the compressor moving toward stall. At higher than design speed, then, it's the back stages of the compressor that tend to stall.

Thus, operation of the multistage compressor appreciably off-design speeds results in stall in some stages of the compressor. At low speeds, the front stages tend to stall and at high speeds the back stages tend to stall. The higher the design pressure ratio of the compressor the more difference in flow area and density between the front and the rear of the compressor and, consequently, the more severe the off-design stall problems.

Stall in the multistage compressor may have large effects on performance. The performance of a typical multistage compressor is shown in figure 5. The over-all pressure ratio developed by the compressor is plotted against weight flow of air through the compressor. Lines are shown which give the over-all pressure ratio and air flow produced by the compressor at a speed lower than design speed and a high speed near the design speed. If the compressor were mounted on a compressor test rig, it could be operated at any flow or pressure ratio on the curves by adjusting a throttle at the compressor outlet. Throttling the outlet

of the compressor at low speed increases the angle of attack and the pressure ratio up to a point at which the first stage of the compressor stalls and rotating stall starts. Even though this rotating stall exists, the over-all pressure ratio can be further increased, with some of the later stages helping out, by additional throttling. If the throttling is continued at the compressor outlet, however, we reach a point which is labeled the compressor-stall limit. At this point stall becomes so severe that performance falls off radically (usually discontinuously as indicated) to a lower branch of the curve. This compressor stall limit marks the limit of useful engine operation. The stall limit is not synonymous with the occurrence of rotating stall. The engine may operate in rotating stall over an appreciable useful operating range. Only when rotating stall becomes very severe is operation of the engine limited. Two different phenomena may occur at this limit. Either performance falls off so radically that overtemperature of the turbine results - which makes the engine inoperable or the engine may go into surge. During surge, very violent low-frequency, high-amplitude pressure oscillations occur throughout the engine, accompanied by overtemperature of the turbine and large thrust losses. No matter which phenomenon occurs - surge or large performance drop off - the stall limit is the limit of useful engine operation. At speeds near the design speed, when the stall limit is reached, the engines invariably go into surge.

The difference between rotating stall and surge is shown in figure 6. Typical hot-wire recordings of flow in the compressor against time are shown for rotating stall on the top and surge on the bottom of the figure. During rotating stall, small amplitude, high-frequency pressure and flow oscillations occur in the compressor. To all outward appearances, the compressor and engine operate stably with these small disturbances. During surge, high-amplitude, low-frequency oscillations are present. Rotating stall is confined to the compressor, whereas surge involves the whole engine. Which phenomenon will occur, surge or rotating stall, depends on the intensity of the stall and how much damping is present, or in other words, on the characteristics of the whole engine. The important thing is that either severe rotating stall or surge will limit the useful operating range of engines.

The significance of the stall and surge limit of an engine can be illustrated best on a compressor map such as figure 7. Compressor pressure ratio is plotted against weight flow through the compressor. Lines are shown for the performance at various constant engine speeds from the design speed (100 percent) down to 50 percent. If the compressor is installed in an engine with a fixed turbine and exhaust-nozzle area, it will operate in steady state at only one pressure ratio at any given speed. The points at which the compressor turbine and exhaust nozzle are matched, determine the steady-state operating line. If the engine is operated at a fixed-throttle setting at any constant speed, the compressor will operate on this steady-state line.

As previously discussed, when the engine speed is reduced appreciably below design speed, the inlet stages tend to stall. In this case, the inlet stages stall at all speeds within the shaded area shown in figure 7. If the engine were operated along the steady-state operating line at reduced speed, rotating stall would, therefore, start at about 65 percent speed and would be present at all lower speeds.

The upper broken curve of figure 7 is the compressor-stall-limit line which is simply a line connecting the stall limit points described in connection with figure 5. This line represents the limit of useful engine operation. Operation above this line is not possible. In the case shown, the stall limit is separated from the steady-state operating line, although as will be discussed later, this separation does not exist in all engines. Even if some margin exists, as in this case, the separation between the two lines is of great importance because it determines the maximum acceleration rate of the engine. To accelerate an engine, the throttle is advanced rapidly, which causes a sudden increase in the turbine-inlet gas temperature, which greatly increases the volume flow of the gases through the turbine. To compensate for this increase in volume flow, the compressor must produce a higher pressure ratio. The operating point, therefore, departs from the steady-state operating line and rises sharply toward the stall limit. Obviously, the greater the displacement between the steady-state operating line and the stall limit the greater the maximum acceleration rate. As indicated in the figure, the margin between the operating line and the stall limit is very small at low engine speeds in our modern engines. This means that acceleration rates of our modern engines are severely restricted unless variable-geometry devices are used.

In addition to limiting the acceleration margin, in some engines the stall limit may actually prevent operation at part-speed conditions, as shown in figure 8. Compressor pressure ratio is plotted against weight flow for a modern, high-pressure-ratio engine. The dashed line is the steady-state operating line, and the solid line is the stall-limit line. There is a sharp dip in the stall limit at speeds between 70 and 80 percent caused by abrupt stall of several stages. The stall line actually drops below the steady-state line, and operation of the engine is not possible in this speed range without variable-geometry devices.

This part-speed stall occurs because the front stages of the compressor are stalled. The back stages of the compressor tend to stall at speeds higher than design. This back-stage stall leads to a high-speed stall problem, which is illustrated in figure 9. In figure 9, compressor pressure ratio is plotted against equivalent engine speed. Equivalent engine speed is the engine rotating speed divided by the square root of the compressor-inlet temperature. If the engine is operating at high altitude where the compressor-inlet temperature is very low, the

compressor equivalent speed may exceed the design speed by as much as 10 or 20 percent. On the figure, the compressor-stall limit is shown by the solid line and the steady-state operating line is shown by the dashed line. Because of back-stage stall, the stall limit bends over and approaches the operating line at speeds above the design. The stall limit and the operating line intersect at an engine speed about 8 percent above the design speed, which makes the engine inoperable at any higher speeds. This high-speed stall limit is a limit existing in most engines, which may restrict the operation of the engines at high-altitude conditions.

The two-spool engine is also affected by compressor stall. Because there is no mechanical connection between the two spools, the operation of the compressor is determined by the flow areas and power-absorption characteristics of the components. The interaction between the components and the resultant behavior of the engine is quite complicated and, therefore, the reasons for its operational characteristic will not be described in detail. Some of the general stall characteristics for a two-spool engine are shown for a hypothetical engine in figure 10.

Over-all pressure ratio, that is, the combined pressure ratio across both spools, is shown plotted against weight flow through the compressor. In the two-spool engine there are, of course, two compressors, which results in two stall limits. The inner-compressor stall limit is the upper limit to useful engine pressure ratio, that is, the engine cannot be operated at pressure ratios higher than the inner-compressor stall limit. The outer-compressor stall limit represents a lower limit to engine pressure, that is, the engine cannot be operated at pressure ratios below the outer-compressor stall limit. The operating line, therefore, must fall between these two stall limits. Although it might seem that this type of operation is more restrictive than one-spool engines, in actual practice the two-spool engine may be designed to operate at higher pressure ratios than the one-spool engine with no more severe stall problems. As illustrated here, the operating line approaches the outer-compressor stall limit at part speed and approaches the inner-compressor stall limit at speeds higher than design. We can see then, that the two-spool engine has similar part-speed and high-speed stall problems to the single-spool engine.

To summarize, stall or flow breakaway, which occurs in wings at high angles of attack, also occurs in compressors. In compressors, stall limits the pressure ratio that can be developed by the compressor. If the single-stage compressor is operated in stall, local regions of stalled flow appear that propagate around the compressor annulus. This propagating stall is called rotating stall.

In the multistage compressor, operation at speeds lower than design forces the front stages of the compressor to stall and causes rotating stall to appear. At speeds higher than design, the rear stages of the compressor tend to stall.

If the pressure ratio of the multistage compressor is increased sufficiently at any speed, a limit of useful compressor operation is encountered. This limit of operation is called the compressor stall limit and is the point at which stall becomes sufficiently widespread in the compressor, or sufficiently severe, to cause a large usually discontinuous drop in compressor pressure ratio and efficiency.

If the compressor as a part of an engine is operated beyond the stall limit, either excessive turbine-inlet temperatures will result, which makes operation impractical, or the engine will surge. Which thing happens depends upon the characteristics of the individual compressor and the amount of damping present in the rest of the engine. Experience has shown that, although either type of limit may occur at low compressor rotative speeds, surge invariably occurs at high speeds. In any case, the stall limit is the real limit of engine operation.

In order to achieve maximum performance with minimum size, modern engines are designed so that the stall limits occur close to the steady-state operating lines of the engine. This proximity of the stall and operating lines introduces two major problems in modern engines: (1) The acceleration margin, and hence the acceleration rate, is limited, or the steady-state operating line and the stall-limit line may actually intersect at part speed, necessitating the use of some remedial device; (2) the stall-limit and steady-state operating lines may intersect at speeds higher than design, which may make the engine inoperative at the lower compressor inlet temperatures accompanying high-altitude flight conditions.

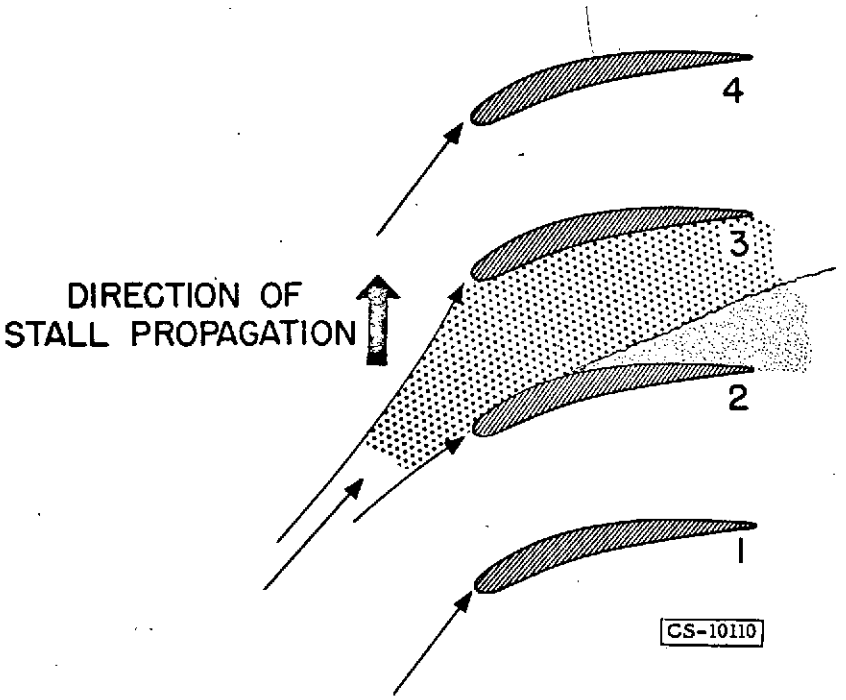

Figure 1. - Stall propagation in cascade.

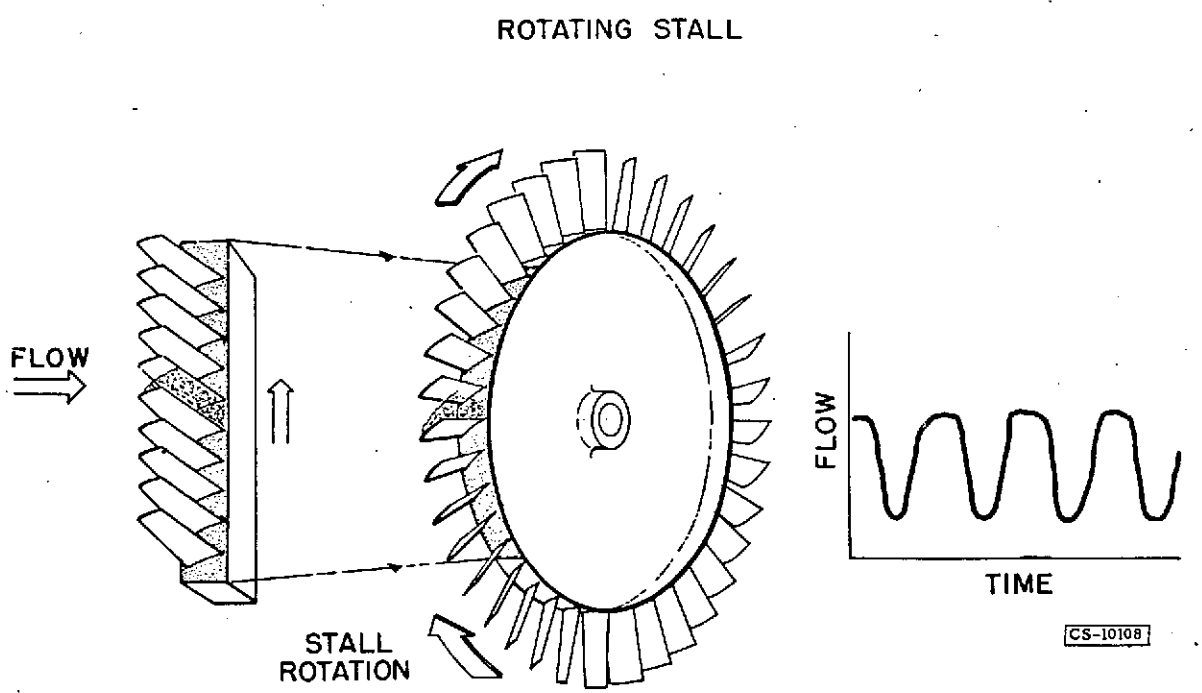

Figure 2. - Stall propagation in rotor or stator.

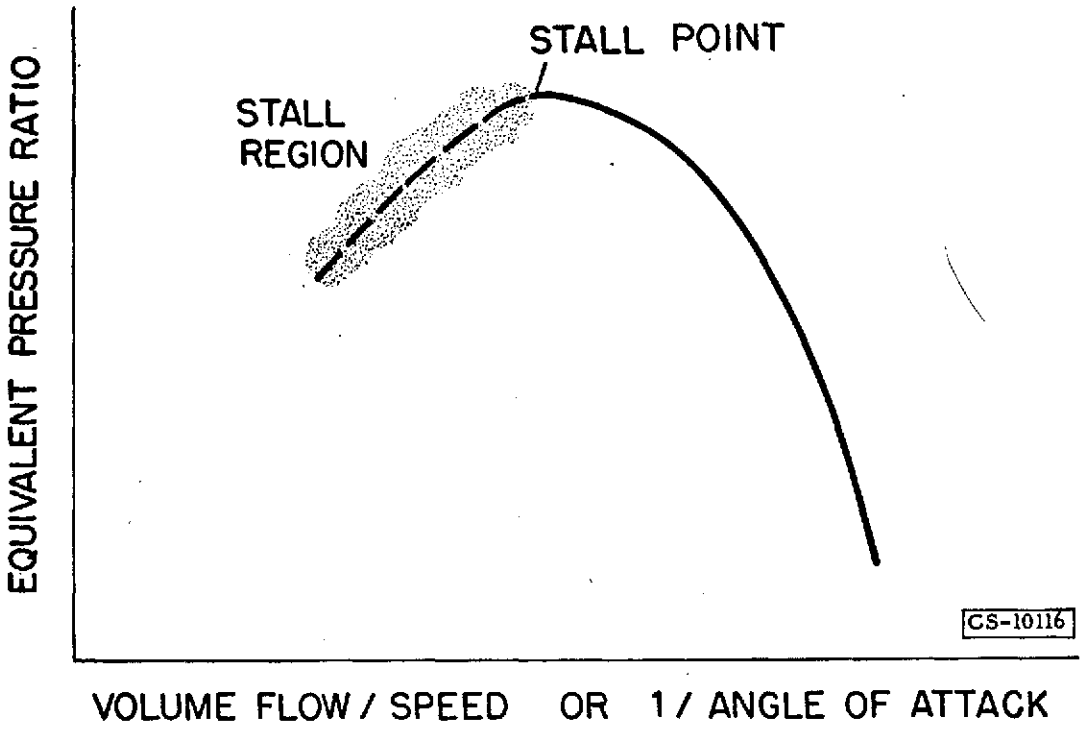

Figure 3. - Performance of a single stage compressor.

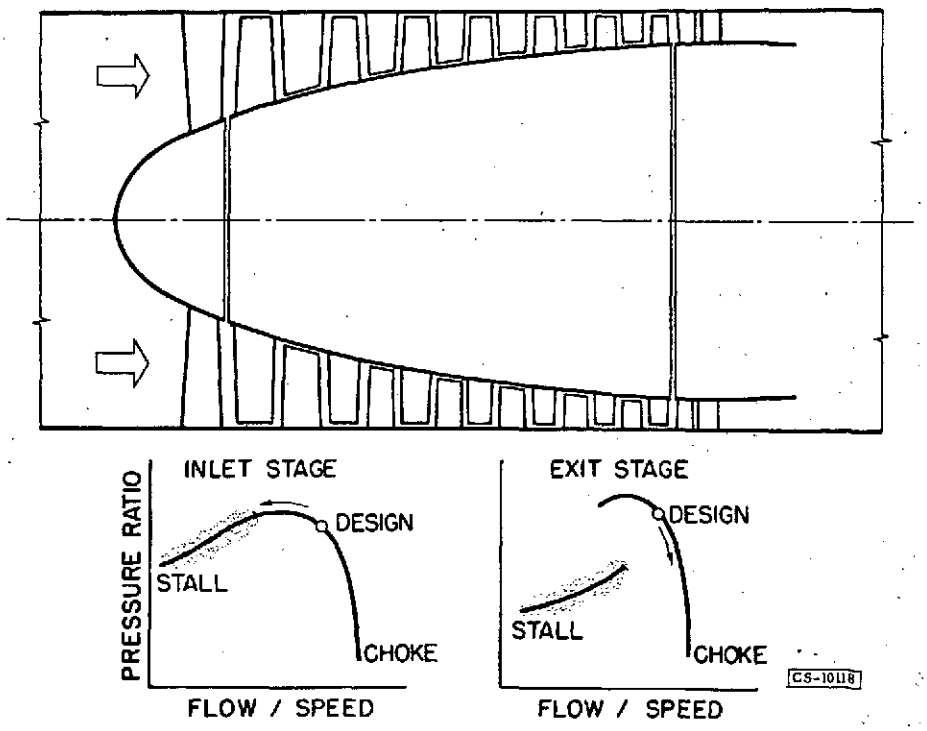

Figure 4. - Axial flow compressor.

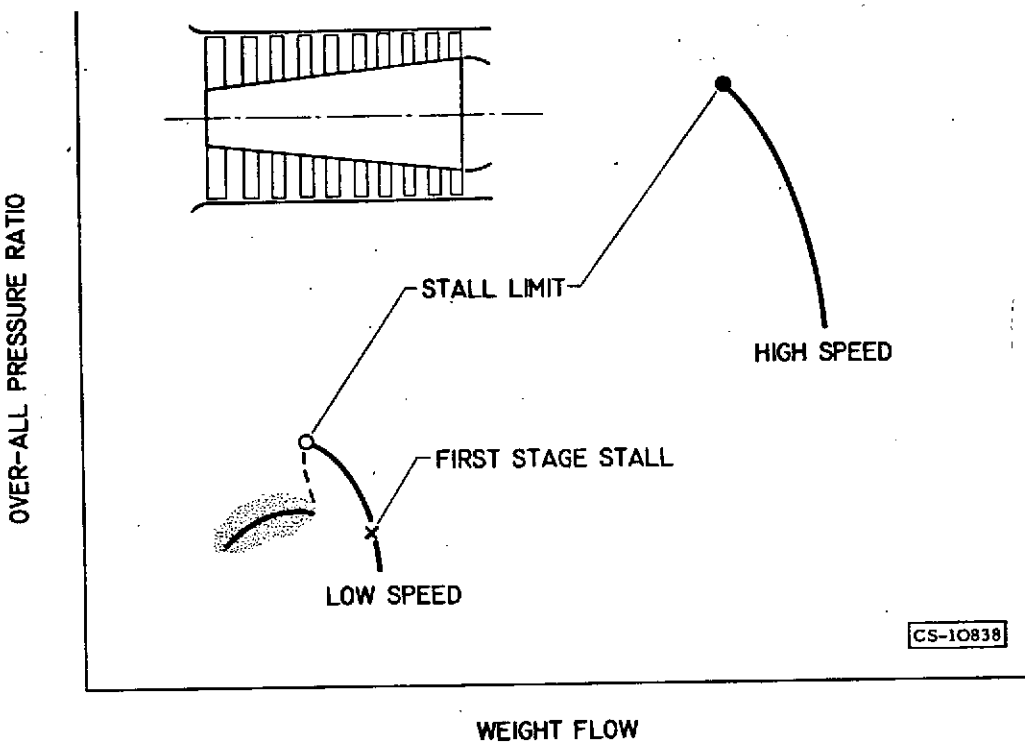

Figure 5. - Multistage compressor performance.

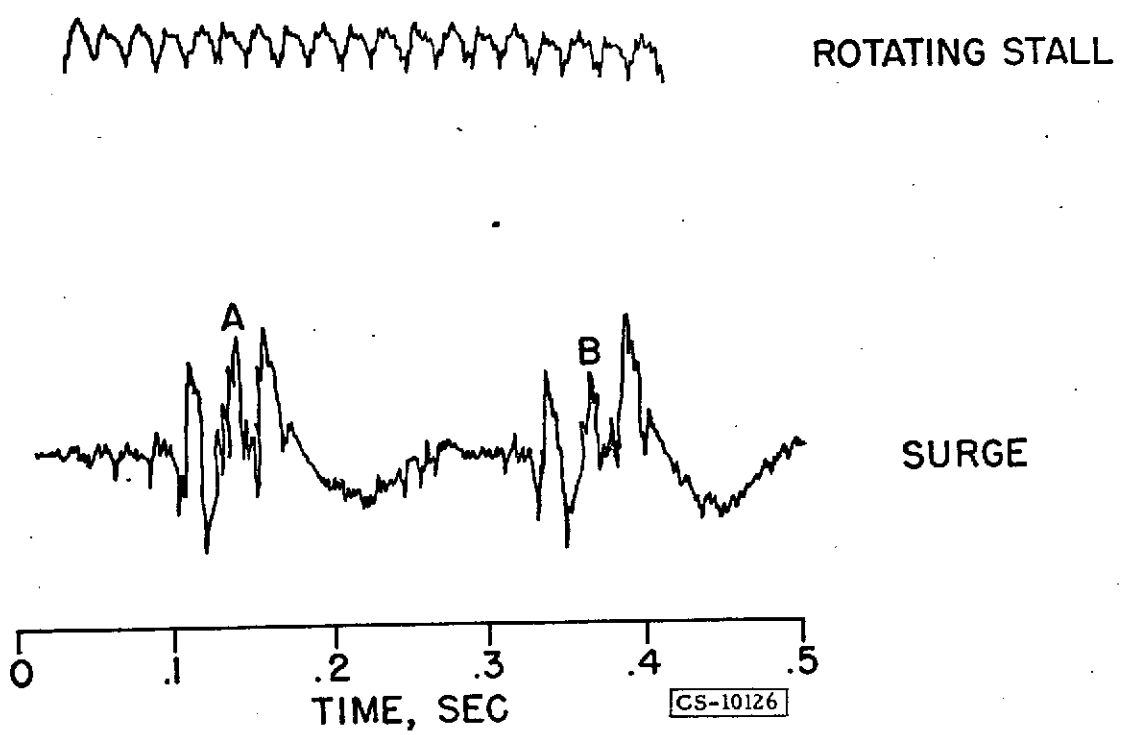

Figure 6. - Flow pulses.

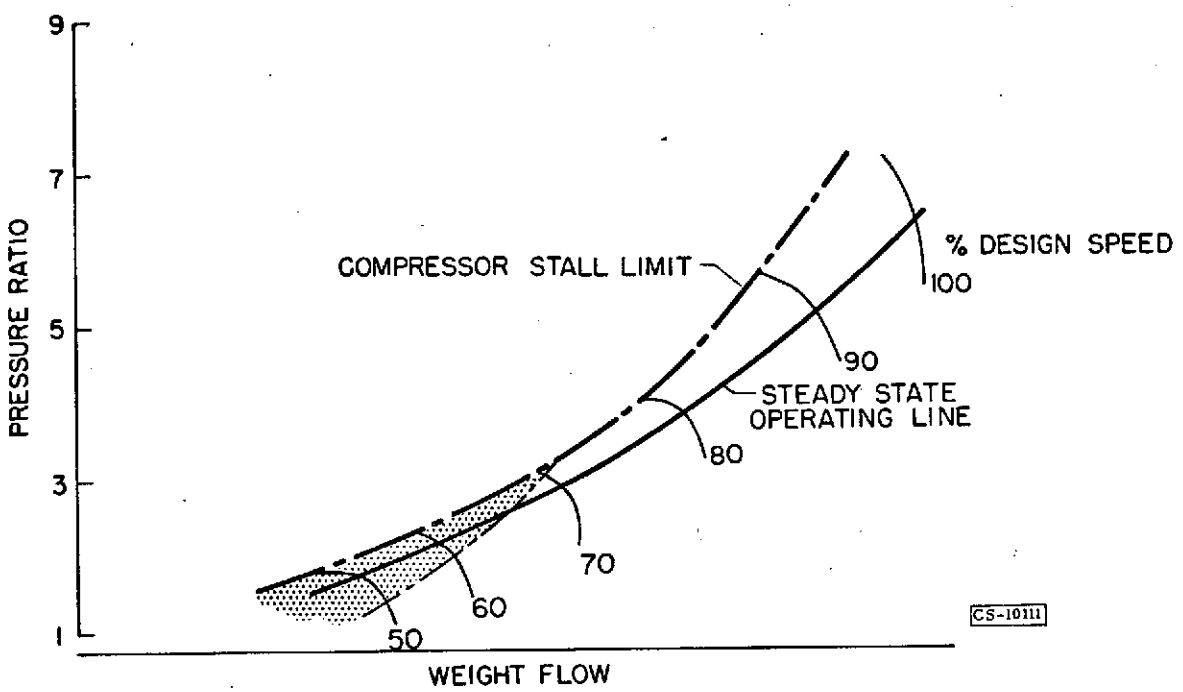

Figure 7. - Steady state operating line.

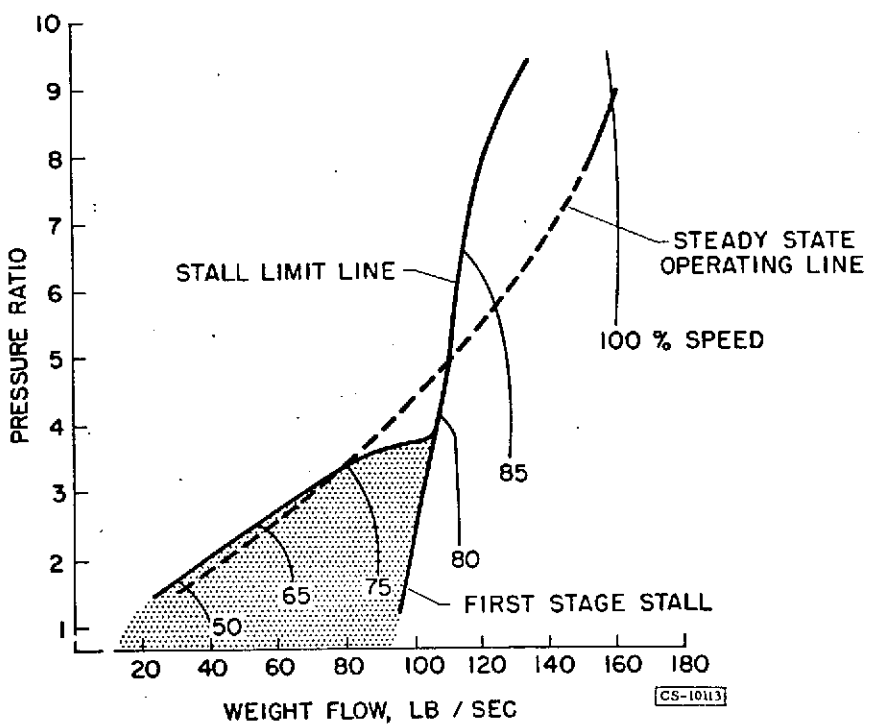

Figure 8. - Part speed surge problem.

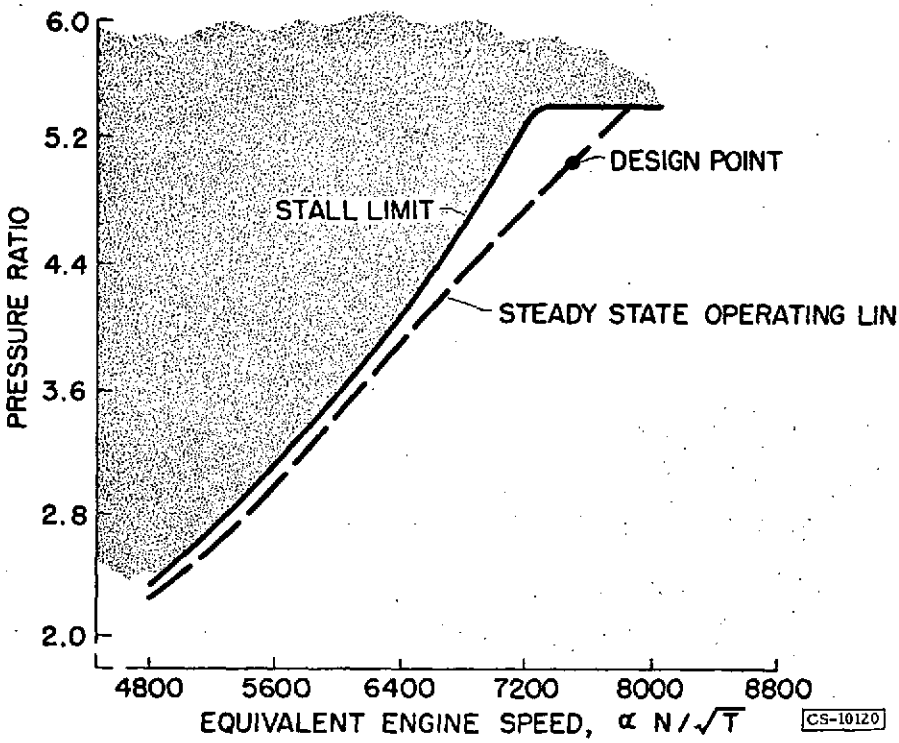

Figure 9. - High speed surge.

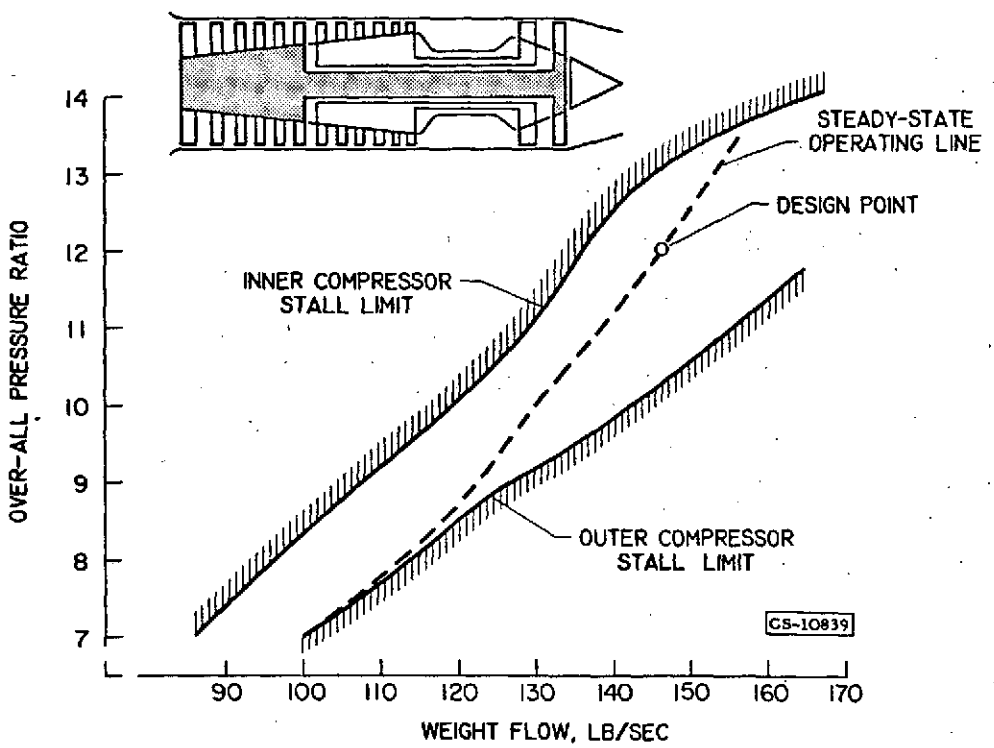

Figure 10. - Two-spool compressor.

II

EFFECT OF ROTATING STALL ON COMPRESSOR BLADE VIBRATION

by

S. S. Manson, A. J. Meyer, A. A. Medeiros, M. P. Hanson

II - EFFECT OF ROTATING STALL ON COMPRESSOR BLADE VIBRATION

By S. S. Manson, A. J. Meyer, Jr., A. A. Medeiros
and M. P. Hanson

INTRODUCTION

One of the important effects of rotating stall is the possibility of inducing compressor blade vibrations. A number of compressor blade failures, both in experimental rigs and in production compressors, have been traced to vibration induced by rotating stall. The present discussion describes the reason that rotating stall induces vibration, indicates some important engine variables that affect vibration, and outlines several remedies that might be used in overcoming this problem.

MECHANISM OF VIBRATION EXCITATION

Relative Velocity between Rotating Stall and Compressor Blades

To demonstrate the reason for vibration excitation by rotating stall, it is necessary first to determine the relative velocity between the stall zones and the compressor blading. For the stator blades the relative velocity is obviously the absolute velocity of the rotating stall. For the rotor blades the relative velocity is determined as in figure 1. In this figure, a row of stator blades is shown, followed by a row of rotating blades. It is assumed that rotating stall has been established. The velocity of the rotating stall in the stators is equal to vector A, and the velocity of the rotor blades is designated by vector B. If a given stall pattern exists within one stage of compressors, in most cases its effect is felt throughout the unit (ref. 1). Thus, the velocity of the rotating stall in the rotor blades, vector A', is equal to vector A. The velocity of the rotating stall relative to the rotor blades is then equal to vector B minus vector A', or vector C.

Because of the relative motion between the stall and the blades, each blade experiences alternate regions of high and low pressure. By use of hot-wire anemometers, various patterns of rotating stall and consequent pressure fluctuations have been determined. Typical configurations are shown in figure 2. The circles represent the annulus of the compressor, and the shaded areas the stalled regions. Figure A represents a hub stall configuration; figure B, a combination of hub stall and a tip stall. In figure C the stall exists over the entire blade span; and in figures D, E, and F are shown tip stalls, both evenly and unevenly spaced. As the pressure variations due to the stall zones pass by the blades, they produce periodic forces that may excite the blades into vibration if they are of the proper frequency.

Condition of Resonance

To determine under what conditions rotating-stall frequencies will produce blade vibrations, a typical response curve of a blade is shown in figure 3 (ref. 2, pp. 61-70). When a blade is excited by a sinusoidal force, the amplitude of vibration depends on the ratio of the frequency of the exciting force to the natural frequency of the blade. For low ratio of excitation to blade natural frequency, the amplitude is relatively low. However, as the exciting frequency approaches the natural frequency of the blade, the amplitude increases rapidly. Were there no damping, the amplitude would become infinitely great when the exciting frequency is equal to the natural frequency. Because friction is always present, the amplitude does not become infinite, but does achieve a high value at this condition of equality between exciting frequency and blade natural frequency. Vibration under such a condition is known as resonant vibration. For exciting frequencies above the natural frequency of the blade, the amplitude again falls off and rapidly approaches zero as the exciting frequency is increased. Thus, to obtain high vibration amplitudes, it is necessary for the exciting frequency to be at or near the natural frequency of the blade.

Exciting Frequencies Contained in Rotating-Stall Signals

The meaning of the exciting frequency of the rotating stall must be clarified. Actually, a given rotating-stall pattern contains a large number of exciting frequencies, as can be seen in figure 4. In the upper part of the figure is shown a typical signal obtained from a hot-wire anemometer. Rather than being sinusoidal, the wave is complex. Since the natural motion of the blade during vibration is, however, sinusoidal, it turns out that, to analyze blade vibrations, the complex wave must be replaced by a combination of waves.

With the use of a Fourier analysis (ref. 2, pp. 19-30), it is found that the upper signal can be replaced by the combination of the signals of the sine signals in the lower part of the figure. There exists first a uniform component, indicated by the horizontal line H, as well as a number of sine and waves. At any point such as P, the sum of OA, OB, OC, OD, and the steady-state component (the distance between the axis and horizontal line H) is equal to the amplitude of the original signal. The effect of the original stall signal is therefore exactly the same as the effect of the combined signals as far as blade vibration is concerned.

The steady-state component does not produce any vibrations, but each of the sine waves can produce a vibration if it is at or near the natural frequency of the blade. For example, if the frequency of the stall signal is 100 cps, then there will exist a wave as shown on the

figure for a frequency of 100 cps, which is called the fundamental. In addition, there will exist a wave having a frequency of 200 cps called the second harmonic, and other waves for 300 and 400 cps, and so forth, as the third and fourth harmonics, and so forth. Thus, because of the complexity of the stall signal, it becomes possible to encounter a large number of resonances within the operating range of the engine.

Critical-Speed Diagram

After the stall signal has been resolved into its harmonic components, it becomes possible to predict the speeds at which resonant vibrations occur by use of a critical-speed diagram such as shown in figure 5. On the horizontal axis is shown engine speed, and on the vertical the frequency of excitation. The frequency of rotating stall is approximately linear with rotative speed, and the lowest inclined line represents the variation of exciting frequency of the fundamental of a given stall pattern. Excitation is also produced at any engine speed by the second harmonic at a frequency exactly twice the fundamental frequency, and by the third harmonic at a frequency three times the fundamental, and so forth. Therefore, a number of exciting lines exist, as shown by the solid lines in figure 5. Also shown in the figure by the dotted line is the natural frequency of the blade, which increases slightly with rotative speed as a result of centrifugal stiffening. Each time the natural-frequency line intersects one of the lines of excitation, resonance occurs.

Figure 6 shows a more realistic critical-speed diagram, in which the natural-frequency lines for the first five stages are shown. Lines of excitation are shown for a single-stall-zone pattern, two-stall-zone patterns, and three-, four-, and five-zone stall patterns. Also shown are the second harmonics of the three- and four-zone stall configurations. The dotted and solid lines intersect at many points, indicating that blade vibrations are possible at many engine speeds. In practice, it is practically impossible to avoid resonance with one or another of the stages and the various exciting lines possible whenever rotating stall occurs. However, not all resonances cause serious vibrations. As indicated in figure 4, the amplitudes of the various harmonics are not all high. The energy available for vibration excitation depends on the amplitude of the particular harmonic which is in resonance with the blade natural frequency. Thus, although resonance occurs in some cases, the amplitude developed may be low if the available excitation energy is low.

SEVERAL FACTORS AFFECTING STALL AND VIBRATION

Measurements of vibrations induced by rotating stall have been made in a large number of engines, both of experimental and production types. In general, it has been found that all engines are subject to rotating stall in certain speed ranges and that in most cases resonance occurs between one or another of the harmonics of the rotating stall and the natural frequency of the blade. The amplitude of vibration in some engines is sufficient to induce blade breakage; in other cases low amplitude vibration exists which does not, however, affect the structural integrity of the blades.

The studies indicate that a number of important variables can seriously affect the vibration in a given compressor. Several of these variables will now be outlined.

Effect of inlet temperature. - It has been found that the tendency toward vibration in a given compressor can be seriously affected by the inlet temperature. Figure 7 indicates the reason for this effect. In this figure the compressor total pressure ratio is plotted against equivalent weight flow for lines of constant equivalent speed. This map is plotted for the low speed range where the inlet stages are operating at stall conditions. The various stall patterns are indicated between ranges labelled 2, 3, 4, and 5. Any point of operation bounded by the lines OA and OB resulted in a rotating stall with two zones; any region bounded by lines OB and OC resulted in rotating stall with three zones, and so forth. Although the regions are shown as distinct from each other, there is in practice some overlap between these regions, and the boundaries separating the regions are not as clear as indicated in the figure. In general, along the stall limit line only one stall zone is experienced, not only at the speeds shown upon the figure, but at all speeds.

Steady state operating conditions are shown by the dot-dash line. At an actual engine speed of 5200 rpm and a temperature of 59° F, three stall zones exist as indicated by the circled point. If the mechanical speed is held at 5200 rpm, but the inlet temperature is changed to 20° F, the equivalent speed is changed to approximately 5400 rpm, and a four-zone stall predominates, as indicated by the triangle. If the inlet temperature is decreased to -67° F, corresponding to the temperature at high altitudes, and the engine speed is still maintained at 5200 rpm, the equivalent speed now becomes 6000 rpm. As indicated by the square, operation now occurs at a condition outside the region of rotating stall and no high amplitude blade vibrations are encountered. Thus, an engine may not have a vibration problem at one inlet temperature and speed, but a change of temperature within the range of expected operation of the engine may induce a severe vibration problem at the same speed.

Effect of exhaust nozzle area. - A change of exhaust nozzle area may also seriously affect vibration at a given speed. Figure 8 shows this effect. Again the regions of various numbers of rotating stalls are delineated by the lines OA, OB, and so forth. Two steady state operating lines corresponding to two positions of the exhaust nozzle are shown by the dotted and dot-dash curves. At a speed of 5200 rpm, it can be seen that operation with the smaller exhaust nozzle area, as indicated by the dotted curve, results in a three-zone rotating stall pattern. Opening the exhaust nozzle produces a condition which changes the stall pattern to a four-zone rotating stall as indicated by the intersection between the dot-dash curve and the 5200 rpm equivalent speed curve. Depending upon the natural frequency of the blade, one or another of these two operating conditions may be more severe in inducing vibrations.

Figure 9 shows the vibration encountered in the second stage of a production engine resulting from a change in exhaust nozzle area. Here, the vibratory stress is plotted against engine speed. For the rated nozzle, the maximum stress encountered was ±26,500 psi, whereas for the closed nozzle the maximum stress reached was ±60,000 psi.

Most engines are not equipped with variable-area exhaust nozzles. The purpose of testing a given engine with a variable exhaust nozzle is to map the complete characteristics of the engine during operation under steady-state conditions. Once this map has been obtained, the characteristics of the engine during transient conditions can be determined. Of particular interest is the prediction of the vibration characteristics during acceleration as described in the next section.

Effect of acceleration. - Figure 10 shows the compressor map for an engine on which acceleration studies were made. In this engine a limited region adjacent to the stall limit line was characterized by a single-zone rotating stall (the very thin shaded region). The predominant region in which rotating stall occurred was characterized by a seven-zone rotating stall. During normal acceleration of the engine, as shown by the lower of the dotted lines in figure 10, the engine remained for an extended period within the region of the seven-zone stall, and since the frequency of this stall pattern coincided with the natural frequency of the blades, high vibrations were encountered during normal acceleration. The single-zone rotating stall was, however, of too low a frequency to induce high vibratory stresses; hence, in this engine it was desirable to accelerate the engine very rapidly to operation very close to the stall limit line where the vibratory stresses were lower. A maximum stress of ±60,000 psi during normal acceleration was reduced to a stress of ±30,000 psi. It should be emphasized, however, that in other cases a change of acceleration rate may increase vibratory stress. The final stress depends on the stall characteristics of the engine and the relation between the frequency of the stalls (and their harmonics) and the natural frequency of the blade.

RELATION BETWEEN VIBRATORY STRESS AND FATIGUE FAILURE

The fact that every engine that has been examined has shown manifestations of rotating stall and associated blade vibration does not necessarily mean that all engines are expected to fail. In some cases the stress levels are below the endurance limit of the material. Even when the vibratory stresses are above the endurance limit, immediate failure is not always to be expected. Figure 11 shows a modified S-N curve for fatigue of compressor blade materials that indicates why some engines fail after a very short period of operation while others can be operated for many hours before failure. In this figure vibratory stress required to produce failure is plotted against the number of cycles. The lowest horizontal dotted line is known as the endurance limit. Any vibratory stress lower than this value can be withstood indefinitely without failure. This stress level has been adjusted to take into account the steady-state centrifugal stress to which the engine is subjected. Blades in engines with vibratory stresses in the neighborhood of 44,000 psi can withstand approximately one million cycles. A blade with a natural frequency of 200 cps can withstand 83 minutes of vibration before failing. At very high stress levels, such as 75,000 psi, which are occasionally experienced as a result of rotating stall, failure can be expected in the very short time of 1000 cycles, or 5 seconds.

Experience indicates that rotating stall is a very common cause of blade failure. Obviously, in some cases, the stresses induced are above tolerable levels. It is thus desirable to indicate several remedies that can be applied in coping with this problem. The most obvious of these is, of course, minimizing the rotating stall itself, as is discussed in a later paper. The present discussion is limited to mechanical approaches.

POTENTIAL METHODS OF REDUCING STRESS AMPLITUDES

Design Modifications

One way of minimizing the problem of failure due to vibration is to provide a structure that will withstand the vibratory stresses. Where these failures are in the blade root region, the use of heavy sections and large radii of curvature can be beneficial. Figure 12 shows roots intended for operation in the same compressor. In design A, four serrations were used and the fillet radii were small. The result was cracking in the root across the second pair of serrations. In design B, the section is heavier and the number of fillets is reduced to three, thereby permitting the use of larger radii in the fillets. Preliminary tests indicate that design B can withstand the stress levels encountered in the engine that caused the failure of blade root A.

Mechanical Friction

Another method of limiting vibration amplitude is the use of loose blades. A blade that is loose in its mount produces considerable friction, thereby inducing damping. Studies have been made on root damping, and some of the results are shown in figure 13 (ref. 3). Here root damping is plotted as a function of rotor speed for several designs investigated. Generally, there is a decreasing trend in the damping with increased speed, because the centrifugal force tightens the blade in its mount, thereby overcoming to some extent the original looseness provided by the designer. At the rated speed of the engine, the root damping is very low; however, at part speed, considerable damping may still be present.

The amount of damping depends on the root design. The fir-tree type of design produced considerably more damping, for example, than the ball-root design. Also shown at the upper right in this figure is a design in which the friction is produced by the side pressure between the tangs of the blade and the disk. At low speeds, the friction was so high that the vibration induced was not sufficient to measure the damping. At the high speeds, the available damping was maintained because the side pressure which caused the friction was not affected by centrifugal force. Thus, new designs conducive to looseness and to the introduction of friction in the mounting should prove beneficial in the solution of vibration problems. In current production engines, the trend has been toward the use of loose blades.

Materials with High Internal Damping

Damping can also be achieved by the use of materials having high internal damping capacity. For example, attention should be directed toward the use of plastic compressor blades (ref. 4). Figure 14 shows a comparison of the damping characteristics of a Bakelite-impregnated fiberglass plastic and several other materials that have been used as compressor blading. Damping capacity depends on stress level, and the figure shows the damping capacity at both 5000 and 25,000 psi, the latter being of greater interest in connection with operation near the point of failure. At a stress level of around 25,000 psi, the damping of the plastic is approximately 20 percent, compared with 4 percent for the type 403 stainless steel used in most of the current engines. Titanium and aluminum have very low internal damping.

Some experience has already been obtained with the use of the Bakelite-impregnated fiberglass plastics (ref. 4). The tests were run on a J47 engine under normal steady-state operating conditions. As previously indicated, no severe vibration due to rotating stall is obtained under these conditions; and, therefore, the evaluation

was not made to determine the applicability in the solution of vibration problems. The preliminary tests were made largely to determine whether the blades were sufficiently durable to withstand normal conditions of operation. A third stage of a J47 compressor was completely fitted with plastic blades and operated at rated take-off conditions for approximately 100 hours. No detectable deterioration was observed.

CONCLUDING REMARKS

Rotating stall induces vibration because the relative motion of the stall and blading results in pressure fluctuations on the blades. Since the wave form of the rotating stall is complex, the number of harmonics available to induce vibration is large. When any of these harmonics is in resonance with the natural frequency of the blade, high vibrations may be induced. In multistage compressors, it is almost impossible to avoid resonant vibration with one or another of the stages whenever rotating stall exists.

The rotating stall and associated vibrations are critically affected by engine operating conditions such as inlet temperature, exhaust-nozzle area, and conditions of acceleration. The sensitivity of the rotating stall to these conditions in some cases results in apparently erratic behavior of the rotating-stall characteristics. Thus, on some occasions, rotating stall will be present during one run but vanish in the next run in which the only difference is a small change in inlet-temperature conditions.

Rotating stall and associated vibrations have been observed in every compressor investigated. However, the stress amplitudes are not always high enough to cause failure. For cases involving high vibration amplitudes, several remedial measures are potentially possible. Among those that have been mentioned are redesign to minimize stress concentration and increased rigidity, incorporation of high root damping, and use of materials with high internal damping. Any conventional approach that would tend to minimize vibration amplitude should prove beneficial. The most valuable approaches involve measures that reduce the tendency for rotating stall to initiate and propagate. These measures are discussed in a later paper.

REFERENCES

1. Huppert, Merle C., and Benser, William A.: Some Stall and Surge Phenomena in Axial-Flow Compressors. Jour. Aero. Sci., vol. 20, no. 12, Dec. 1953, pp. 835-845.

2. Den Hartog, J. P.: Mechanical Vibrations. Second ed., McGraw-Hill Book Co., Inc., 1940, pp. 19-30.

3. Hanson, M. P., Meyer, A. J., Jr., and Manson, S. S.: A Method of Evaluating Loose-Blade Mounting as a Means of Suppressing Turbine and Compressor Blade Vibration. Proc. Soc. Exp. Stress Analysis, vol. 10, no. 2, Nov. 1952, pp. 103-116.

4. Johnson, Donald F., and Meyer, André J., Jr.: Preliminary Investigation of the Strength and Endurance of Plastic-Impregnated Fiberglass Compressor Blades. NACA RM E54I27a, 1955.

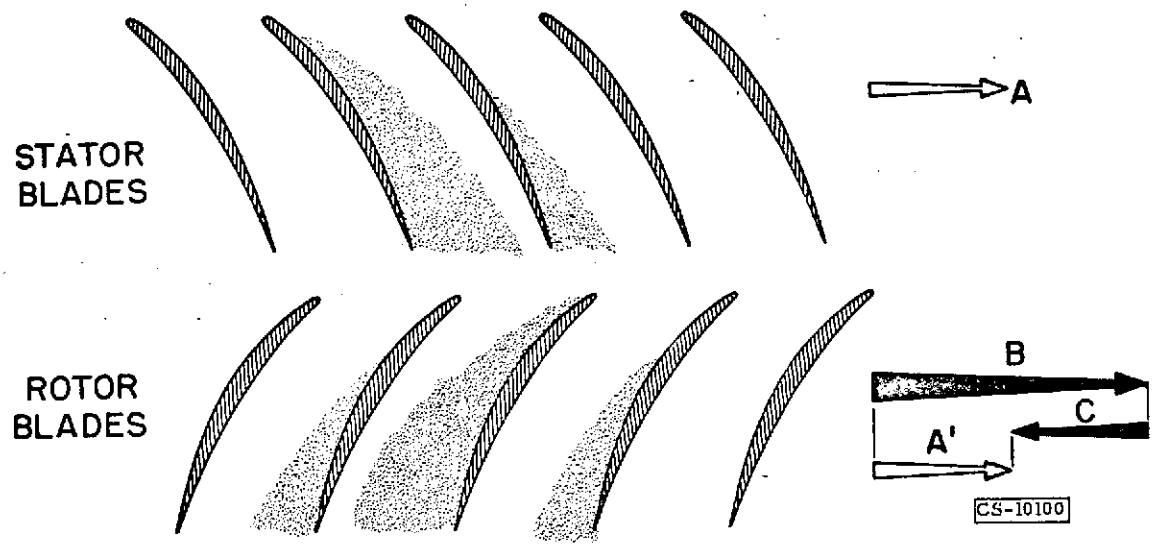

Figure 1. - Relative motion of stalled zones.

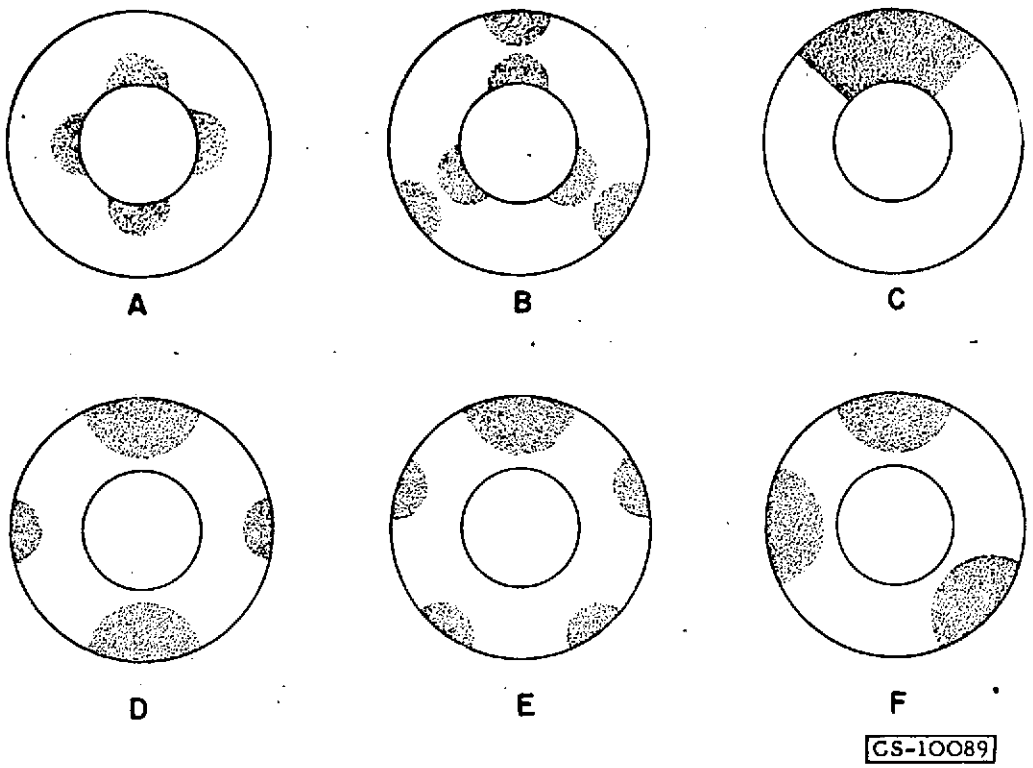

Figure 2. - Types of rotating stall patterns observed.

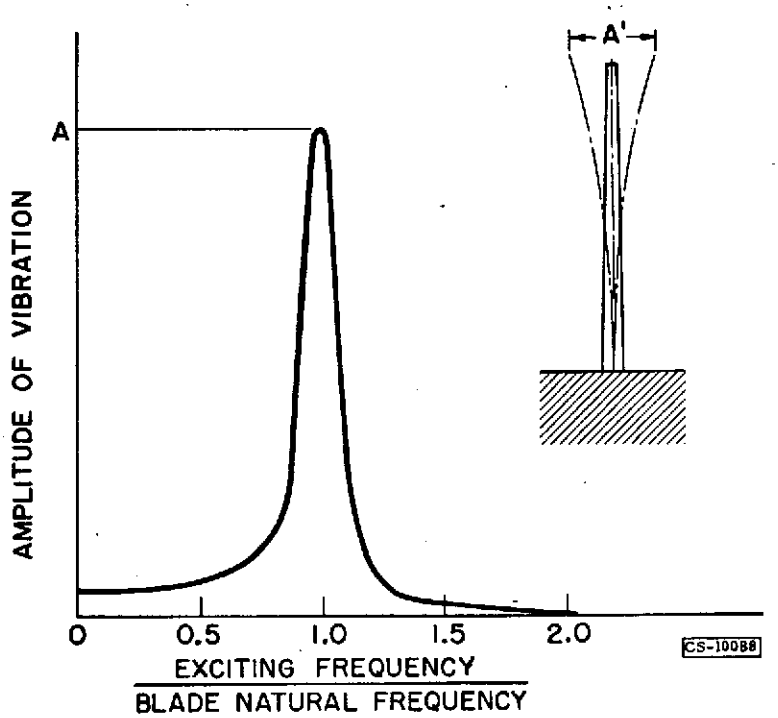

Figure 3. - Typical resonance curve.

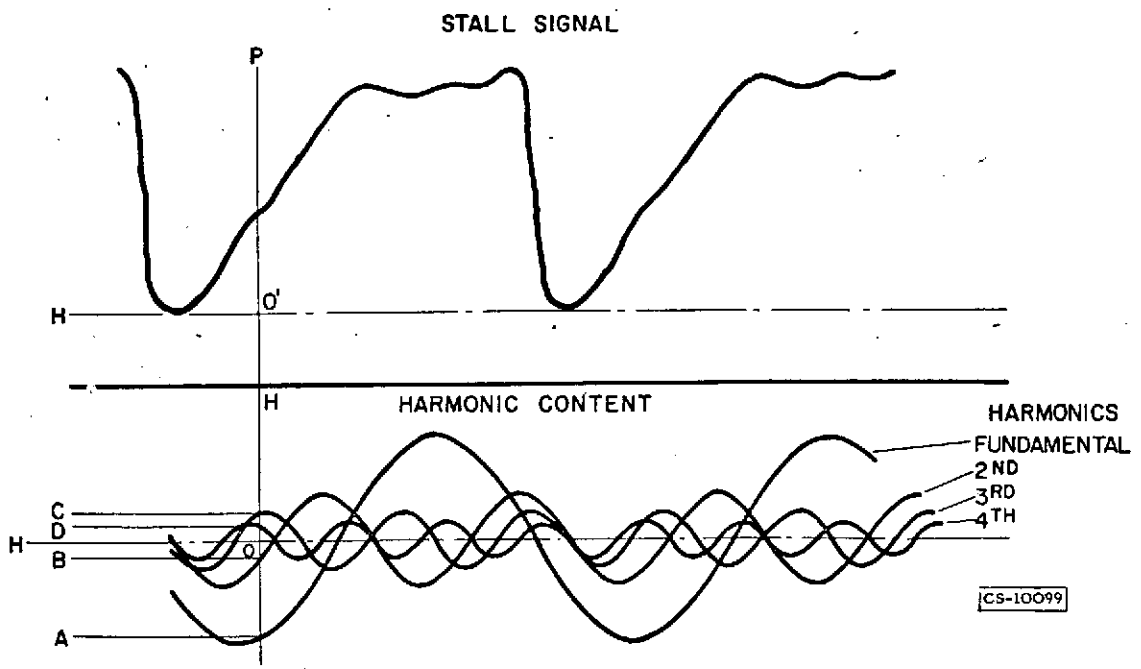

Figure 4. - Rotating-stall wave form and harmonic content.

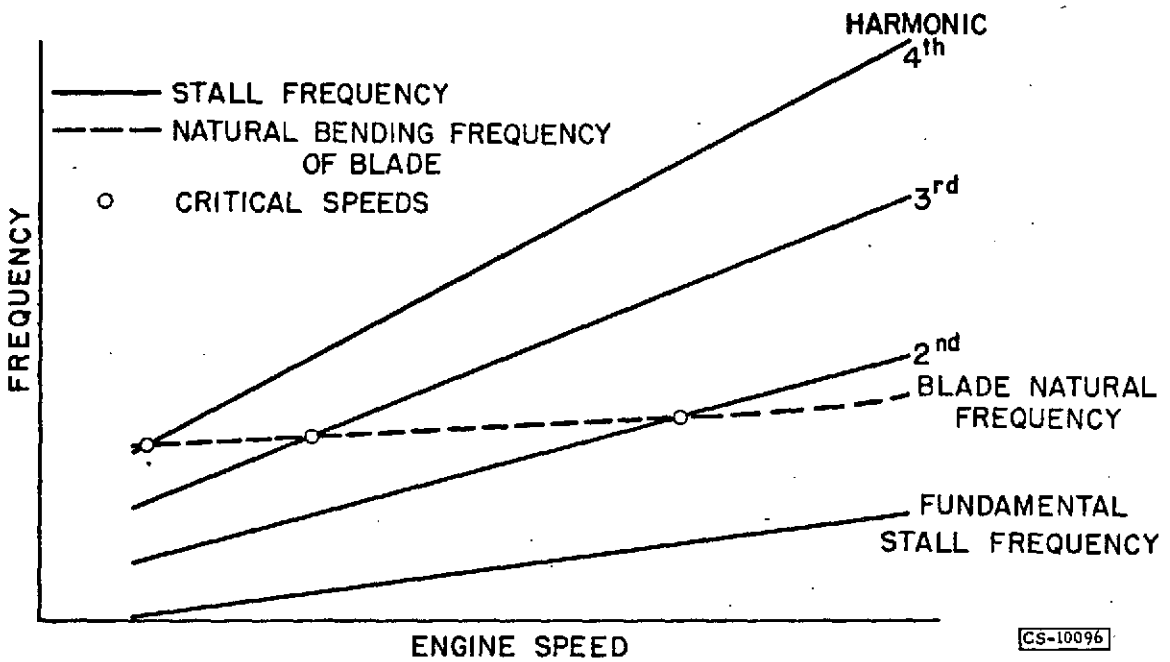

Figure 5. - Typical critical-speed diagram for a single blade row.

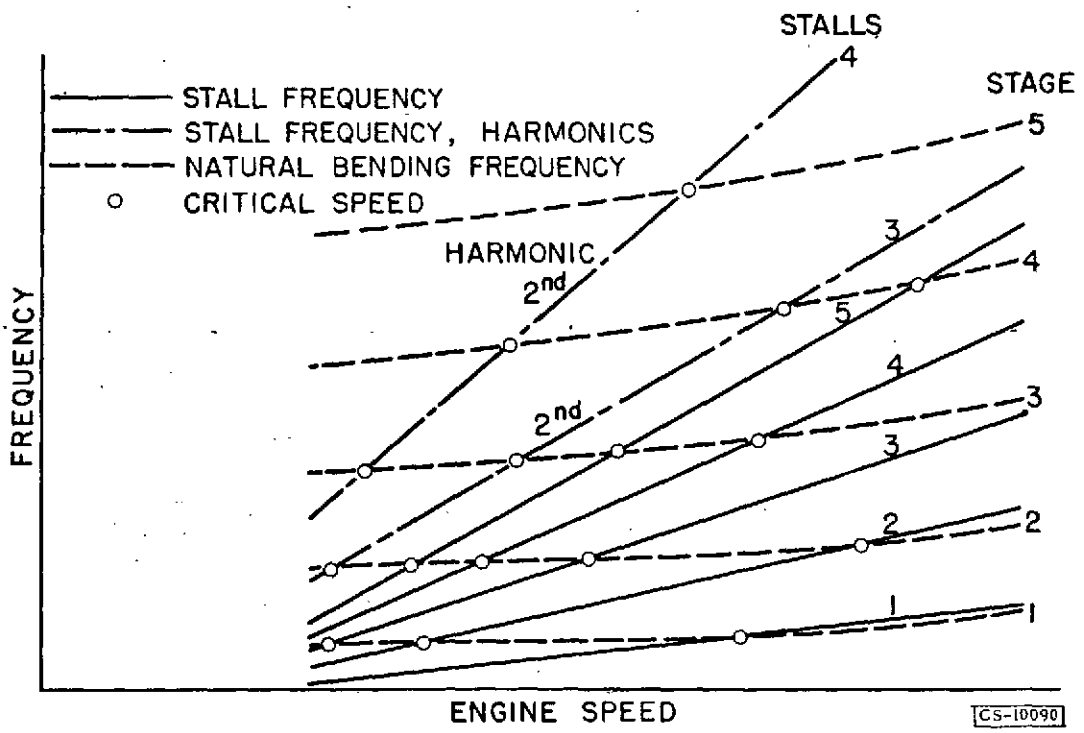

Figure 6. - Typical critical-speed diagram for multistage compressor.

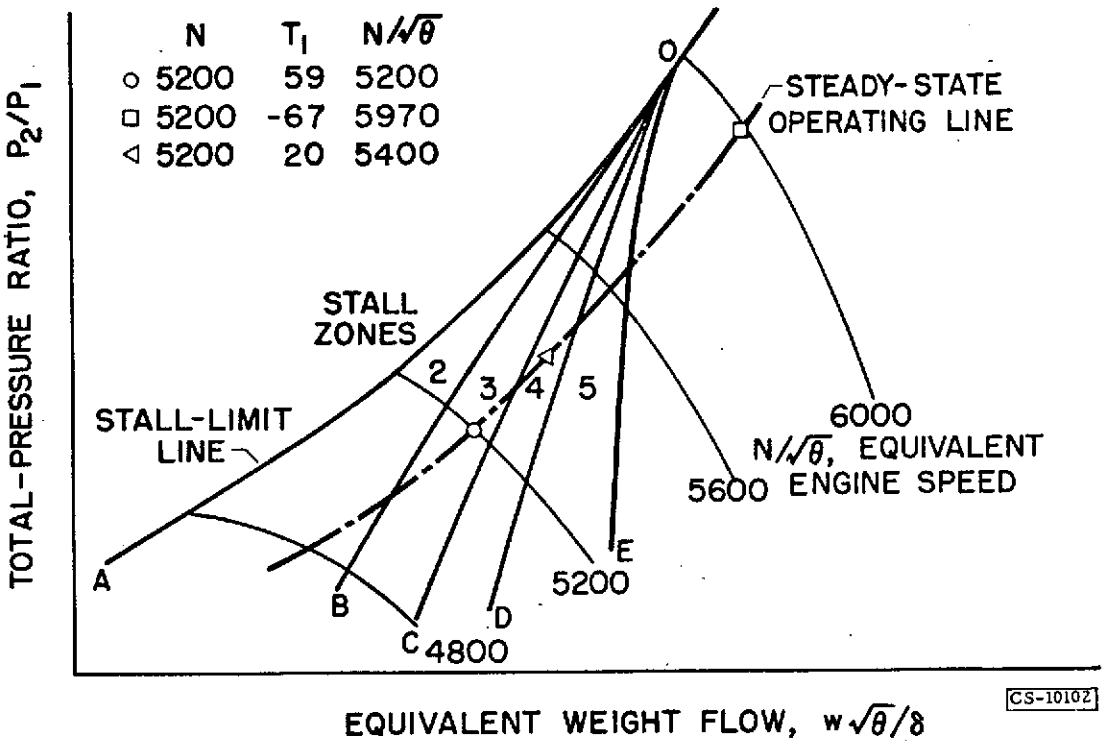

Figure 7. - Inlet temperature and stall.

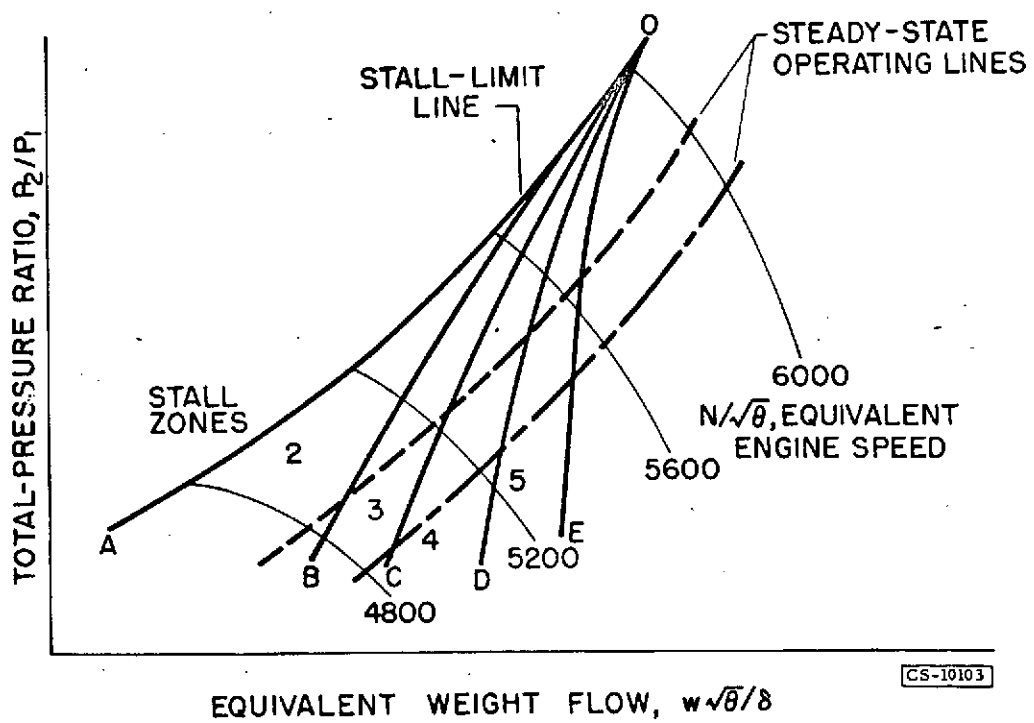

Figure 8. - Nozzle area and stall.

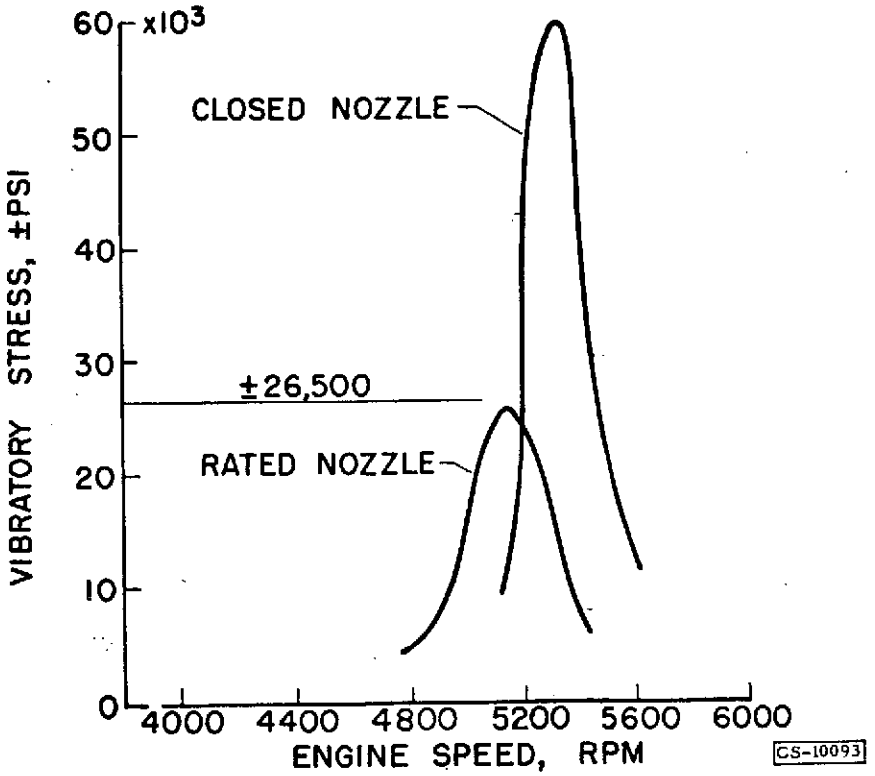

Figure 9. - Second-stage vibration due to rotating stall.

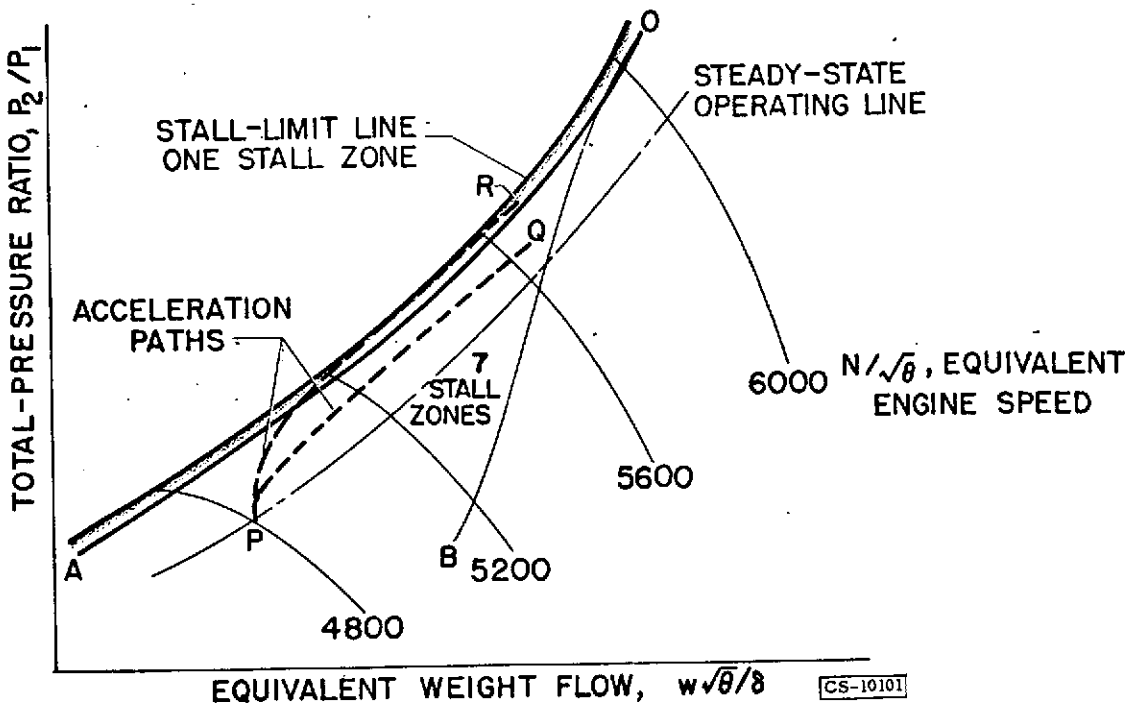

Figure 10. - Acceleration and stall.

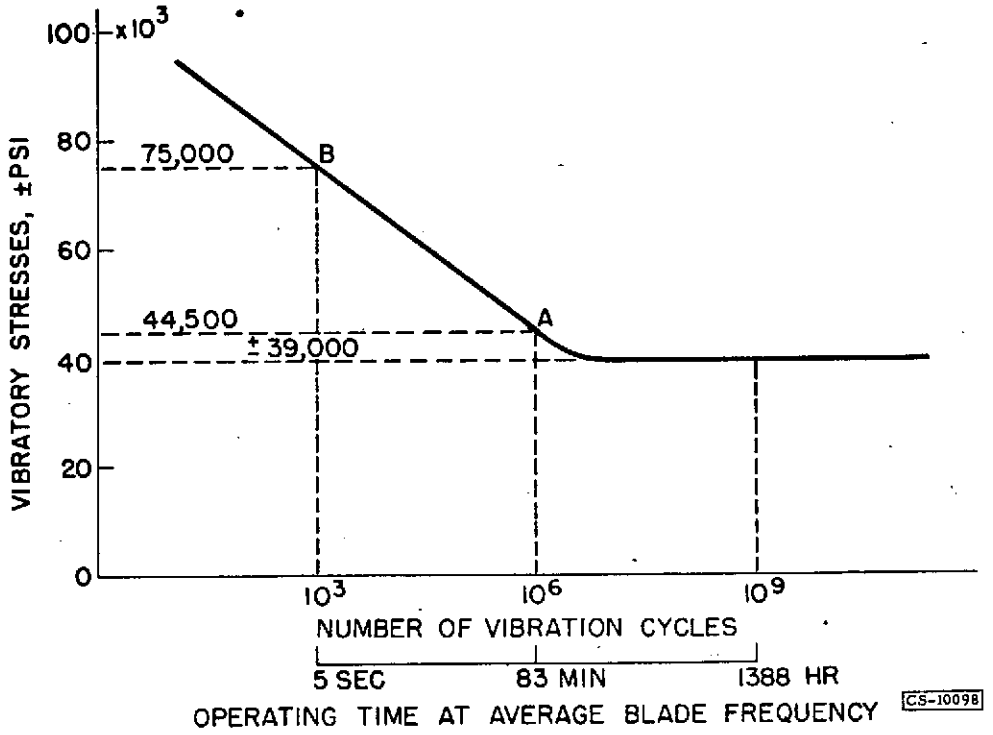

Figure 11. - Modified S-N curve.

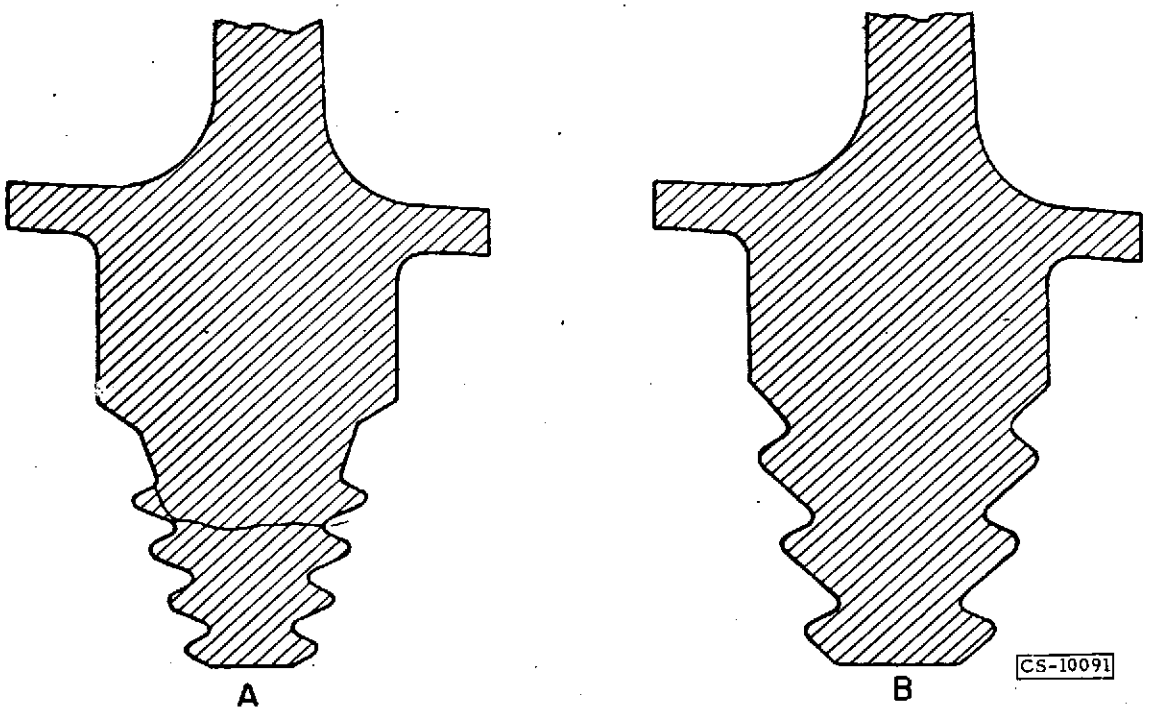

Figure 12. - Elimination of failure by root redesign.

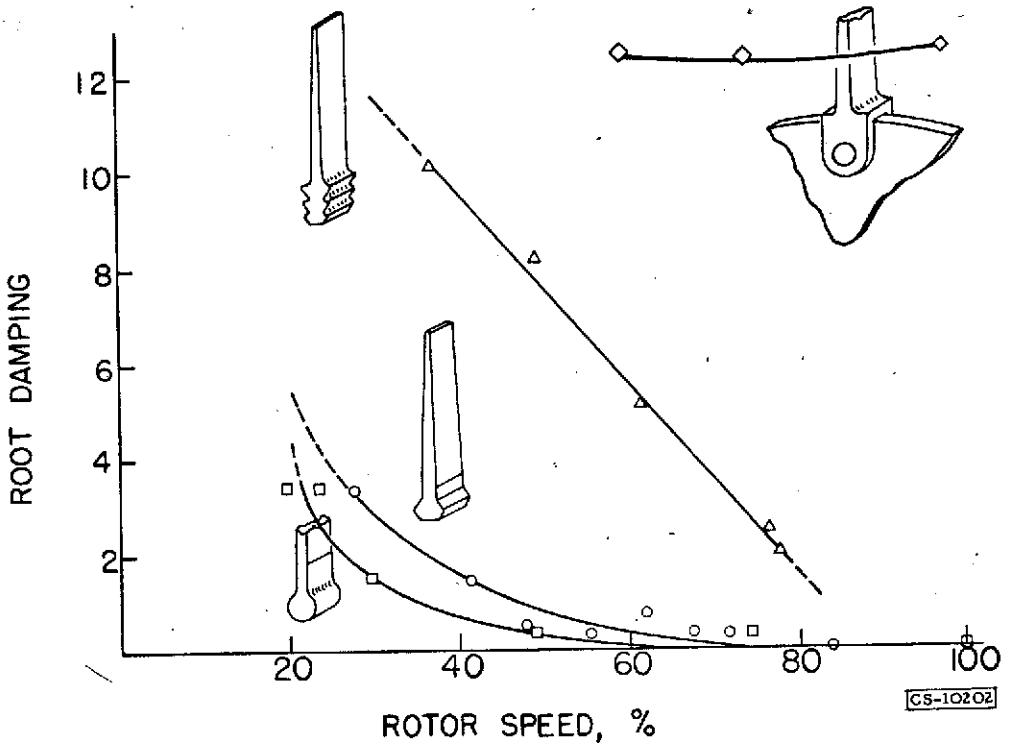

Figure 13. - Root damping for several designs.

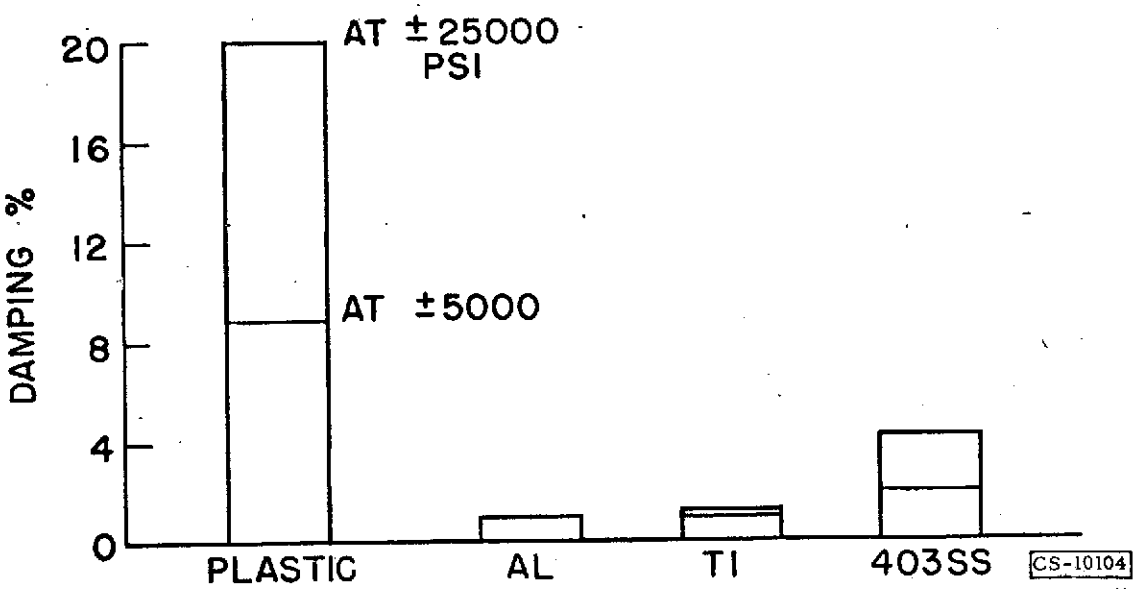

Figure 14. - Material damping.

III

INLET FLOW DISTORTION

by

D. D. Wyatt, L. J. Obery, T. G. Piercy, M. J. Saari

III - INLET FLOW DISTORTION

By D. D. Wyatt, L. J. Obery, T. G. Piercy, and M. J. Saari

INTRODUCTION

Typical total-pressure distortions observed in current subsonic and transonic airplanes and in duct model tests of projected supersonic airplanes and missiles are discussed herein. The results of some preliminary investigations into methods of reducing the distortion level at the engine inlet are also presented. The effects of inlet-flow distortions on turbojet-engine performance are not analyzed.

DISTORTIONS IN SUBSONIC AND TRANSONIC AIRPLANES

The military services and various airframe manufacturers have furnished the NACA with total-pressure distortions measured on several current subsonic and transonic airplanes. These data are presented on figures 1 to 3. An individual quantitative comparison between configurations should not be attempted inasmuch as the relative severity of the flight conditions represented by the various data is not known.

The distortions for two current Navy airplanes are shown on figure 1. The upper portion of the figure shows the total-pressure contours measured at the engine face. The contours indicate the variation in total pressure from the average value. For example, a 0 contour line represents the average pressure region in the duct. A -3 contour is a line of pressure 3 percent below the average value. A value of $\Delta P/P_{av}$ is indicated alongside each contour plot. This value will be referred to as the maximum distortion value for the duct flow and is the maximum total pressure minus the minimum total pressure divided by the average total pressure.

The left-hand contour indicates a flow that is essentially radial in character, that is, there are only minor distortion changes in a circumferential path around the duct at a constant radius. The right-hand contour, on the other hand, shows a circumferential as well as radial distortion of the flow. (In this case only half of the inlet contour is presented inasmuch as the engine is supplied air by two symmetrical inlets.) Pure circumferential contours without radial distortion are seldom observed.

In many cases insufficient instrumentation is available to determine the contour plot of the distorted flow. In such cases the total-pressure distortions are frequently measured and presented as profiles

of the flow field at the engine face. Two typical profiles for each of the airplanes are presented at the bottom of figure 1. One of the profiles shows the radial variation in total pressure from the accessory housing to the outer duct wall just ahead of the engine intake at an arbitrary circumferential location. The other profile shows the circumferential variation in total pressure at an arbitrary radius.

Only profile data are available for the Air Force airplanes for which distortion data are shown on figure 2. Although these airplanes had different inlet configurations and different flight conditions, the profiles are all qualitatively similar. The total distortions for the airplanes varied from 15 to 19 percent, with maximum pressures from 3 to 5 percent above the average value and minimum pressures 12 to 14 percent below average.

The distortion data presented in figure 4 for several nacelle-type bomber engine installations indicate that the symmetrical, short inlet systems produce flow distortions of about the same magnitude as those experienced in fighter planes. Total distortions of from 10 to 20 percent may be noted for these configurations.

These relatively meager distortion data available for currently flying subsonic and transonic airplanes indicate that total-pressure distortions of as high as 20 percent are being encountered, and not infrequently. It can generally be presumed that the air inlet configurations in this speed range should have little or no total-pressure loss from the free stream to the throat. Consequently, the total-pressure distortion at the throat of the inlet should be zero. The pressure distortions observed with subsonic configurations therefore probably arise in the subsonic diffuser passages between the throat and the engine inlet. In general it is believed that the source of the distortions lies in local separations, generally followed by reattachment, of the internal flow.

DISTORTIONS IN SUPERSONIC AIRPLANES AND MISSILES

Although it appears probable that flow distortions are internally induced in subsonic-inlet systems, such does not seem to be the primary cause of flow distortions at supersonic speeds. In the supersonic inlet the flow generally undergoes some degree of compression before entering the subsonic diffuser. This supersonic compression is seldom uniform across the whole face of the cowl and therefore results in a nonuniform velocity profile at the cowl inlet. The terminal (normal) shock system is thus of nonuniform strength and the air enters the subsonic diffuser in a state of considerable total-pressure distortion. The distortion may be considerably aggravated by further shock - boundary-layer interactions which are known to promote the tendency for separation.

As a result of the nonuniform compressions and the shock - boundary-layer separations in the supersonic inlets, the role of the internal diffuser passage is markedly different from that of the subsonic intake system. Instead of being required to maintain the characteristics of a good entering flow, the passage behind a supersonic inlet must correct a poor throat flow if low distortions are to be delivered to the engine face. This correction must be obtained by a mixing process within the subsonic-diffuser passage. During this mixing process the diffuser must not induce flow separations of the previously discussed subsonic type if low engine-inlet distortions are to be realized.

The variable nature of distortions from supersonic inlets is illustrated by the data on figure 4. The axially symmetric inlet is one of the proposed configurations for the B-58 bomber. The data are presented from quarter-scale model tests at Mach 2.0 for a range of mass-flow ratios at 0° angle of attack.

With critical inlet flow, the maximum total-pressure distortion was 10 percent. When the inlet mass flow was reduced to give subcritical operation, the distortion increased slightly to 13 percent. For the indicated nonuniform compression of the entering air flow a minimum theoretical distortion of 18 percent would be expected at the cowl inlet without considering shock - boundary-layer interaction. The lower measured distortion at the engine face indicates that some mixing has taken place between the cowl inlet and the engine inlet.

When the back pressure on the inlet was reduced to give supercritical flow (shock drawn into the subsonic diffuser), the distortion increased rapidly and for the condition presented reached a value of 30 percent. This increase in distortion level as the inlet becomes supercritical is a common characteristic of all inlets and illustrates the general advisability of avoiding supercritical operation.

Although the flow distortions of figure 4 are largely radial in character, the details of the contours change markedly as the mass-flow ratio is varied. With subcritical operation the highest energy air is located in the vicinity of the centerbody where the entering air flow has passed through both an oblique and a normal shock. As the mass flow is increased into the supercritical regime the high energy portion tends to move outboard and a layer of the lowest energy air occurs on the centerbody.

When the symmetrical nose inlet is operated at angle of attack, the character of the distortion changes from a pure radial to a mixed radial and circumferential type as shown by the data on figure 5. At positive angles of attack the compression is strongest on the undersurface of the compression cone. This high energy air enters the bottom of the cowl inlet but, due to inertia, flows across the centerbody and enters the

engine inlet in the upper quadrant. The magnitude of the distortion did not change appreciably for angles of attack up to 6°, however, it increased almost 300 percent for angle of attack changes from 6° to 10°.

As might be anticipated, side inlets rarely display a symmetrical, purely radial, discharge profile at any operating condition. As illustrated by the data of figure 6, the discharge profile can generally be related to the inlet compression nonuniformities and to the expansion and turns inherent in the internal ducting. The configuration of figure 6 was a ramp-type inlet with a semicircular cowl. The inlet was located on the upper portion of a roughly triangular fuselage with base down. The relative positions of the inlet and the discharge duct are indicated by the dotted inlet lines superimposed on the discharge contour plots.

For this particular installation the magnitude of the total-pressure distortion did not change appreciably through the angle of attack range up to 12°. The high energy residual core, from 11 to 12 percent above the average value, moved counterclockwise as the angle of attack was increased, however. At 0° angle of attack this high-energy core was located directly downstream of the cowl inlet, indicating that the inertia of the entering air flow resisted the turn into the inboard side of the discharge duct. As the angle of attack increased the upper cowl portion received the greatest supersonic compression as a result of reflected cowl shocks and a concurrent expansion around the lower cowl corner. The inertial resistance to turning therefore caused the high-energy core to move in a counterclockwise direction. It should be noted that at angle of attack operation a portion of the duct flow remained separated back to the diffuser discharge as indicated by the shaded portions of the duct.

The ramp compression surface of the configuration on figure 6 initially turned the air outboard from the fuselage and hence accentuated the curvature of the duct floor. The inlet configuration shown on figure 7 incorporated a compression surface outboard of the fuselage. This scoop-type inlet, therefore, initially directed the air toward the fuselage centerline and reduced the amount of internal duct curvature. At critical operating conditions the total-pressure distortion at the engine inlet was not appreciably less than that of the side inlet configuration of figure 6, indicating that the final distortion is predominantly a residue of the badly distorted inlet flow rather than the result of a flow breakdown inside the diffuser. When this inlet was operated subcritically the terminal shock wave interacted with the fuselage boundary layer and reduced the total pressure of the entering air near the fuselage. This low pressure air flowed rearward in the duct and appeared at the engine face as a reduced pressure region near the top of the duct. When the inlet was operated in the supercritical range

the lowest pressures appeared near the bottom of the duct. The large magnitude of distortion for this regime again indicates the desirability of avoiding supercritical operation of supersonic inlets.

Not all side inlets have large distortions. Data are shown on figure 8 for a twin-inlet configuration having ramp inlets mounted on the sides of the fuselage and feeding a common engine. This inlet had an adjustable ramp to improve engine-inlet matching and the conditions indicated correspond to the scheduled engine-inlet operating condition. At each Mach number there was a high-energy core discharged from each duct into the engine face. The magnitude of the distortion was comparatively low, however. At subsonic flight speeds the maximum distortion was only 6 percent and the level rose only slightly at supersonic speeds.

A study of the maximum total-pressure distortions from a number of supersonic side-inlet configurations showed that the magnitude of distortion at critical operating conditions varied widely. If the analysis of the supersonic-inlet distortion problem given earlier is correct, this distortion is predominantly a result of incomplete mixing of the distorted throat flow. Although the amount of distortion at the throat would be expected to vary with different inlet configurations the internal mixing-passage length should have some correlating effect on the observed distortions. Figure 9 presents the results of such an attempted correlation.

Figure 9 includes the maximum distortions measured for a number of supersonic side-inlet configurations at critical flow conditions and at 0° body angle of attack plotted as a function of the internal-passage length-diameter ratio of the configuration. The diameter in the abscissa is the equivalent hydraulic diameter of the minimum throat passage area.

Although the data of figure 9 scatter, there is a definite trend of reduced critical flow distortion as the mixing length of the subsonic passage is increased. This trend is indicated on the figure by the solid curve. The configurations represented include a wide variety of inlet types and degrees of curvature of the subsonic ducts. Test Mach numbers vary from 1.5 to approximately 3.0. The fact that the data follow a definite trend in spite of these differences further substantiates the reasoning that the major cause of distortion in supersonic inlets lies ahead of the subsonic diffuser and is more or less common to all inlets at all supersonic speeds.

METHODS OF REDUCING DISTORTION

Supersonic inlet data cited thus far tend to show that low values of engine-inlet flow distortion can only be expected when the entering

air flow has had adequate opportunity to mix. Several recent preliminary experimental investigations have been undertaken at the NACA Lewis laboratory to determine the utility of several obvious methods of improving the mixing process between the inlet throat and the engine face. The effectiveness of several methods of adding mixing length is shown on figure 10.

Two inlet configurations having different subsonic diffuser lengths were investigated at Mach 3. For simplicity the diffusers are designated long and short on figure 10 although both were considerably longer than current airplane practice allows. A straight discharge section was located downstream of each diffuser so that the relative merits of mixing length during and after diffusion could be evaluated. The abscissa on the figure represents the over-all length to the point of distortion measurement divided by the inlet hydraulic diameter.

The short diffuser had a total distortion of 16 percent at its discharge. As straight sections were added after diffusion this distortion decreased rapidly. The long diffuser had an initial distortion of only 12 percent and the addition of straight sections reduced this value at the same rate as for the short diffuser. Although the distortion following diffusion was lower with the long diffuser, indicating the effectiveness of the additional flow passage length, for a corresponding over-all length the short diffuser plus straight section had the lower distortion. This is qualitatively explainable from mixing considerations. The maximum shears in the fluid are obtained at the lowest mean fluid velocity. In the length-diameter range from 11 to 14.5 the flow Mach number in the short diffuser is at a minimum value, whereas the Mach number is still decreasing in the long diffuser. The increased shearing action in the short-diffuser straight-section combination was therefore more effective than the lesser shear over the same path length in the long diffuser.

The mixing process can be accelerated if some sort of forced mixing device is inserted into the air stream. Figure 11 shows the distortions resulting from the use of full-passage screens of varying solidity. The abscissa indicates the length of straight section downstream of the screen location and hence the figure shows the combined effect of screens and straight sections. These data were obtained using the short diffuser of the preceding figure. With no screen (0 solidity) the distortion curve therefore corresponds to the short diffuser curve of figure 10.

The use of screen blockage to force mixing markedly reduced the distortion level of the diffuser system. The observed distortion decreased as the blockage factor was increased until with 40 percent blockage the distortion was reduced to 5 percent at one-half diameter downstream of the screen (located at the end of diffusion) as compared

with 13 percent distortion at the same station for the unblocked flow. These reduced distortions were, of course, obtained at the expense of over-all total-pressure losses in the duct. The pressure losses were found to be approximately those predicted from screen theory for uniform inflow.

Another method of forced mixing that has been theoretically investigated is summarized on figure 12. This method uses a freely rotating fan stage to interchange flow energy differences due to distortion. The figure shows the axial Mach number and total-pressure leveling that can theoretically be achieved with a single stage and a contrarotating two-stage fan for an arbitrarily assumed initial radial distortion. An initial total-pressure distortion of 17 percent was assumed in the form of a linear Mach number distribution from hub to tip at a mean Mach number of approximately 0.5. The 17 percent total-pressure distortion could be reduced to about 9.5 percent with a single blade row and to about 2 percent with the contrarotating blade rows (with no intervening stators). Within the limitations of the analysis there would be no net loss in total pressure across the fan. This point, as well as the action of the fan on circumferential distortions, awaits experimental verification.

The proposed methods of promoting mixing in the duct flow all have undesirable aspects. Either they would increase the installation weight and reduce the useful volume inside the aircraft or they would add undesirable pressure losses in the induction system. Methods of reducing inlet distortion without these undesirable aspects are obviously needed. If, as proposed, the main source of distortion in supersonic inlets lies in the nonuniform compression and shock - boundary-layer interaction in the supersonic portion of the inlet, then attempts to improve the local flow structure in this region should be rewarding. Several research efforts which indicate that this method of approach may be fruitful are illustrated on figures 13 and 14.

Figure 13 shows improvements in flow distortion obtained with the short diffuser configuration as a result of bleeding the boundary layer from the throat and of refairing the compression surface centerbody. As measured at the station at the end of the diffuser, the use of throat bleed resulted in nearly a 50 percent reduction in distortion. Somewhat lower percentage reductions were measured in the straight section following the diffuser.

The centerbody was refaired by raising the after portion from the floor of the diffuser into the duct passage. The mechanism by which this improved the distortion is not understood, but a reduction of more than 50 percent was obtained.

Other experiments with the removal of internal boundary layer are shown on figure 14. This inlet was a ramp-type configuration mounted underneath a body of revolution with a flattened section approaching the inlet. Provision was made for the removal of the fuselage boundary layer by a diverter system. In addition an internal adjustable scoop was provided for the removal of boundary layer accumulating on the ramp surface. The height h of this internal scoop is plotted as the independent variable in the figure. With the scoop closed, critical flow distortions of from 15 to 20 percent were measured over the Mach number range from 1.5 to 2.0. When the scoop was opened to about 14 percent of the throat height the distortions were reduced to the order of 4 to 7 percent. As a consequence of the removal of the disturbed air behind the shock - boundary-layer interaction, the pressure recovery of the inlet was increased, thus compensating for the drag loss due to bleeding the mass flow.

CONCLUDING REMARKS

This analysis of typical inlet flow distortions shows that large distortions may be encountered at subsonic as well as supersonic speeds. The principal sources of the distortions are believed to be different in the two speed ranges, however, so that research results applicable to one may not constitute a solution to the other. For subsonic airplanes the principal need seems to be a better understanding of the effects of passage shape variables on the introduction of low energy filaments into the flow. While these results have application to supersonic inlet systems, the principal need in the latter case appears to be a better understanding of the local details of the supersonic compression region with a view towards an improved uniformity of this flow.

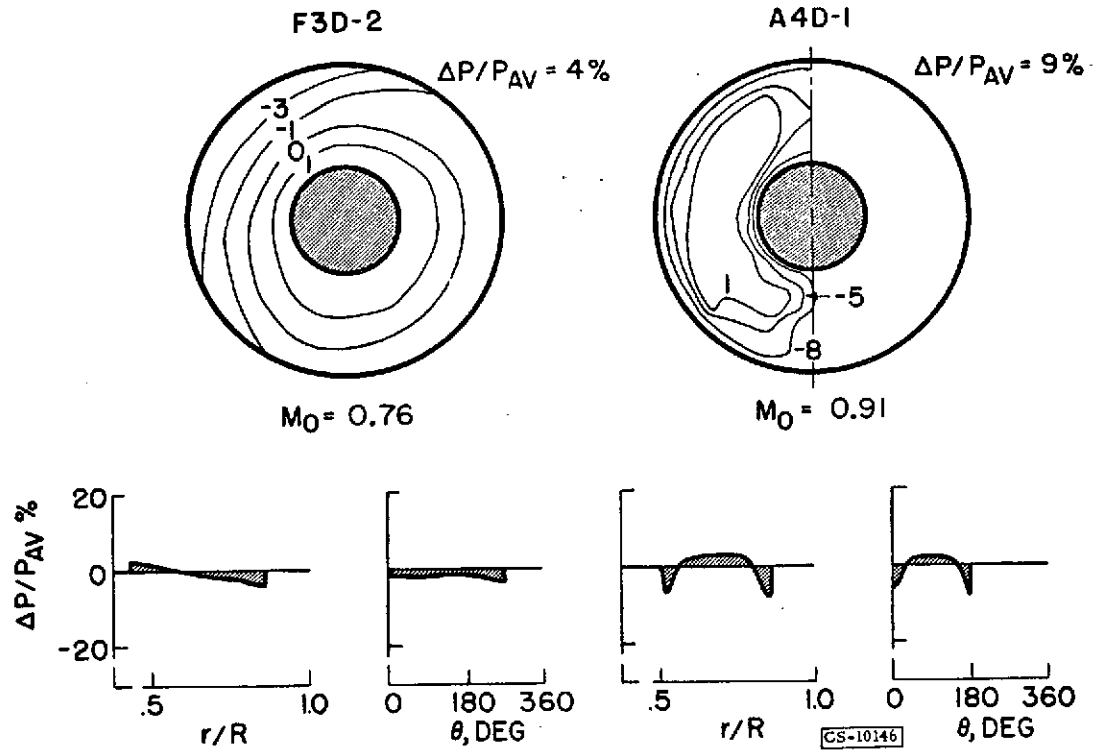

Figure 1. - Engine inlet flow profile for current airplanes.

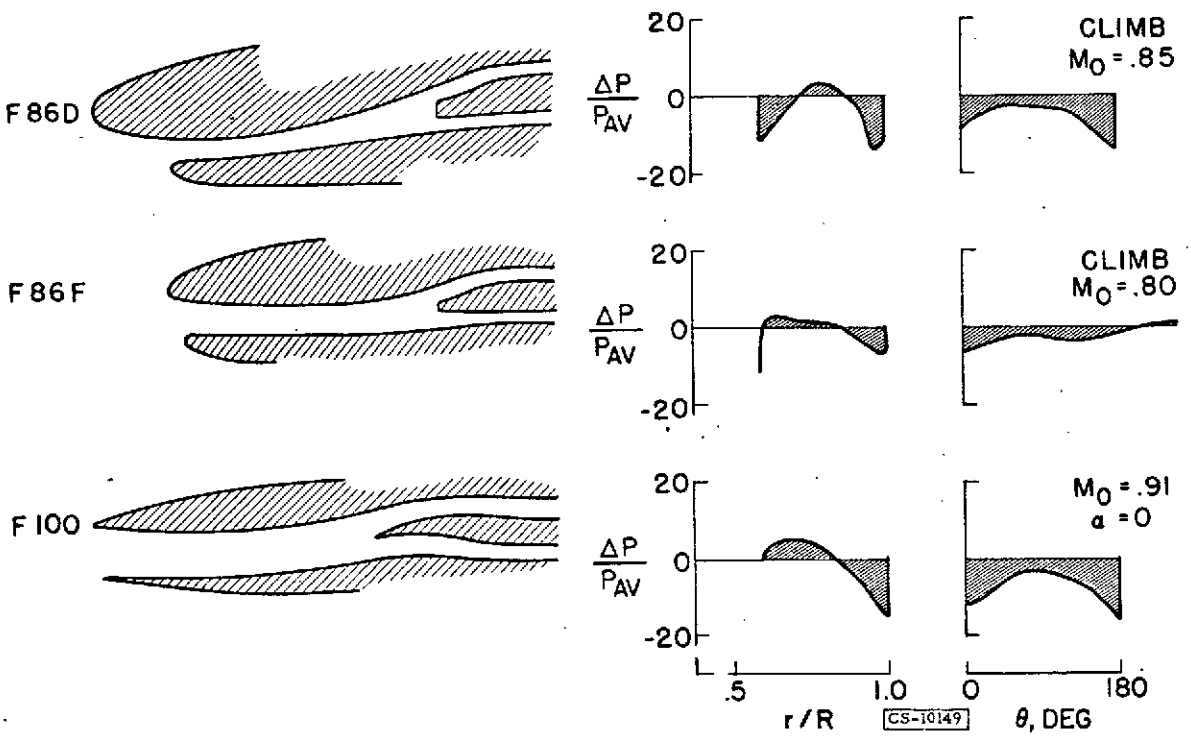

Figure 2. - Engine inlet profiles for current airplanes.

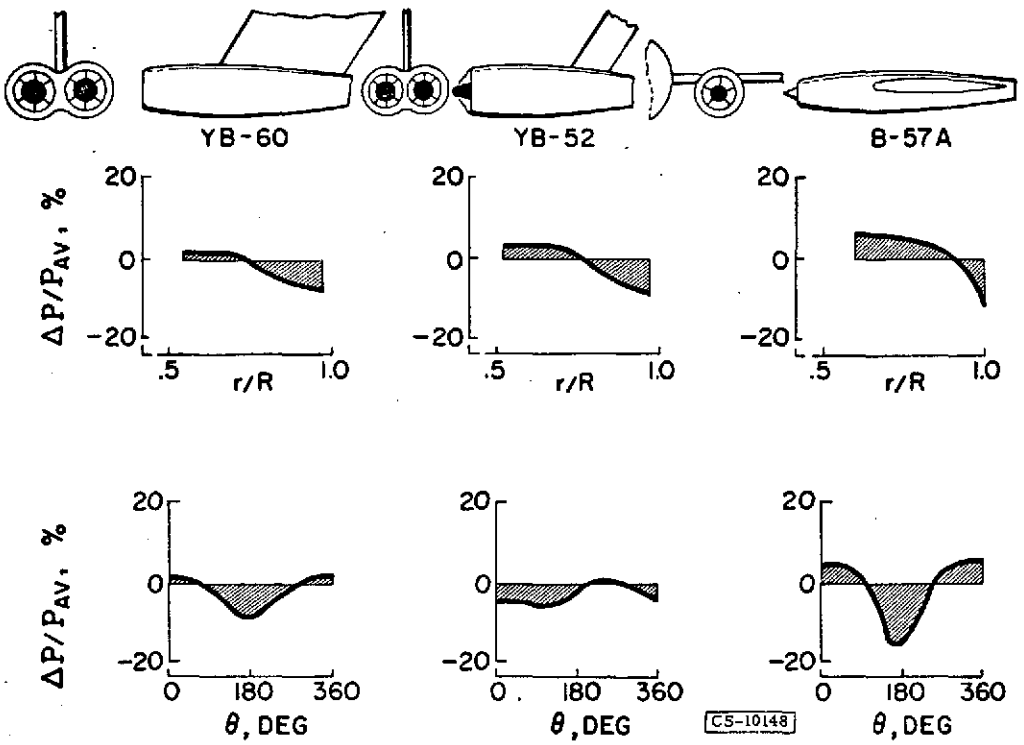

Figure 3. - Engine inlet flow profiles for current airplanes.

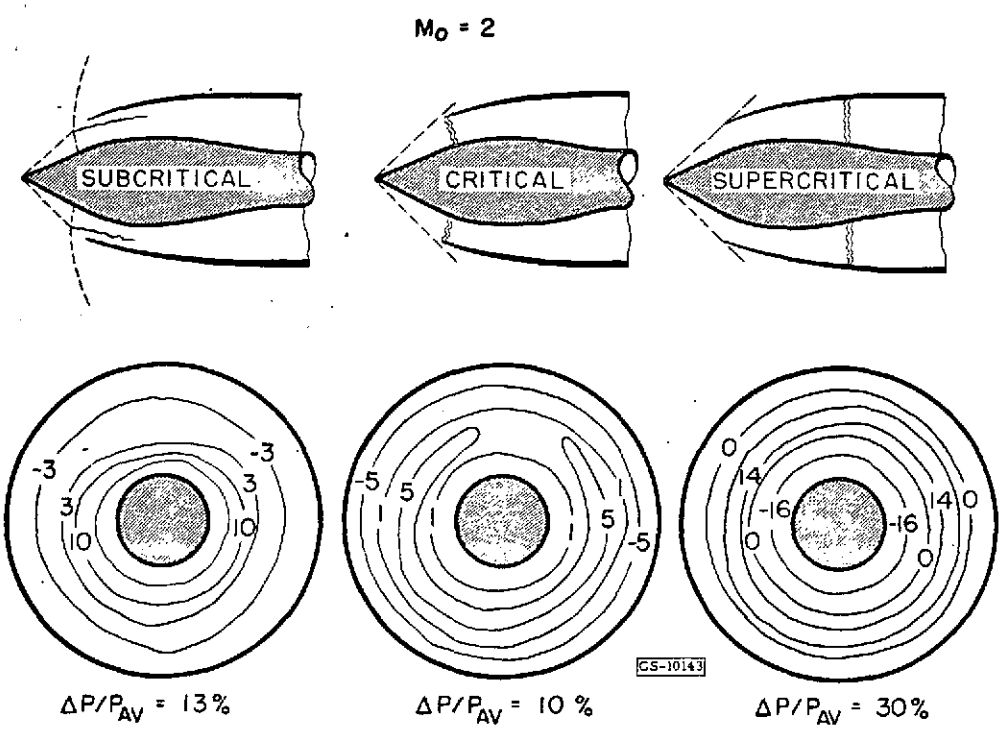

Figure 4. - Effect of mass flow ratio for nose inlet, B-58 nacelle.

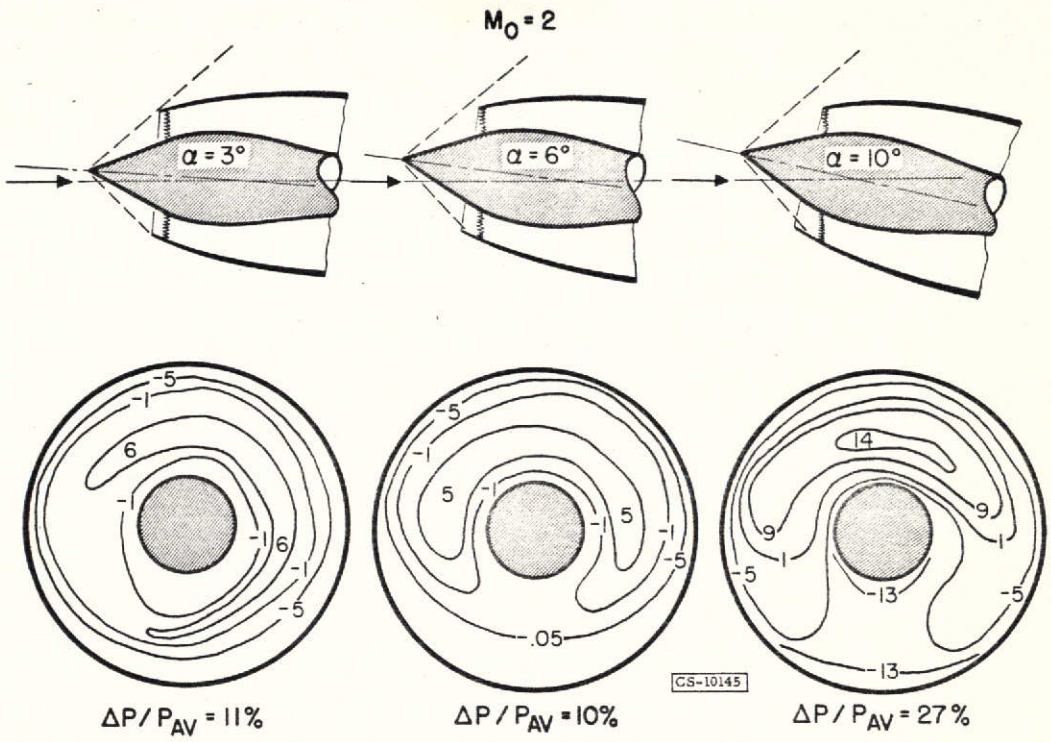

Figure 5. - Effect of angle of attack for nose inlet, B-58 nacelle.

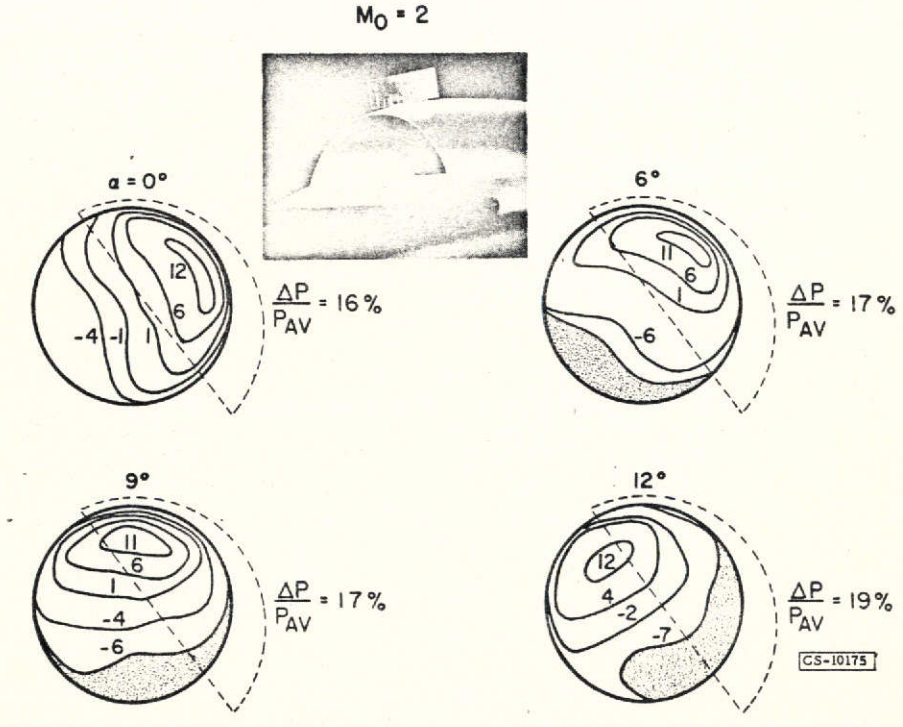

Figure 6. - Diffuser discharge contours for X-3 airplane with ramp inlet.

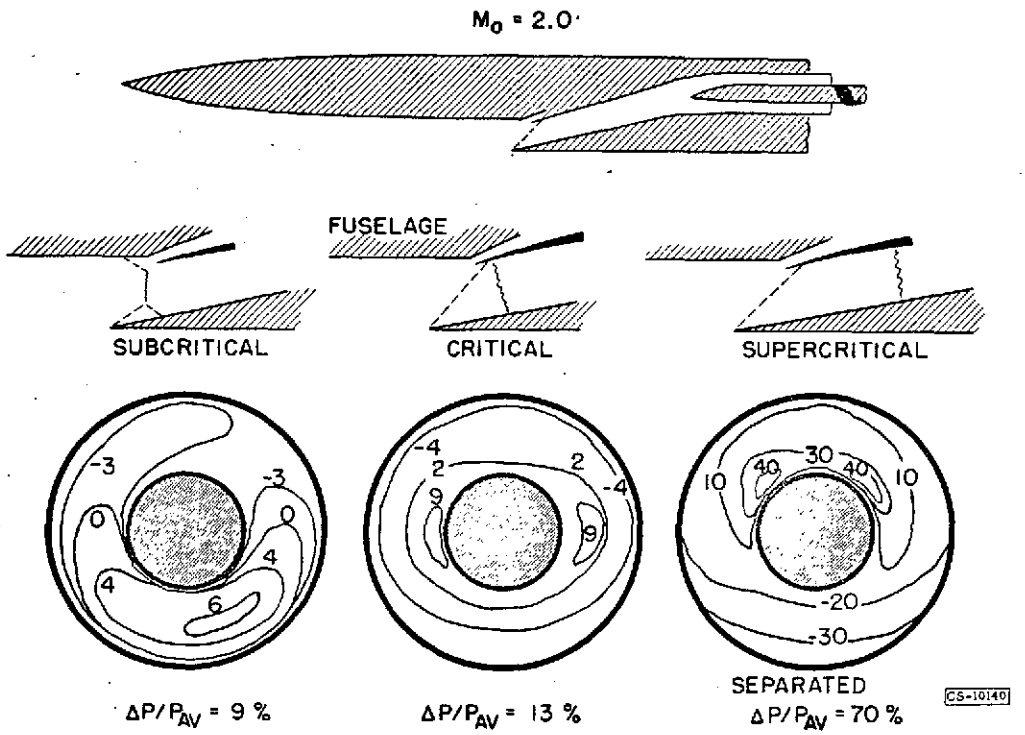

Figure 7. - Effect of mass flow ratio on scoop type inlet, Regulus missile.

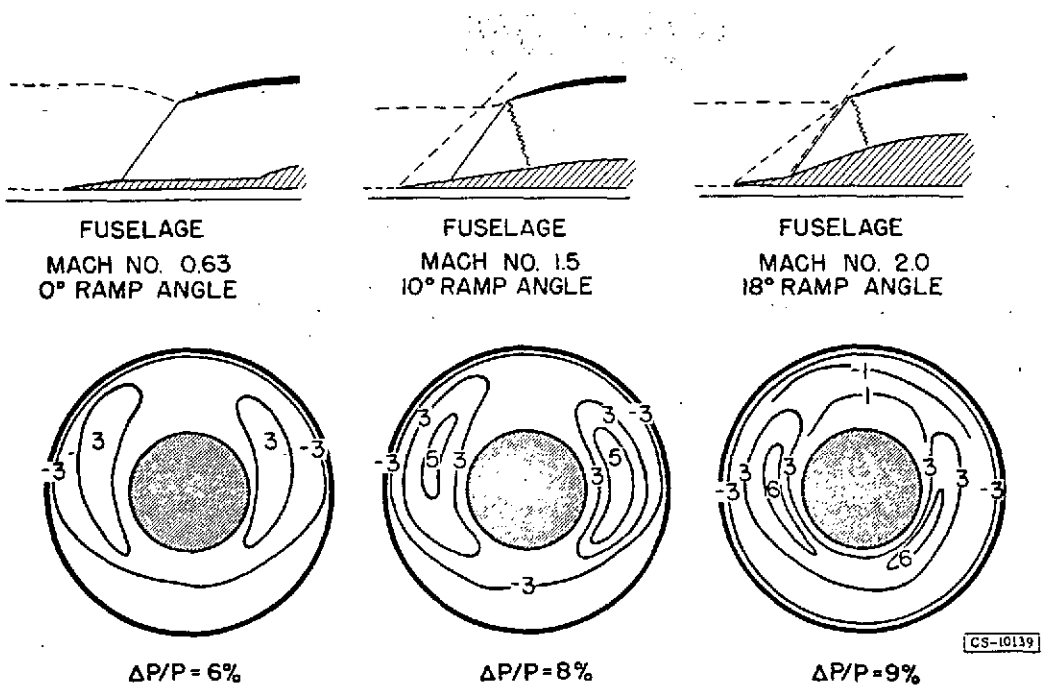

Figure 8. - Effect of flight mach number, F-102 airplane.

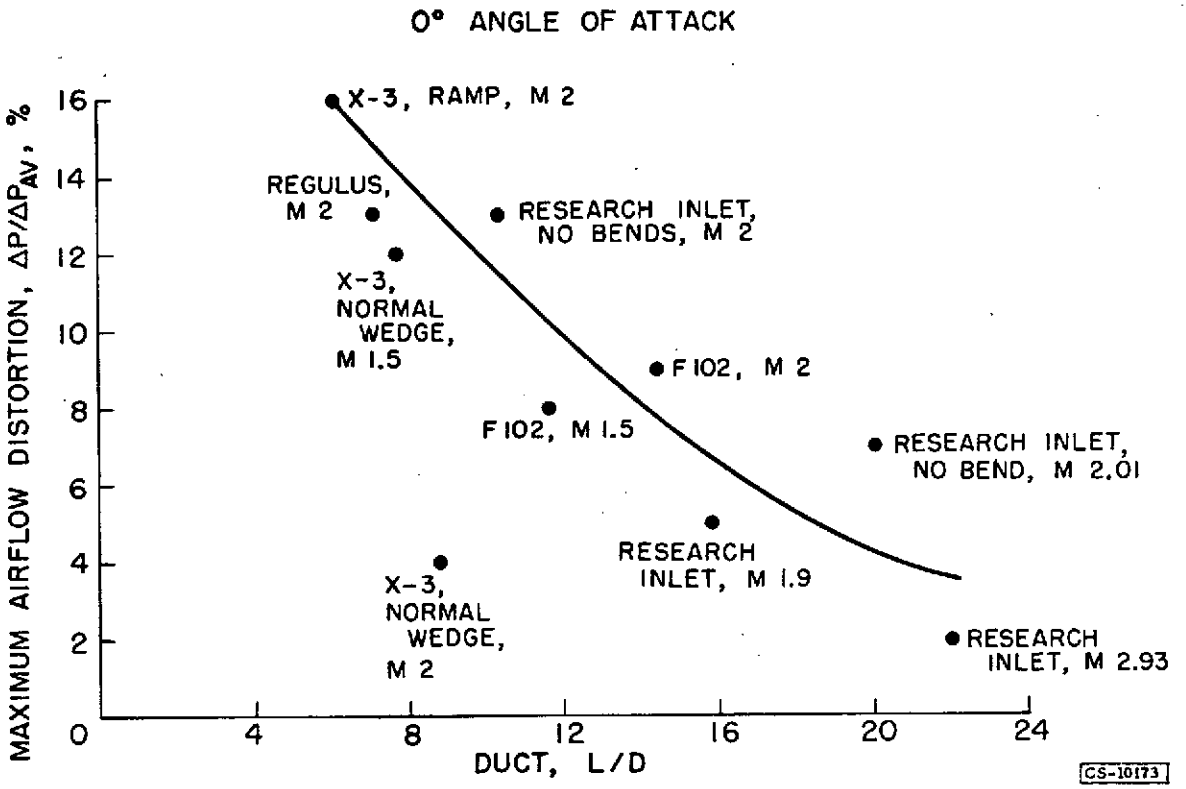

Figure 9. - Influence of diffuser length on distortion with side inlets.

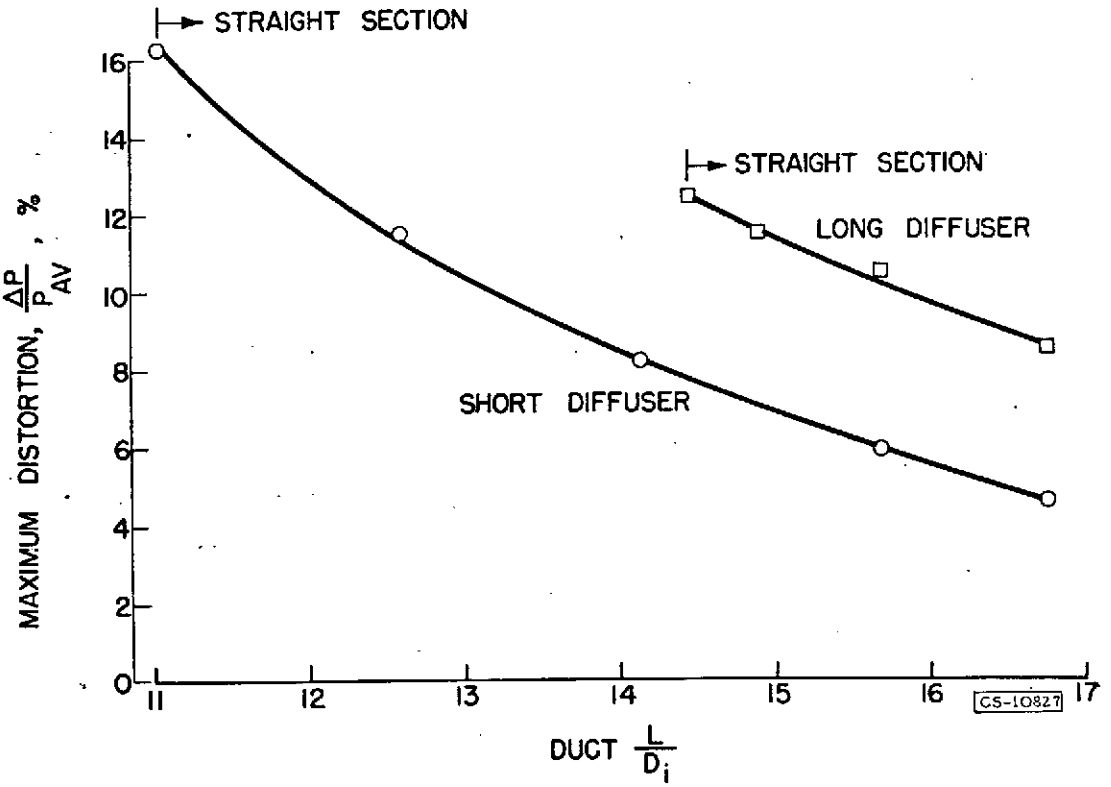

Figure 10. - Effect of length on distortion.

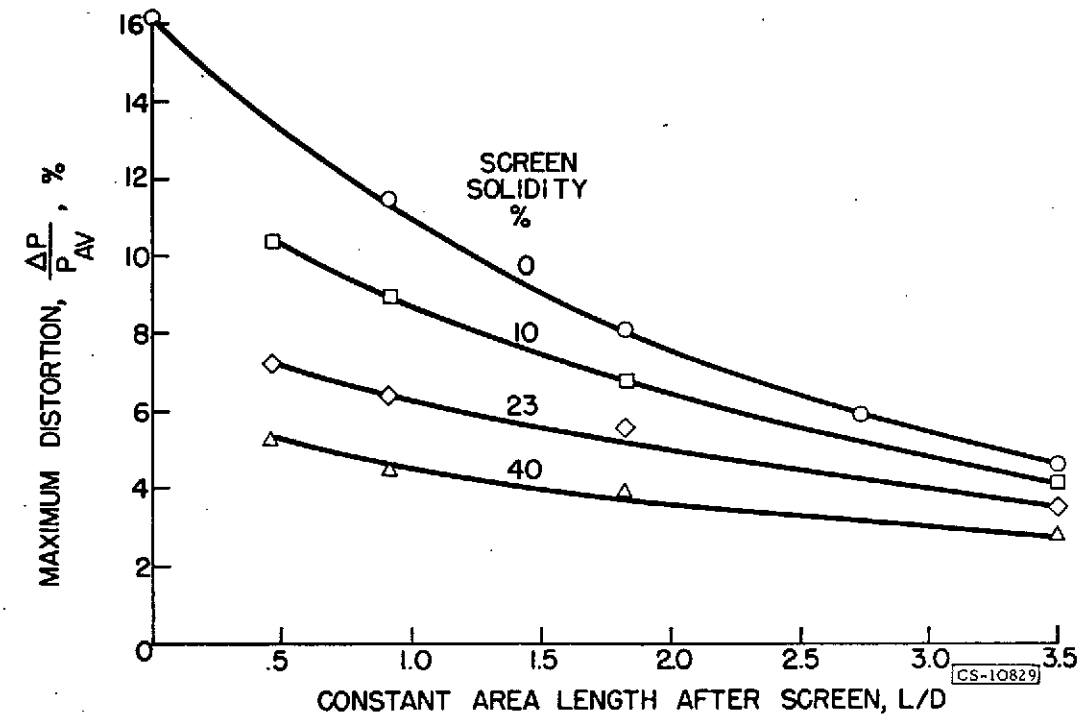

Figure 11. - Effect of screens on distortion.

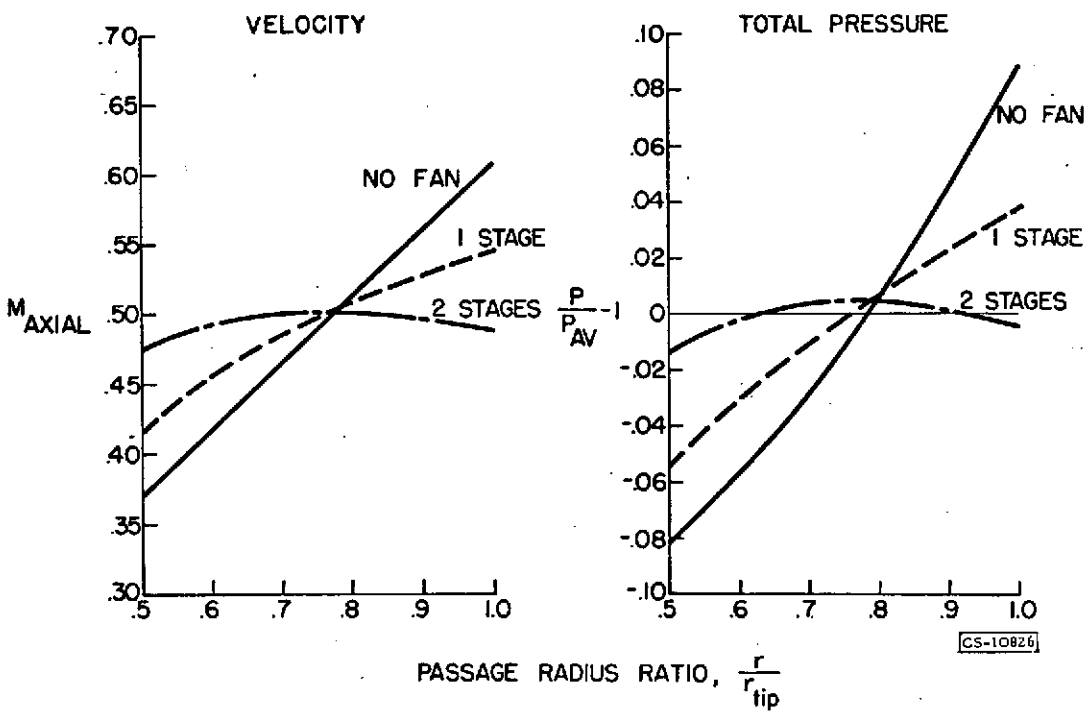

Figure 12. - Effect of fan on radial distortion (theoretical).

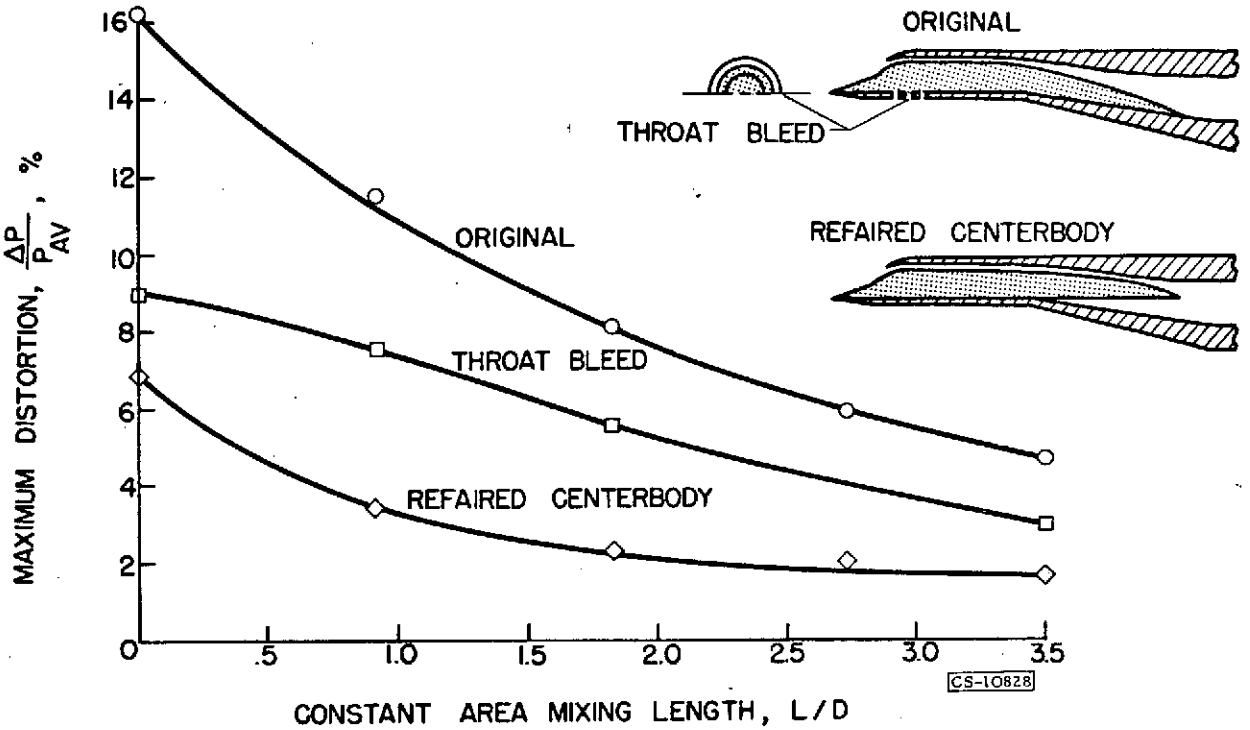

Figure 13. - Effect of diffuser alterations on distortion.

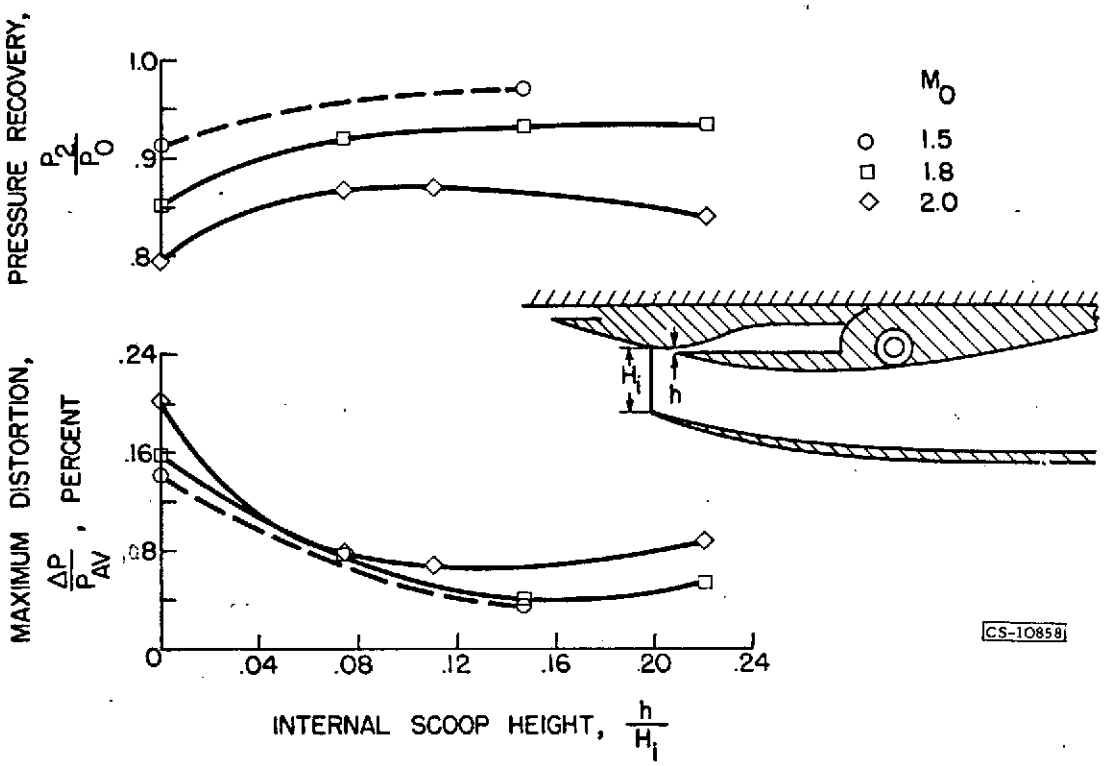

Figure 14. - Distortion reduction by throat bleed.

IV

EFFECT OF DISTORTION ON PERFORMANCE

by
W. A. Fleming, B. T. Lundin

IV - EFFECTS OF INLET-PRESSURE DISTORTIONS ON TURBOJET ENGINE PERFORMANCE

By W. A. Fleming and B. T. Lundin

The effects of inlet-pressure distortion on the performance of turbojet engines has been under investigation at the Lewis laboratory for the past 3 years. This work has been carried out on five different types of engine, over a considerable range of flight and engine operating conditions and with many different types of pressure-distortion pattern. A brief review of some of the highlights and more general aspects of this work is presented in the following discussion.

As discussed in the preceding paper, the pressure fields existing in representative engine-inlet ducts may be considered as distorted, or uneven, in both a radial and a circumferential direction. For purposes of studying their effects on engine performance and operating characteristics, however, radial and circumferential components of these distortions were, for the most part, investigated separately. The magnitude of the pressure difference and the extent of the distortion across the inlet passage used for the engine investigations simulated, of course, those existing in most inlets.

The pressure distortions at the engine inlet were produced by screens installed in the engine-inlet duct. The screen arrangements used and some typical radial and circumferential distortions produced are shown in figure 1. The radial distortions were produced by an annular section of screen in the duct and the circumferential distortions by segments of screens of varying density. The screens were installed from 1 to 3 feet ahead of the compressor inlet. Typical pressure distortions are shown in the lower part of this figure as a plot of local total pressure across the blade height from hub to tip for the radial distortion and around the circumference from 0° to 360° for the circumferential distortion. The magnitude of the distortion is expressed in the same manner as in the previous paper, that is, as the difference between the highest pressure at any point minus the lowest pressure at any point divided by the average pressure.

Four general and closely related aspects of distortion effects on engine performance will be briefly reviewed:

(1) The extent to which inlet pressure distortions persist through the engine

(2) The effect of distortions on steady-state engine performance

(3) The manner in which distortions affect the compressor stall and engine-surge limits

(4) The effect of distortions on engine altitude limits

Extent Distortions Persist Through Engines

The degree to which a radial pressure distortion persists through an engine is illustrated in figure 2. Shown here are radial surveys of total pressure at the compressor inlet, at the fourth stage, and at the tenth stage of the compressor. It is apparent that the substantial radial pressure distortion at the inlet has disappeared by the exit of the fourth compressor stage. No effect of the distortion on the pressure or temperature profiles in the combustor or turbine would therefore be expected. The lower inlet pressure at the tip regions of the early compressor stages would, however, considerably increase the blade loadings in this region, which, as shown later, has a very considerable effect on the stall limits of these stages and on the stage-matching characteristics of the complete compressor.

A similar examination of the extent of an inlet circumferential distortion through an engine is shown in figure 3. Circumferential pressure surveys at the compressor inlet and at the compressor outlet are shown in the upper part of the figure, and corresponding temperature surveys at the compressor inlet, compressor outlet, and at the turbine outlet are shown in the lower part of the figure. Examining first the pressure data, it can be seen that a 20 percent variation in pressure at the compressor inlet is attenuated to only 3 or 4 percent at the compressor outlet. Thus, the compressor essentially pumps up to a common pressure around the circumference. It is to be noted, however, that the segment of the compressor directly behind the low inlet pressure region operates at a considerably higher over-all pressure ratio than does the segment behind the high inlet pressure region. For the case presented in figure 3, the part of the compressor where the inlet pressure was low operated at a pressure ratio some 8 percent above the average and about 16 percent above the pressure ratio of the portion of the compressor where the inlet pressure was high.

The temperature distribution at the compressor inlet is, of course, uniform. As a result of the varying over-all pressure ratio across the compressor in a circumferential direction, there is a 6 percent circumferential variation in compressor-outlet temperature. In addition to this variation in compressor-outlet temperature, a distorted, or uneven, temperature rise also occurs circumferentially around the combustor because of the circumferentially uneven air-flow rate arising from the variations in compressor outlet pressure and temperature and the uniform fuel-flow rate to the combustor. This variation in combustor-inlet

temperature and combustor temperature rise combine to produce a considerable temperature profile at the turbine outlet. As shown by these data, the normal 120° peak to peak turbine outlet temperature variation for this engine was increased to 280°. Thus for the same average turbine-outlet temperature the peak turbine-outlet temperature was increased from 1340° without inlet distortion to about 1450° F with the 20 percent circumferential inlet-flow distortion.

Effect of Distortions on Steady-State Performance

The increase in local turbine temperature discussed above will, of course, have little effect on the turbine rotor but has, during distortion investigations, resulted in local over-heating and failure of turbine stators. To avoid these failures, it is necessary to derate, or reduce the average turbine temperature sufficiently to bring the peak local temperature down to the normal safe level. The amount of this temperature derating, and the accompanying loss in net thrust, is shown in figure 4 for a range of inlet-pressure distortions and for four different engines. For the range of conditions investigated, temperature reductions of between 50° and 125° have been necessary, the general magnitude increasing, of course, as the inlet distortion is increased.

Reducing the turbine-outlet temperature by these amounts, either by decreasing engine speed or opening up the exhaust nozzle, results in a 5 to 10 percent loss in net thrust at this flight Mach number of 0.8. It should also be noted that the temperatures considered here are those at the turbine-outlet, and even more severe temperature profiles would be present at the turbine inlet. The temperature reductions shown here are, therefore, nonconservative and the thrust losses correspondingly optimistic.

Effect of Distortions on Compressor Stall Limits

The third aspect of the distortion problem is the effect of inlet-pressure distortions on compressor-stall limits. If the compressor-stall limit is reduced, there will result, of course, a reduction in the acceleration capacity of the engine, a reduction in the range of speeds over which the engine can operate, and a lowering of the maximum altitude limit. The effects of a given inlet distortion on the compressor-stall limit will also have an increasingly serious effect on the engine operation as the altitude is increased because of the normal Reynolds number effects on the basic compressor performance.

A rather typical effect of a circumferential-inlet distortion on the stall limit of a compressor is shown in figure 5. The circumferential distortion for these data varied from 17 to 32 percent over the

range of engine speeds investigated. As shown here, it is generally found that the steady-state operating line of an engine is essentially unaffected by the distortion. The acceleration margin between the steady-state line and the stall-limit line was greatly reduced by the distortion and, in this case, the two curves intersected, resulting in a maximum speed limit at about 108 percent of rated speed. This corrected speed of 108 percent corresponds to engine operation at rated mechanical speed at an inlet-air temperature of -15° F.

It was previously indicated that under these conditions of circumferentially uneven inlet pressure, one portion or segment of the compressor is operating at a higher pressure ratio than another segment. It may be possible, for example, to have a high pressure ratio across the top half of the compressor and a low pressure ratio across the bottom half. In this case, when the pressure ratio across the top portion, which is the high-pressure-ratio region, reaches the normal stall limit of the compressor, the whole compressor stalls, even though the bottom portion is operating at a low pressure ratio. Thus, in figure 5, the stall limits shown by the square points are the average pressure ratios; part of the compressor is operating at the pressure ratios of the normal stall limit shown by the dashed curve, and part of the compressor is operating at correspondingly lower pressure ratios.

This situation is shown somewhat more directly, and for several different engines, in figure 6. The solid curves in this figure are the stall-limit lines of the compressors of the different engines with a uniform inlet flow. The data points, on the other hand, are the maximum local pressure ratios at which compressor stall occurred with a circumferential inlet-pressure distortion. As previously noted, these local pressure ratios are higher than the average pressure ratios, with the difference being in direct proportion to the amount of the inlet distortion. The ordinate scales for these three curves have been separated slightly for clarity of presentation. The very good agreement between the local maximum pressure ratios with distortion and the normal stall limit with uniform flow reveals that whenever any portion, or segment, of the compressor reaches its normal stall limit, the compressor can no longer maintain a pressure rise and the whole compressor stalls, even though part of it is operating at a much lower pressure ratio. Similar considerations apply to both single and two-spool compressors. The data presented here cover pressure distortions from 6 to 32 percent, of both abrupt and more gradual, or sinusoidal, shapes and with the low-pressure region extending from 60° to 180° of the inlet circumference. It is, of course, quite possible that this agreement between maximum local pressure ratio and the normal stall limit of the compressor will not hold for distortions of smaller extent than 60° of circumference or for some of the more complex types of distortions that may exist in aircraft ducts. It does, however, provide a good understanding of the gross effects of the distortion on the compressor performance and affords a useful method of predicting the stall limits of a compressor with an inlet-flow distortion that is predominately circumferential in nature.

Compared to these effects of a circumferential distortion, the mechanism by which a radial distortion affects the stall limits is rather complex, and no simple concept is available at present to indicate the magnitude or permit the prediction of their effects. One effect of a radial distortion on the stall limits of an engine is, however, presented in figure 7. The solid curve represents the steady-state operating line, and the two dashed curves the stall-limit lines with and without the inlet distortion. The shaded area of this figure indicates the regions of operation in which steady-state rotating stall occurred. Two effects of the radial distortion are immediately apparent. First, the stall-limit line throughout the entire speed range is lowered and, secondly, the region of rotating stall is extended to higher speed regions, with the knee in the stall line moved nearer the steady-state operating line. There is thus a decrease in the stall margin, or acceleration capabilities, of the engine throughout the speed range, especially in the intermediate speed region. The extension of the rotating-stall region to higher speeds has also introduced blade-vibration problems on some engines when the frequency of rotating stall in these regions becomes in resonance with the fundamental frequency of the blades, as discussed in the paper on rotating stall and blade vibration.

As pointed out in the paper on inlet flow distortions, a combination of radial and circumferential distortions usually occurs in practice rather than each one separately. Such combinations of a radial and a circumferential distortion have been investigated on two different engines, and the results are summarized in figure 8. Plotted here in bar-graph form is the stall margin of the compressor between the steady-state operating line and the stall-limit line at rated engine speed. These stall margins are shown, for each engine, for four types of inlet condition: For uniform flow, for a circumferential distortion, for a radial distortion, and for a combined radial and circumferential distortion. The combined distortions had about the same peak-to-peak pressure variation as the circumferential distortion but, of course, included both radial and circumferential components.

For engine A, shown in the left portion of the figure, the stall margin with the circumferential distortion was only slightly smaller than with uniform flow. With a radial distortion, however, the stall margin was reduced to about one-half that with uniform flow, indicating the large effect of a radial distortion on this engine. The stall margin with the combined distortion was about the same as that with the radial distortion.

With the other engine, the stall margin was decreased much more by the circumferential distortion than by the radial. In fact, for this engine, the presence of the radial distortion actually increased the stall limit slightly. The performance with the combined distortion in

this case approximates that with the circumferential distortion alone. Thus for each engine, one sensitive to a radial distortion and the other to a circumferential distortion, each component of the combined distortions naturally contributed its own predominant characteristics, and the effect of the combined distortions was about the same as that of the more serious component alone.

Effect of Distortions on Altitude Limits

The reduction in the stall limit of the compressor by the inlet-flow distortion shown in figures 5 to 8 will not only reduce the acceleration margin of the engine but also reduce the speed at which the steady-state operating line and the stall line intersect. In other words, the maximum operable engine speed will be reduced. Because of the Reynolds number effects on compressor performance previously mentioned, this maximum speed limit will be reduced more at high altitude than at a low altitude.

This general characteristic is shown for one engine in figure 9. The three curves show the maximum speed and altitude limits at which the engine could be operated due to compressor stall for the various inlet-flow conditions. With the more severe circumferential distortion, indicated by the lower curve, the maximum speed limit was reduced about 3 percent. Much more important was the fact that the altitude limit was reduced from over 60,000 feet with uniform inlet flow to under 50,000 feet with this inlet distortion.

These data are, of course, illustrative of the general trend of operating limits with inlet distortion but are for only two different distortions and for a single engine. Data presenting the altitude limits for a range of inlet distortions at a given engine speed for five different engines are shown in figure 10. These data are for circumferential inlet distortions of various shapes and with the low pressure regions extending over at least 60° of the inlet circumference. The different engines have, of course, different altitude limits but the effect of the inlet distortion was similar for all engines. As the inlet distortion was increased, the altitude limit was reduced rather rapidly with, in general, a 20-percent distortion decreasing the altitude limit 15,000 to 20,000 feet.

SUMMARY

In summary, a circumferential inlet-pressure distortion is felt throughout the engine as a distorted or uneven pressure ratio around the compressor and as a distorted circumferential temperature profile at the turbine. This uneven compressor pressure ratio reduces the average, or

useful, stall margin in a predictable manner and increases turbine-temperature gradients, thus necessitating a derating of the engine to avoid turbine failures. The decreased stall margin in the compressor has the effect of reducing the engine acceleration potential, the maximum operating speed limits, and the altitude limit of the engine. For a typical 20-percent circumferential distortion, the maximum engine speed is reduced 2 or 3 percent, and the altitude limits may be reduced as much as 15,000 to 20,000 feet. The effects of a radial pressure distortion are to alter the spanwise blade loadings in the early stages of the compressor, and consequently their over-all effects vary considerably among the engines. In some engines, rather small radial distortions may greatly reduce the stall margin and speed limits and extend the operating region of rotating stall to higher speeds, giving rise to increased blade vibration.

BIBLIOGRAPHY

1. Huntley, S. C., Sivo, Joseph N., and Walker, Curtis L.: Effect of Circumferential Total-Pressure Gradients Typical of Single-Inlet Duct Installations on Performance of an Axial-Flow Turbojet Engine. NACA RM E54K26a, 1955.

2. Walker, Curtis L., Sivo, Joseph N., and Jansen, Emmert T.: Effect of Unequal Air-Flow Distribution from Twin Inlet Ducts on Performance of an Axial-Flow Turbojet Engine. NACA RM E54E13, 1954.

3. Wallner, Lewis E., Conrad, E. William, and Prince, William R.: Effect of Uneven Air-Flow Distribution to the Twin Inlets of an Axial-Flow Turbojet Engine. NACA RM E52K06, 1953.

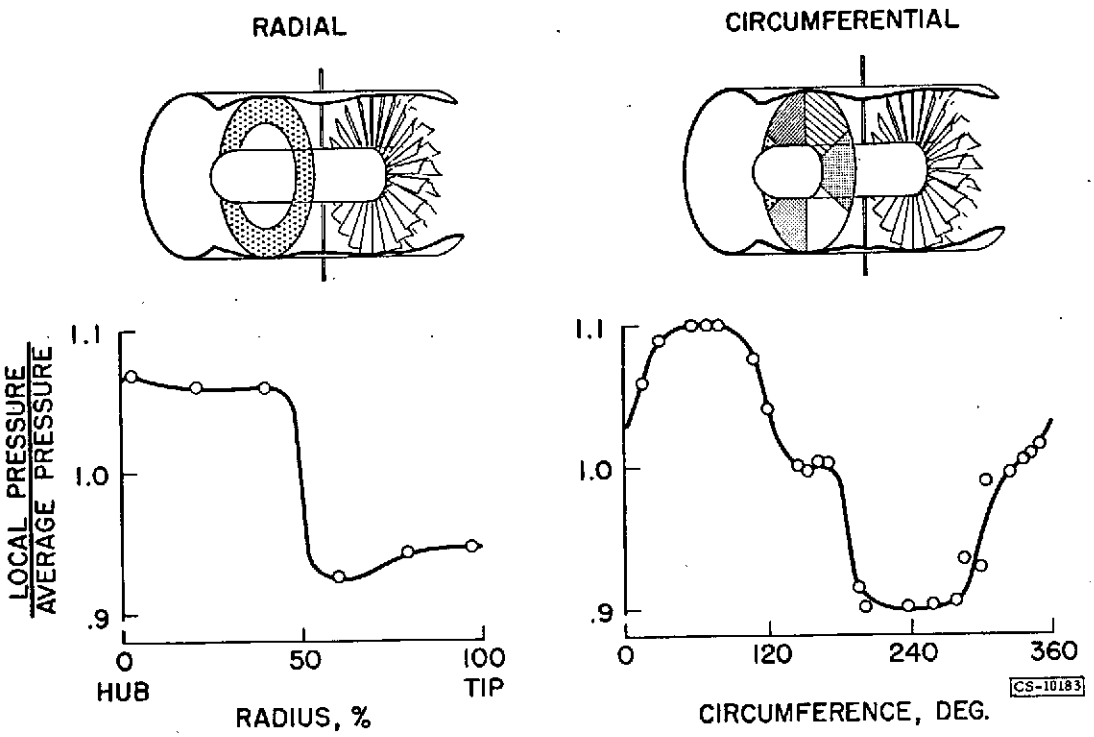

Figure 1. - Typical inlet flow distortions.

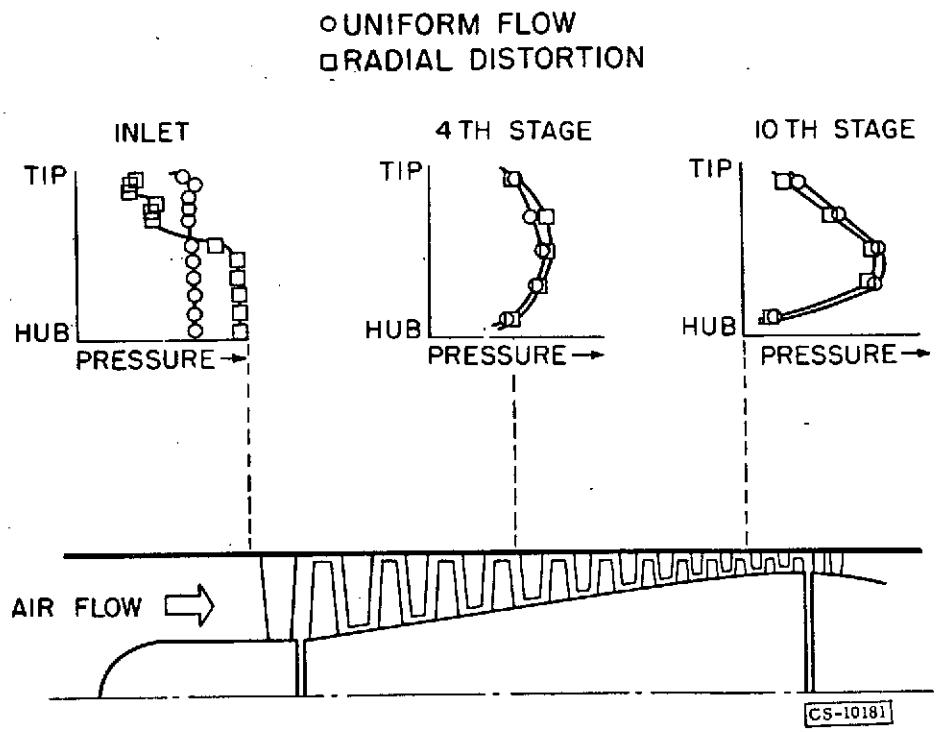

Figure 2. - Extent of radial distortion through compressor.

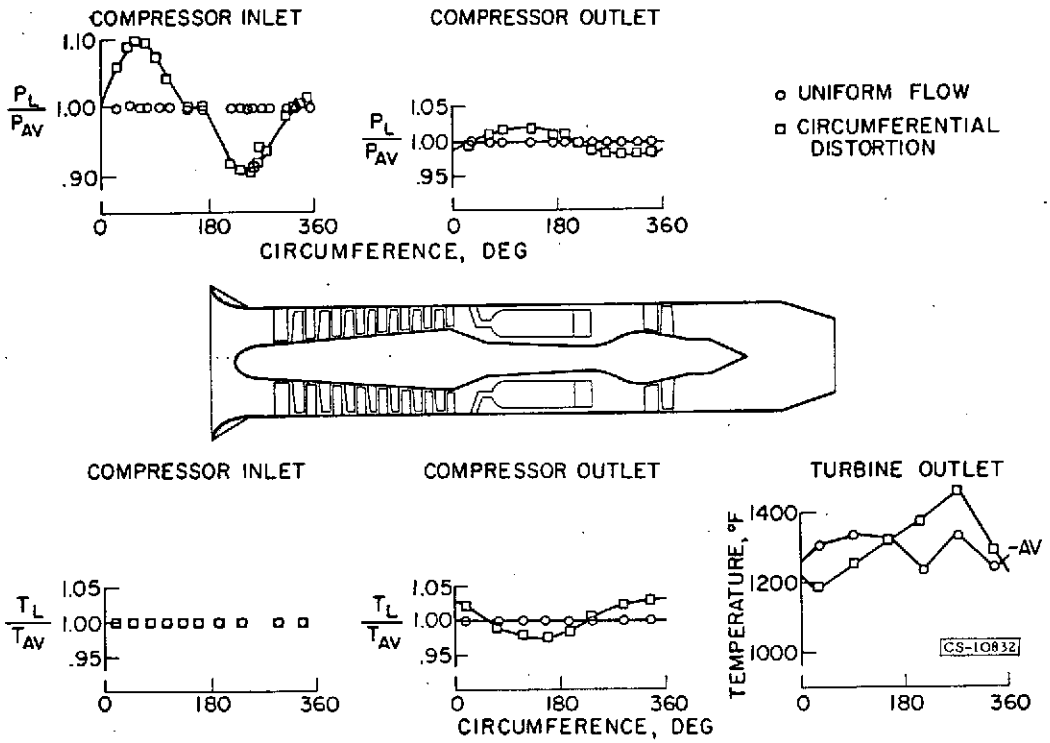

Figure 3. - Extent of circumferential distortion through engine.

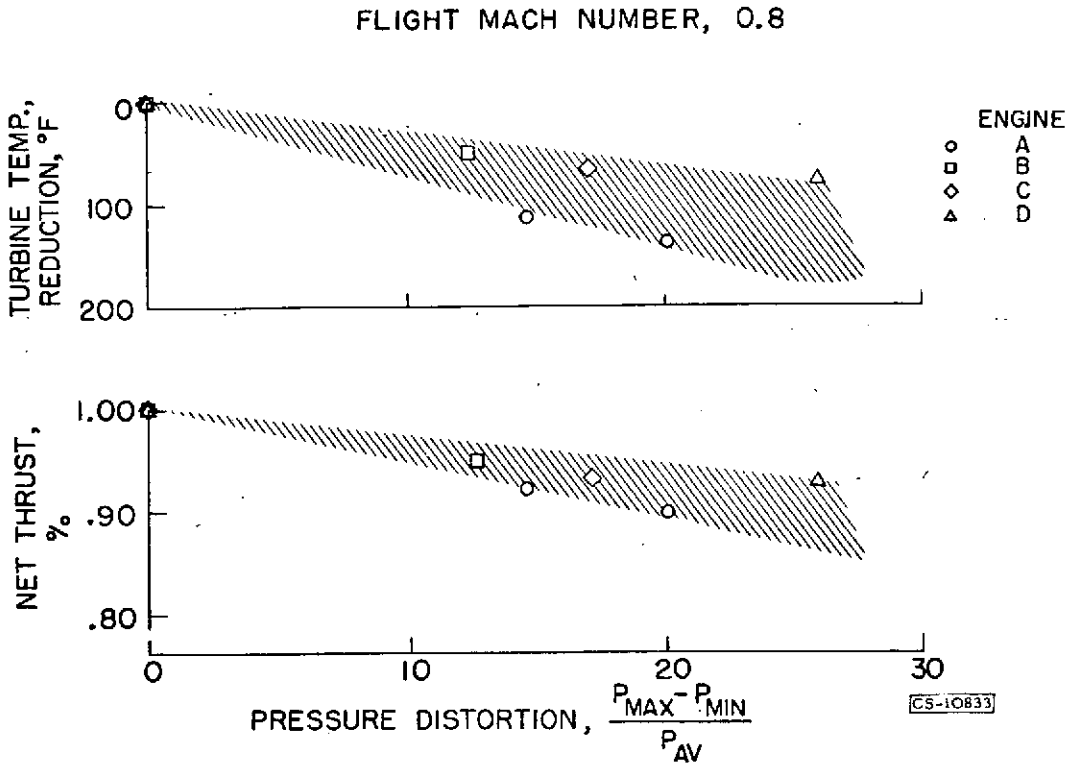

Figure 4. - Performance derating with circumferential distortion.

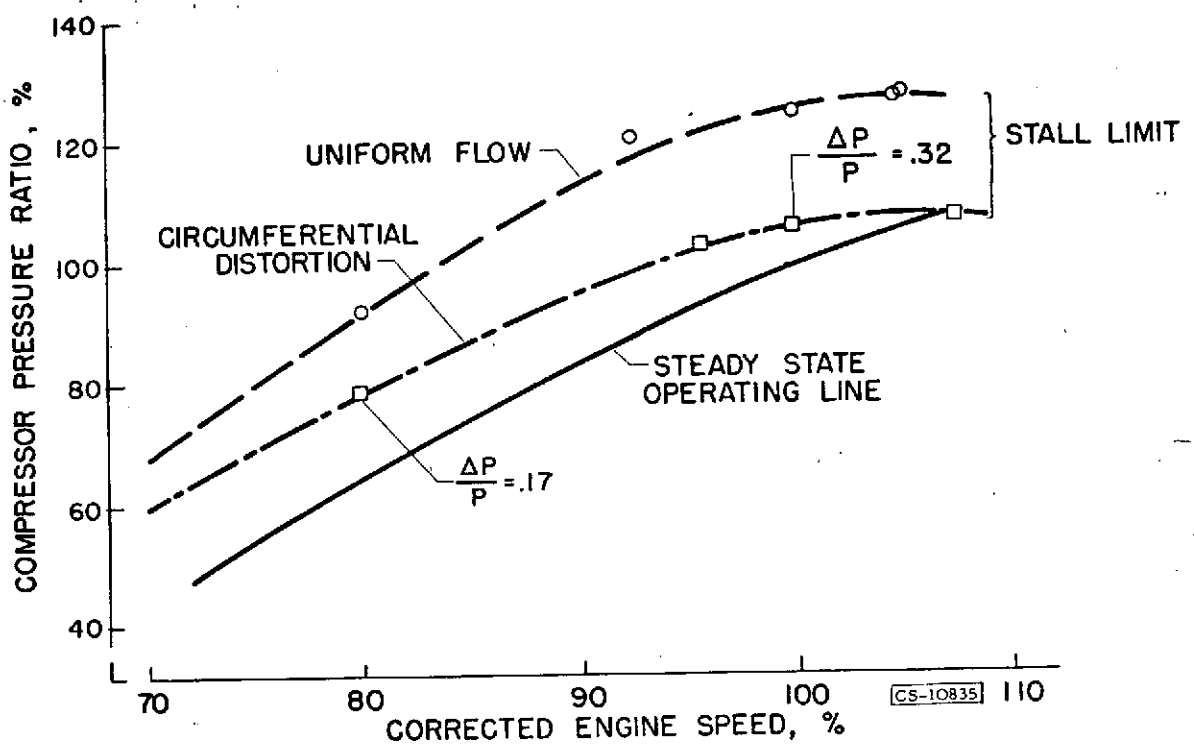

Figure 5. - Effect of circumferential distortion on stall limit.

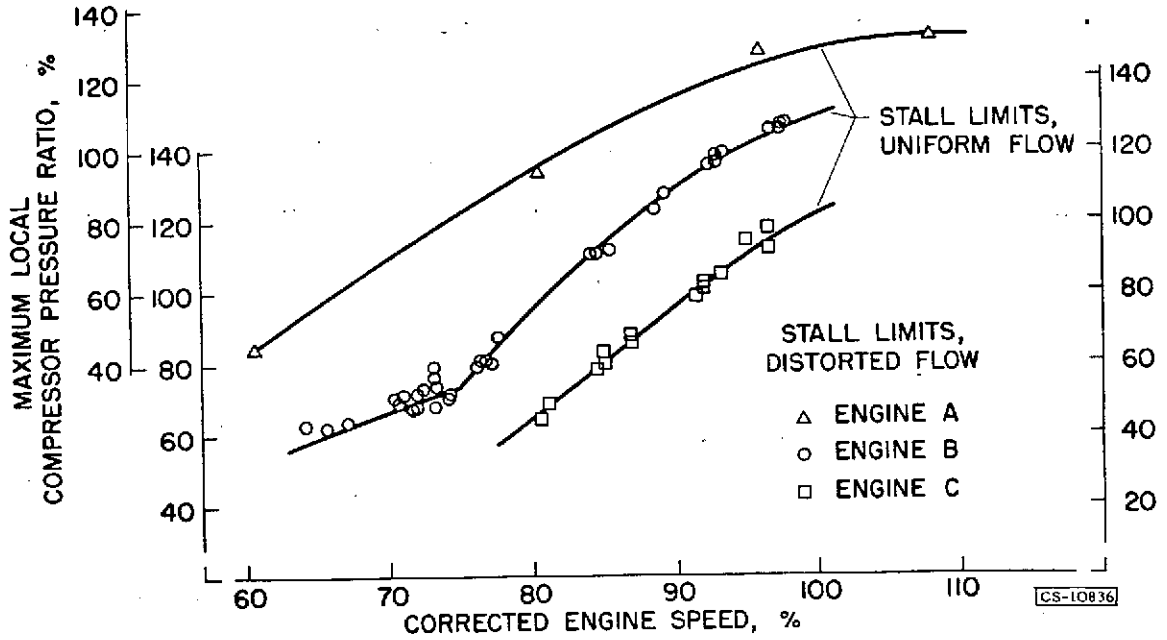

Figure 6. - Generalization of stall limits with circumferential distortion.

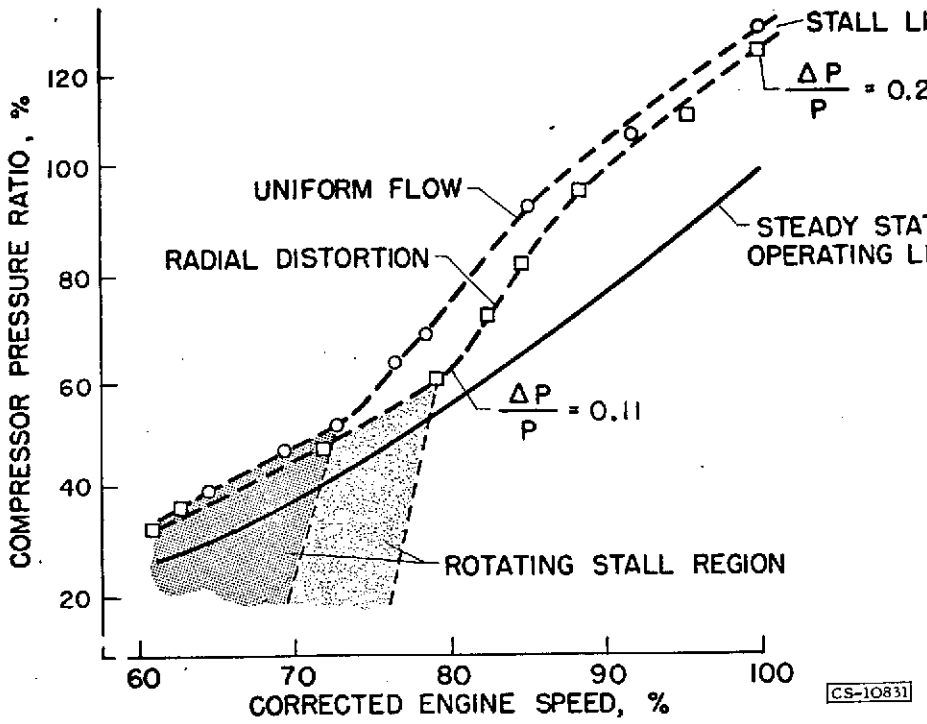

Figure 7. - Effect of radial distortion on stall limit.

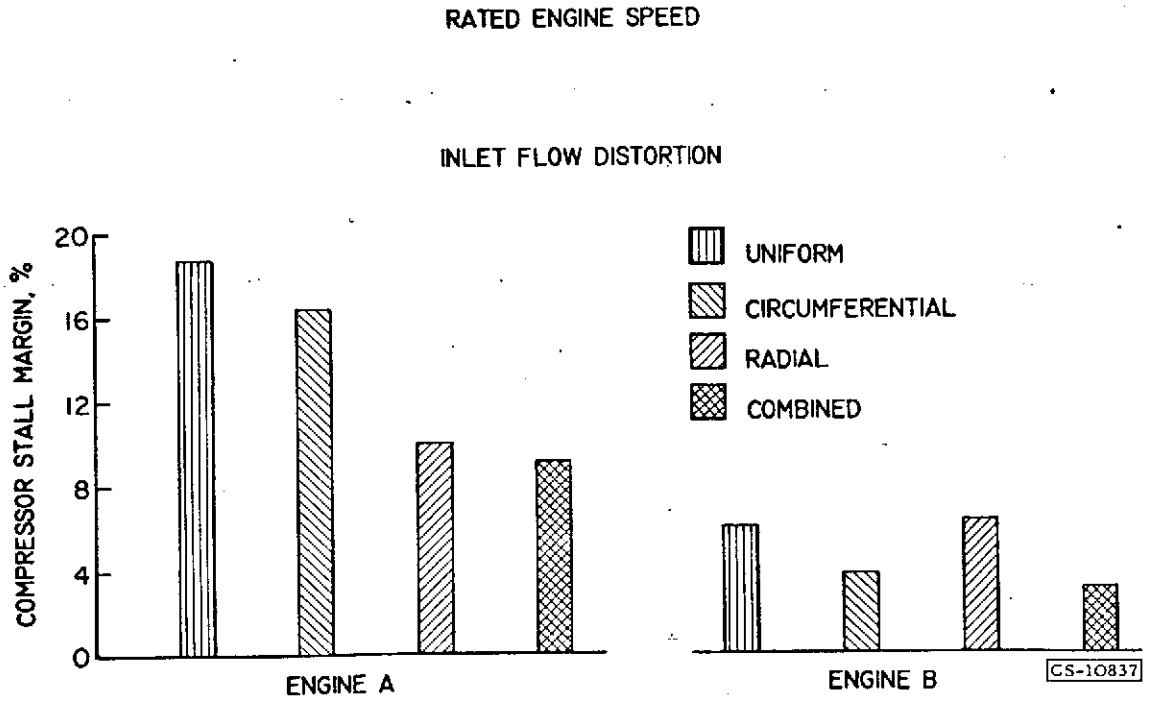

Figure 8. - Stall limits with combined circumferential and radial inlet distortions.

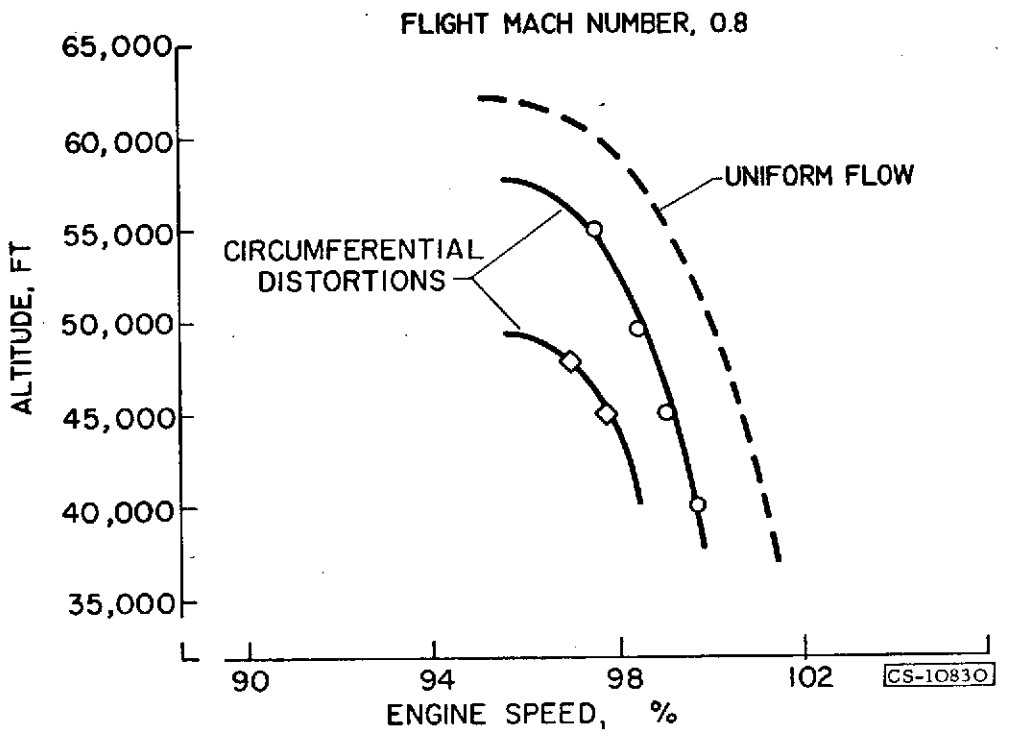

Figure 9. - Effect of circumferential distortions on speed and altitude limits.

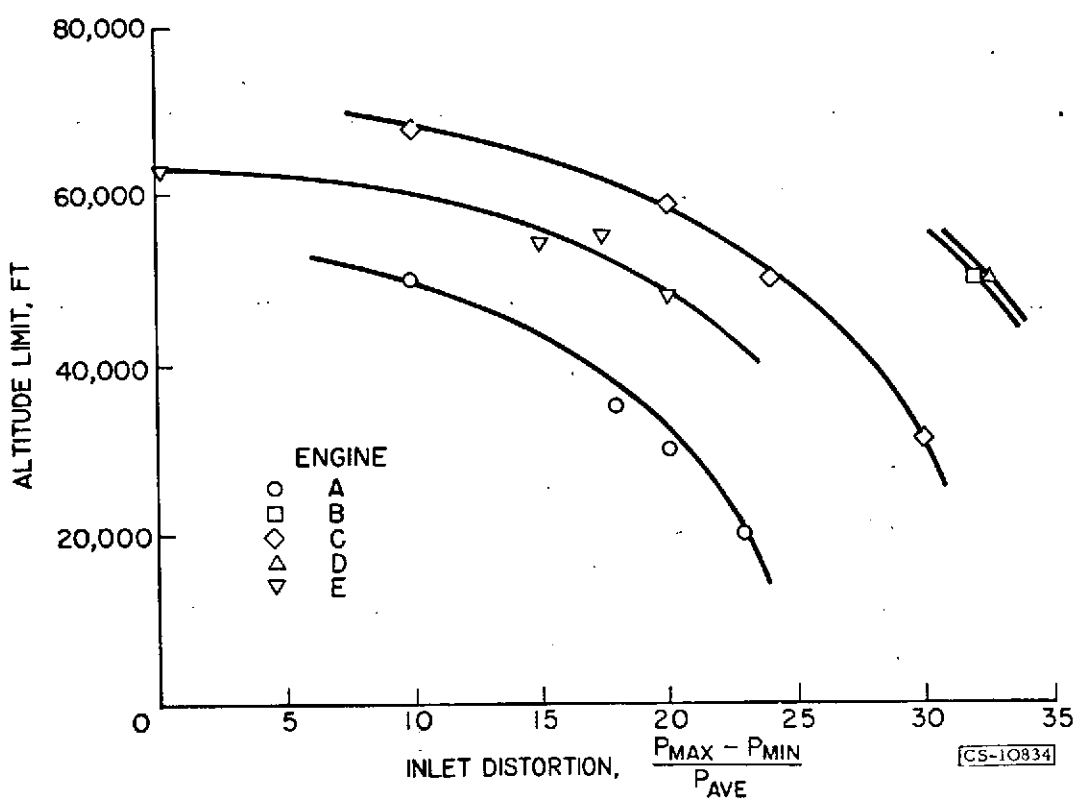

Figure 10. - Effect of circumferential inlet distortion on altitude limits.

V

REMEDIES FOR COMPRESSOR STALL AND BLADE VIBRATION

by
W. A. Benser, M. C. Huppert, L. E. Wallner, H. F. Calvert

V - REMEDIES FOR COMPRESSOR STALL AND BLADE VIBRATION

By W. A. Benser, M. C. Huppert, L. E. Wallner
and H. F. Calvert

INTRODUCTION

In the past few years, the pressure ratio of axial-flow turbojet-engine compressors has been increased appreciably in order to improve altitude performance and engine fuel economy. As a result, compressor stall at low engine speeds has become a serious problem in regard to engine acceleration. Furthermore, rotating stall, which exists in the compressor at these low engine speeds, is a prevalent source of compressor blade vibrations, as discussed in paper II. Recent studies show that inlet-air flow distortion has severe adverse effects on the stalling characteristics of axial-flow compressors at all engine speeds (paper IV). As discussed in paper III, some improvement in inlet flow distribution may be achieved by research on inlets and their associated ducting, but variations in flight conditions such as angle of attack and flight Mach number may still result in appreciable flow distortions at the compressor inlet.

In order to obtain satisfactory acceleration even with uniform inlet flow, adequate margin between the steady-state operating line and the compressor stall-limit line is required, particularly at low and intermediate values of engine speed. To avoid compressor stall problems resulting from inlet flow distortions, the stall margin at all speeds must be increased from that which is normally considered adequate for operation with uniform flow at the compressor inlet. To eliminate blade vibrations due to rotating stall, resonance between the compressor blading and rotating-stall zones must be eliminated.

This paper considers some of the methods available for alleviating the compressor-stall and blade-vibration problems discussed in papers II and IV. The modifications, or remedies, for the compressor-stall problem are used to control the location of the compressor stall-limit line with respect to the engine steady-state operating line so as to avoid encountering compressor stall. The remedies for blade-vibration problems are aimed at eliminating rotating stall as a source of blade excitation. The single-spool engine and the two-spool engine are considered separately.

SINGLE-SPOOL ENGINE

The remedies to be considered for the single-spool engine are (1) exhaust-nozzle adjustment, (2) turbine-stator adjustment, (3) compressor-discharge bleed, (4) compressor interstage bleed, (5) inlet-guide-vane adjustment, and (6) inlet baffles. Exhaust-nozzle and

turbine-stator adjustments are primarily remedies for compressor stall at high engine speeds where compressor stall may be aggravated by inlet flow distortions. Compressor-discharge bleed, compressor interstage bleed, and adjustable inlet guide vanes are remedies for stall problems at low and intermediate speeds, and the inlet baffle is primarily a remedy for compressor blade-vibration problems due to rotating stall. Inasmuch as no single engine incorporates all these features, the data presented are for several different engines. In addition to these remedies, compressor design compromises to improve stall margin are discussed briefly.

Definition of Problem

The low-speed stall problem of high-pressure-ratio single-spool turbojet engines is illustrated in figure 1, which shows the variations of stall-limit pressure ratio with speed for two high-pressure-ratio engines for uniform inlet flow. The steady-state operating line for rated jet nozzle area and no variable-geometry remedies is also shown on these plots. For engine A, the compressor stall limit is extremely close to the steady-state operating line at low engine speeds but is appreciably above the operating line at higher speeds. For engine B, a severe dip or knee occurs in the compressor stall limit between 60 and 80 percent of rated engine speed. In this case, the stall-limit line intersects the operating line at 65- and 75-percent speed. Engine operation between these speeds is impossible without the use of some stall remedy.

A convenient parameter for indicating the margin between the compressor stall limit and the steady-state operating line at a given speed is the ratio of the pressure ratio at stall to the pressure ratio required for steady-state operation at that speed. Figure 2 shows a plot of this stall margin parameter against engine speed for engine A. A value of 1 for this parameter represents an intersection of the operating line and the stall-limit line and is the limit of engine operation. The solid curve on figure 2 is for no inlet distortion and indicates a small stall margin at low engine speeds and a sizable stall margin at high engine speeds.

A comparison of the solid and dashed curves in figure 2 shows the effect of a radial distortion of inlet flow on the stall margin of engine A. The magnitude of distortion decreased with engine speed. The value of $\Delta P/P$ at rated speed was 12 percent and decreased to 5 percent at 90-percent speed. As noted in this figure, the effect of distortion is to move the dip or knee in the stall limit to higher speed and to severely decrease the stall margin at high engine speeds. More severe inlet flow distortions would further reduce the stall margin and could conceivably render this engine inoperable both at intermediate and at high engine speeds.

The two ranges of engine speed that are of particular interest are indicated by figure 2. The first is the high-speed range, where inlet distortions may impose severe stall limitations. The second is the low-speed range, where an adequate stall margin is required in order to obtain satisfactory engine acceleration, with or without inlet flow distortions.

When inlet flow distortions are encountered, the stall margin over the entire speed range must be increased above that which is necessary for a uniform inlet flow.

Exhaust-Nozzle Adjustment

Within limits, increasing the exhaust-nozzle area of a single-spool engine increases the stall margin by decreasing the pressure ratio required for steady-state operation at any speed. When the exhaust nozzle is opened, the back pressure on the turbine is decreased. Thus, the work required to drive the compressor can be obtained at lower turbine-inlet pressure and temperature, and the compressor can operate at a reduced pressure ratio or increased flow.

Effect on stall margin. - The effect of exhaust-nozzle area on the stall margin of engine B is shown in figure 3, where stall margin is plotted against engine speed. The solid curve is for rated exhaust-nozzle area. As engine speed is increased from 40 to 65 percent, the stall margin parameter decreases to a value of 1.0. Thus, at 65-percent speed, the operating line intersects the stall-limit line, and the engine is not operable in the speed range of 65- to 75-percent speed without the aid of some stall remedies. Above 75-percent speed, the stall margin increases rapidly.

The stall margin obtained for an exhaust-nozzle area that is 60 percent greater than the rated area is shown by the dotted curve in figure 3. This change improves the stall margin somewhat at low engine speeds, but the inoperable region remains essentially the same. At high engine speeds, there is a considerable improvement in stall margin. This increase in stall margin at high speeds is beneficial when inlet flow distortions are encountered.

Effect on engine performance. - At rated speed, the thrust of engine B decreases rapidly as the exhaust-nozzle area is increased, as shown in figure 4. For a 60-percent increase in area, the thrust is decreased about 30 percent. This thrust loss results from the drop in turbine-inlet temperature. The 60-percent increase in exhaust-nozzle area causes a 450° drop in turbine-inlet temperature (fig. 4). Thus, exhaust-nozzle-area increase may improve stall margin but only at the expense of a thrust penalty.

Turbine-Stator Adjustment

A combination of turbine-stator-area and exhaust-nozzle-area changes can be used to improve stall margin. As shown previously, increasing the exhaust-nozzle area decreases the compressor pressure ratio and, thus, improves stall margin. In order to operate with this decreased compressor pressure ratio without reducing the turbine-inlet temperature, the turbine-stator area must be increased. Increases in turbine-stator area can be achieved by simply resetting the angle of the first row of turbine stator blades.

Effect on engine performance. - Thrust and fuel consumption in percent of rated values are plotted in figure 5 against turbine-stator area. These data are for engine C, and serve to illustrate the effectiveness of a combination of turbine stator and exhaust-nozzle-area changes. This engine had a two-stage turbine; however, only the stators for the first stage were reset. As the turbine-stator area was increased to 110 percent of rated area, the exhaust-nozzle area was increased to 115 percent of the rated area to maintain constant turbine-inlet temperature. These changes of area had little effect on engine thrust (fig. 5) The fuel consumption of the engine, however, was increased about 4 percent.

Effect on stall margin. - Stall margin is plotted against engine speed in figure 6. The data in the lower curve give the stall margin for engine C when it was operated with standard exhaust-nozzle and turbine-stator areas. The upper curve presents the stall margin when the engine was operated with 110-percent turbine-stator and 115-percent exhaust-nozzle areas. At rated speed, these area changes increased the stall margin approximately 12 percent. The stall margin was increased over the entire speed range; therefore, these area changes could be permanent changes.

Increasing compressor stall margin by turbine-stator adjustment can be considered as derating the engine in terms of pressure ratio. If the pressure ratio is reduced too much, the compressor efficiency will be lowered appreciably, and a large loss in engine thrust and efficiency will result. The reduced pressure ratio also results in a decreased air density at the compressor discharge and, therefore, increases the combustor-inlet velocities. This velocity increase may adversely affect the altitude performance of the combustor.

In most cases the engine components have some flow margin, and moderate increases of turbine-stator and exhaust-nozzle area can be effectively used to increase stall margin. Extremely large area changes, however, will severely decrease component efficiencies and will decrease thrust as well as increase fuel consumption.

Compressor-Discharge Bleed

Compressor-discharge bleed is a simple method of improving stall margin at low engine speeds. Air is bled from the compressor discharge, and the compressor pressure ratio for steady-state operation is decreased. The turbine-inlet temperature, however, is increased. When compressor-discharge bleed is used, the bleed ports must be closed at high engine speeds to avoid severe thrust penalties and to avoid overtemperature of the turbine. Achievement of noticeable gains in stall margin by means of discharge bleed may require 20 percent or more air bleed. This technique of improving low speed stall margin is not considered to be good because of the large quantities of bleed required. It can be used, however, where only small gains in stall margin are required.

Compressor Interstage Bleed

As pointed out in paper I, stall of the compressor at low engine speeds is a result of insufficient flow through the front stages of the compressor. Interstage bleed is a basic approach to this low-speed stall problem, in that it tends to remove the cause of compressor stall. With interstage bleed, the flow through the front stages of the compressor is increased; midway through the compressor, the excess air is bled off through a system of bleed ports and dumped. This increase of flow through the front stages improves the matching between the front and rear halves of the compressor at low speeds and thus delays compressor stall in this speed range.

Effect on stall margin. - The improvements in stage matching obtained by use of interstage bleed in engine B resulted in the improvement in stall margin shown in figure 7. The solid line which shows the stall margin without bleed, is the same plot shown in figure 3. Four-percent interstage bleed resulted in the large improvement in stall margin shown by the dotted curve.

The bleed ports would be closed at about 80-percent speed, because no improvement in margin is obtained beyond that speed. These data show that interstage bleed is a very effective method of improving low-speed stall margin for engines that use high-pressure-ratio single-spool compressors.

Effect on blade vibration. - Inasmuch as interstage bleed increases the flow through the inlet stages of the compressor at low engine speeds, this remedy will diminish the maximum speed at which rotating stall will exist. Thus, interstage bleed may eliminate some critical blade vibrations. This modification, however, will not necessarily eliminate rotating stall over the entire low speed range, and, therefore, will not always completely eliminate the blade vibration problem.

Inlet-Guide-Vane Adjustment

Inlet-guide-vane adjustment is another method of improving compressor stall margin at low engine speeds. Adjustment of the inlet guide vanes alters the performance of the inlet stage of the compressor and, thus, delays stall of the front stages of the compressor at low speed. The effect of guide-vane adjustment on the performance of a typical inlet stage is shown in figure 8, which is a plot of stage pressure ratio against weight flow. The solid curve is for the guide vanes in the open position, and the dashed curve is for the guide vanes in the closed position. The orientation of the guide vanes with the inlet flow direction for the opened and closed positions is shown at the right of figure 8. For the open position, the guide vane is set at a small angle with the inlet flow direction, which is indicated by the arrow. In the closed position, the guide vane is rotated about a radial line so as to make a much larger angle with the inlet flow, as shown at the bottom of this figure.

Comparison of the solid and dashed curves in figure 8 shows the effect of guide-vane positions on the stage performance characteristic. With the guide vanes in the closed position, the maximum flow through the stage is decreased, and the stall point of the stage is shifted to a much lower flow. This shift of stall point delays front-stage stall at low engine speeds and thus improves the stall margin in this speed range.

The following discussion is limited to the effects of inlet-guide-vane adjustment. If necessary the principle of vane adjustment can be applied to additional stages in the front end of the compressor.

Effect on stall margin. - The effects of guide-vane adjustment have been investigated in several turbojet engines. Results of tests with engine B are shown in figure 9, where stall margin is plotted as a function of engine speed. Closing the inlet guide vanes 20° increased the stall margin for the entire speed range shown, and made the engine fully operable in the mid-speed region. Although the stall margin is increased at top speed, it would be impractical to use inlet-guide-vane adjustment in this speed region because of the reduction in mass flow and, therefore, engine thrust. Obviously then, the blades must be opened at high engine speeds. Inlet-guide-vane adjustment, however, is an effective means of obtaining additional stall margin in the low-speed region and, thus, would be an aid to acceleration of the engine. The effectiveness of inlet-guide-vane adjustment in improving low speed stall margin depends on the specific compressor design. In most designs, however, inlet-guide-vane adjustment is an effective method of improving low speed stall margin for high-pressure-ratio engines.

Effect on blade vibration. - Inlet-guide-vane adjustment may decrease the range of speeds over which rotating stall is encountered, but does not completely eliminate rotating stall over the entire low speed range. Closing the guide vanes tends to push the stall zones from the blade tips to the blade roots and may alter the number of stall zones. Closing the guide vanes, therefore, may eliminate some critical resonance conditions, but this modification is not considered as a complete remedy for blade vibrations induced by rotating stall.

Inlet Baffles

The inlet baffle is primarily a device for eliminating blade vibration excited by rotating stall. The principle of the inlet baffle is illustrated by the sketch in figure 10. This device reduces the compressor-inlet area by use of hinged flaps at the inner diameter of the compressor inlet. These flaps operate in a manner similar to the cowl flaps on a radial reciprocating engine. When the baffle is extended, a separated-flow region exists behind the baffle. This separated region gradually dissipates as it flows back through the compressor, and effectively alters the flow area to more nearly match that required for low-speed operation. In addition, the baffle forces the air out towards the rotor tips and in so doing tends to eliminate the rotating-stall region that normally exists at the blade tips.

Effect on blade vibration. - The baffle was the only one of the remedies considered for the single-spool engine that eliminated the periodic nature of the stall in the front stages of the compressor. When the periodic rotating stall was eliminated, the blade-vibration problem was also eliminated.

Figure 11, a plot of vibratory stress against engine speed, presents the results of an investigation in which engine D was operated with a baffle at the inner diameter of the compressor inlet. The solid curve presents the maximum vibratory stresses measured in the first and second stages when the engine was operated without the baffle. These stresses were excited by a three-zone stall pattern, as shown by the upper sketch. The dashed curve represents the stresses measured when the engine was operated with the baffle. The stresses were reduced to a minimum, because the periodic nature of the stall had been removed. With baffle, the compressor operated with a continuous stall region around the annulus, as shown by the lower sketch in figure 11.

Thus, the baffle, by eliminating the periodic nature of rotating stall, satisfactorily eliminates blade vibration. This baffle must, of course, be retracted at high engine speeds to avoid severe thrust penalties.

Effect on stall margin. - Inasmuch as the separated-flow region behind the inlet baffle tends to alter the effective area ratio through the compressor to favor low-speed performance, it might be expected that the baffle could improve low-speed stall margin. To date, no stall-limit data have been obtained on an engine incorporating a retractable baffle. Some compressor component tests have indicated some improvement in low speed stall margin. The improvement in stall margin obtained by the use of only an inlet baffle, however, would probably not be adequate to insure good acceleration characteristics for most high-pressure-ratio engines.

Design Compromises

The items discussed are concerned primarily with remedies for existing compressors. Early low-pressure-ratio compressors were designed to match the individual stages at design or rated rotative speed. As pressure ratio was increased, however, engines became plagued with low-speed stall problems. These stall limitations were in some cases so acute that acceleration of the engine to rated speed was impossible. In order to alleviate this situation, the stages were matched at less than rated speed. This tended to improve the stall problem at low speed at the expense of high-speed stall margin. It has been demonstrated, however, that variable-geometry features that provide adequate stall margin at low engine speeds are available. It has also been shown that, when inlet flow distortions are encountered, large stall margins are required at high engine speeds. Therefore, compressors could be designed for optimum high-speed operation, and variable-geometry features such as guide-vane adjustment or interstage bleed could be used to facilitate engine acceleration. It should be noted that such stage-matching compromises should be effective for applications up to a flight Mach number of about 1.5. For higher flight Mach numbers, this problem must be reevaluated.

TWO-SPOOL ENGINES

For the two-spool engine, the interactions between the two compressors and two turbines operating in series are extremely complex. The discussion of this type engine, therefore, will only consider remedies to the stall problems in comparison to those for the single-spool engine.

Definition of Problem

As shown on the composite compressor performance map (fig. 12), the steady-state operating line for the two-spool engine lies between the inner- and the outer-compressor stall limits (paper I). As indicated

here for uniform inlet flow distributions, stall of the outer compressor is expected at low engine speed, and stall of the inner compressor is expected at high engine speeds. This is analogous to the single-spool engine, which exhibits front-stage stall at low speed and rear-stage stall at high engine speeds. During rapid accelerations, however, both compressors of the two-spool engine will move towards their stall limits. At low engine speeds, inlet flow distortions will tend to make the stall limitations of the outer compressor more severe. For high engine speeds, it has not been definitely ascertained whether inlet flow distortions induce premature stall in the inner or the outer compressor. Therefore, both of these possibilities will be considered.

The variable geometry features to be discussed for the two-spool engine are indicated on the engine sketch at the top of figure 12.

Outer-Compressor Stall at Low Engine Speeds

Outer-compressor stall at low speeds for the two-spool engine is analogous to front stage stall in the single-spool engine and is amenable to the same treatments. For the single-spool engine interstage bleed was shown to be an effective remedy for low speed stall problems. For the two-spool engine interspool bleed as indicated on figure 12 has proven to be an effective remedy. Of course, the bleed ports must be closed at high engine speeds so as to avoid penalties in thrust and fuel consumption.

Inner-Compressor Stall at High Engine Speeds

It has been shown that high-speed or rear-stage stall of the single-spool engine can be alleviated by a combination of turbine-stator and exhaust-nozzle area changes. Analysis has indicated that inner-compressor stall of the two-spool engine can be effectively handled by these same geometry changes. In this analysis, the outer-compressor operating condition was held constant and the pressure ratio required of the inner compressor reduced to increase the stall margin of the inner compressor. In order to maintain turbine-inlet temperature when the pressure ratio was reduced, it was necessary to reset the stators of both turbines and to adjust the exhaust-nozzle area. These changes have the same effect on the performance of the two-spool engine as on the single-spool engine. The specific fuel consumption is increased, but the thrust is not appreciably reduced. Of course, as in the single-spool engine, the allowable magnitude of such changes will be limited, because radical changes will result in large losses in component efficiency and will adversely affect combustor performance.

Outer-Compressor Stall at High Engine Speeds Due to Inlet Distortions

As discussed previously, outer-compressor stall may occur at high engine speeds as a result of inlet flow distortions. Although this problem is not completely understood, analysis to date has indicated that any attempt to increase the stall margin of the outer compressor without compressor design changes will result in an appreciable reduction in engine thrust.

This reduction in thrust may be qualitatively explained as follows: When the inner compressor of a two-spool engine is operated at a constant speed, the inlet volume flow to this compressor must remain essentially constant. The flow capacity of the inner compressor might be increased by overspeeding of this unit, but this may result in a serious turbine stress problem. Therefore, if the pressure ratio of the outer compressor is reduced to improve stall margin, the weight flow through the engine must also be reduced in order to maintain constant volume flow at the inlet of the inner compressor. A reduction in weight flow, of course, results in a thrust penalty. In order to reduce both the flow and pressure ratio of the outer compressor, the speed of this unit must be reduced. As the speed of a compressor is reduced, the obtainable pressure ratio is also reduced. Therefore, the benefits obtained in stall margin, as a result of turbine and exhaust-nozzle-area changes, will depend on the shape of the stall-limit line of the outer compressor. Very large changes of speed and thrust may be required to avoid outer-compressor stall when serious inlet flow distortions are encountered. Thus, it appears that increases in stall margin of the outer compressor without sacrifices in engine thrust will require compressor design modifications.

CONCLUDING REMARKS

The study of stall remedies for single-spool engines indicated that the stall margin on this type engine can be improved and blade vibration due to rotating stall can be virtually eliminated. A combination of turbine-stator and exhaust-nozzle-area changes can be used to alleviate compressor stall problems at high engine speeds. These can be fixed changes and need not be adjustable features. For moderate changes, this remedy has little effect on engine thrust, but it does increase fuel consumption somewhat. Interstage bleed and adjustable inlet guide vanes have proven to be effective remedies for compressor stall problems at low engine speeds. A retractable inlet baffle is an effective means of eliminating compressor blade vibrations induced by rotating stall.

Stall remedies for the two-spool engine are not well defined. Interspool bleed appears to be an effective means of avoiding low-speed stall of the outer compressor during engine acceleration. Remedies for a high-speed stall of the inner compressor have not been proved by test, but

calculations indicate that this problem can be solved by the use of turbine-stator and exhaust-nozzle area changes. As for the single-spool engine these changes should have little effect on thrust but probably will increase fuel consumption somewhat. Analysis to date has shown no simple remedy for an outer-compressor stall problem at high engine speeds without a severe thrust derating of the engine. At present, the only satisfactory solution to this problem appears to be a modification of the compressor to provide sufficient stall margin to cope with inlet distortions.

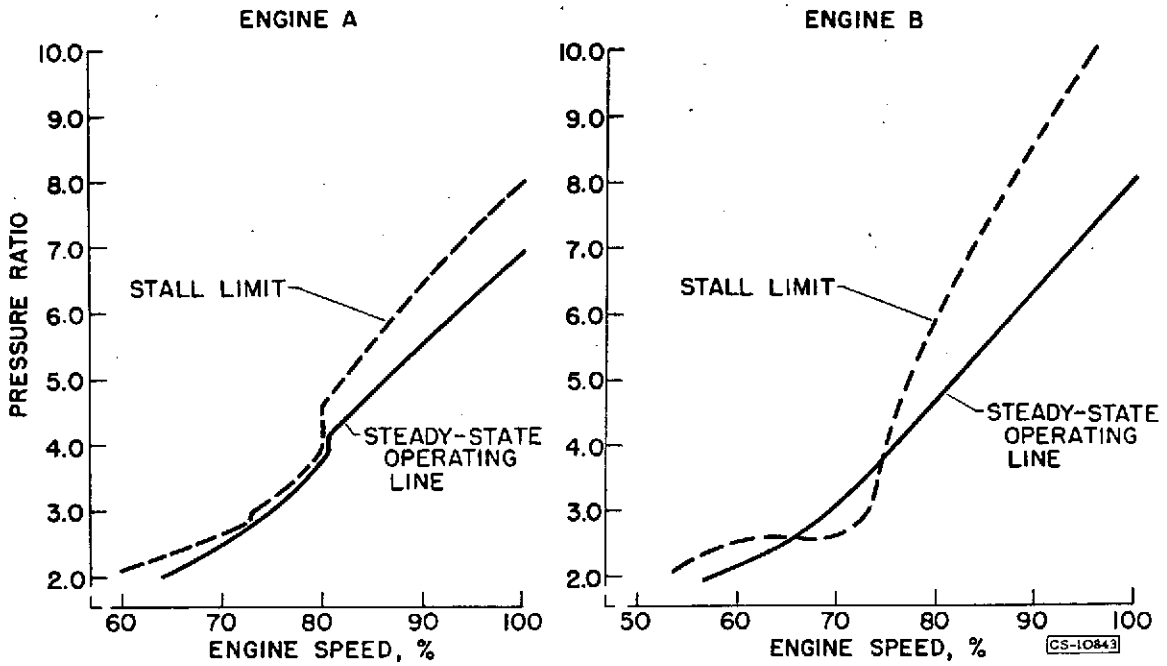

Figure 1. - Operating and stall lines for two high-pressure-ratio turbojet engines.

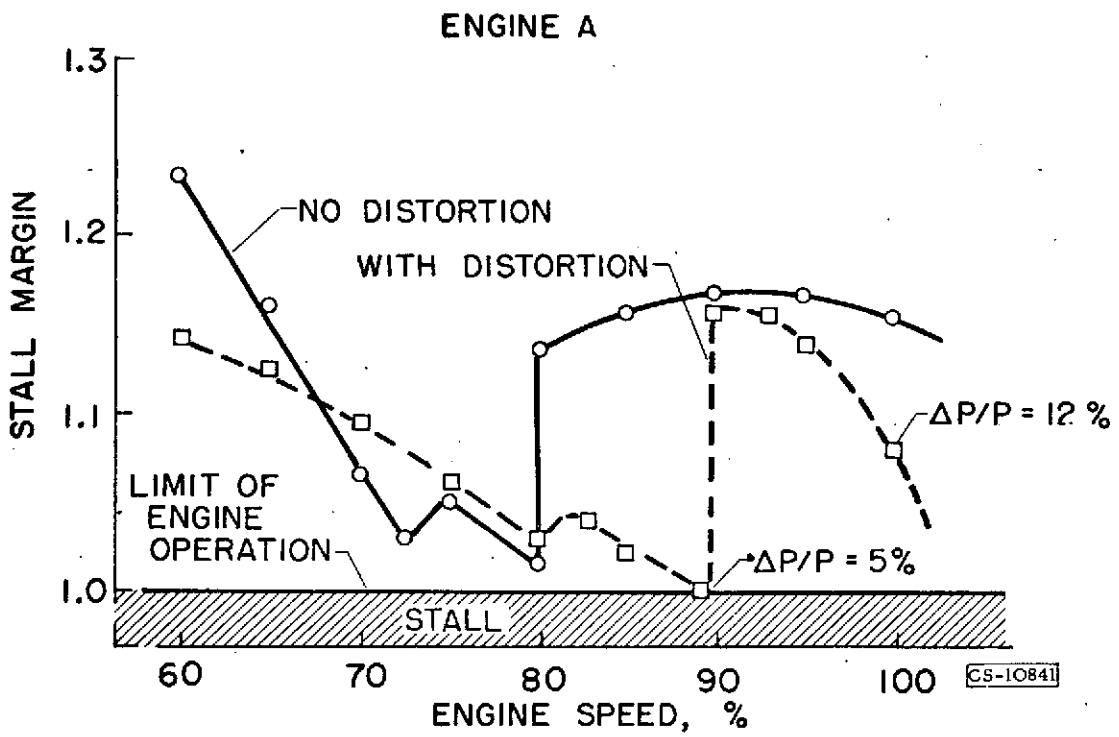

Figure 2. - Effect of inlet flow distortion on stall margin.

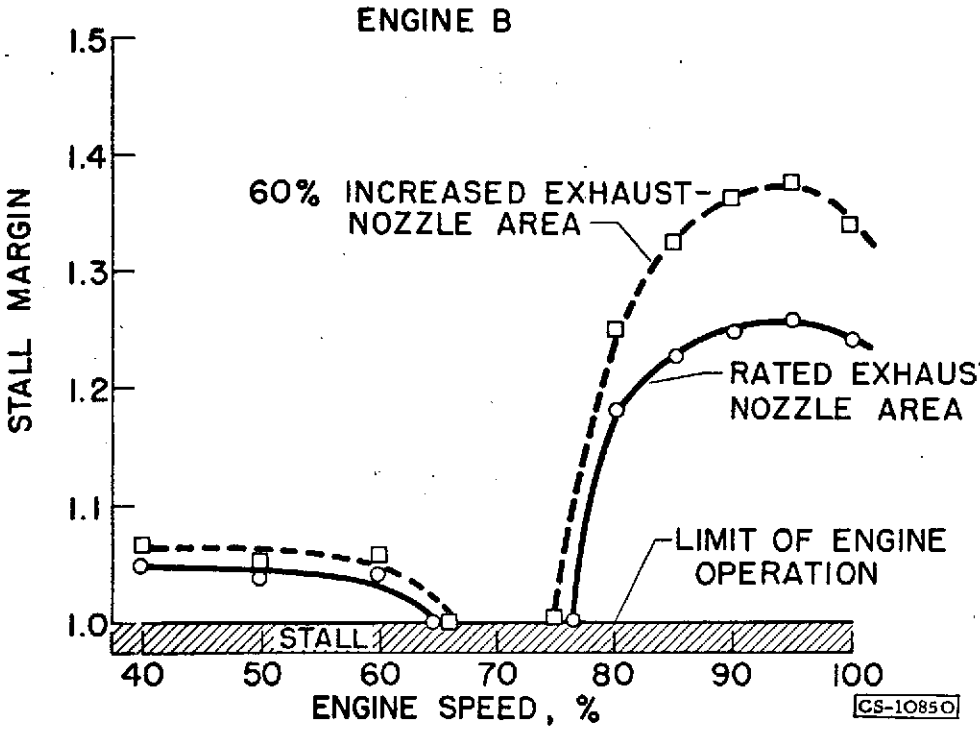

Figure 3. - Effect of exhaust-nozzle area changes on compressor stall margin.

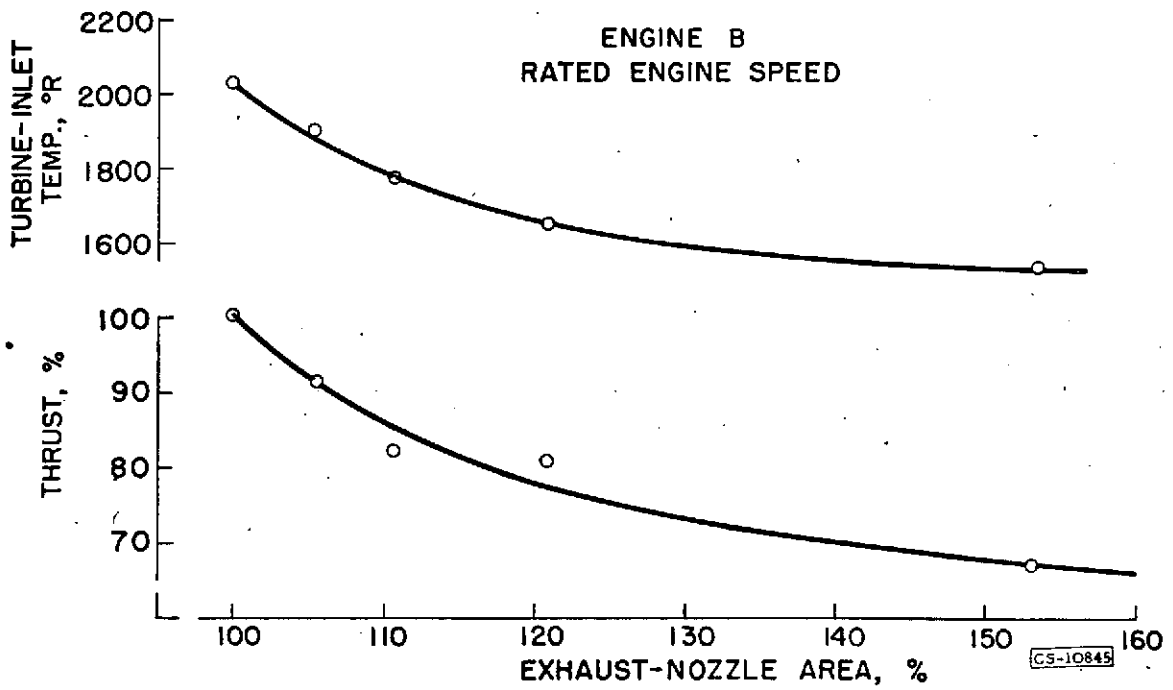

Figure 4. - Effect of exhaust-nozzle area on turbine-inlet temperature and thrust.

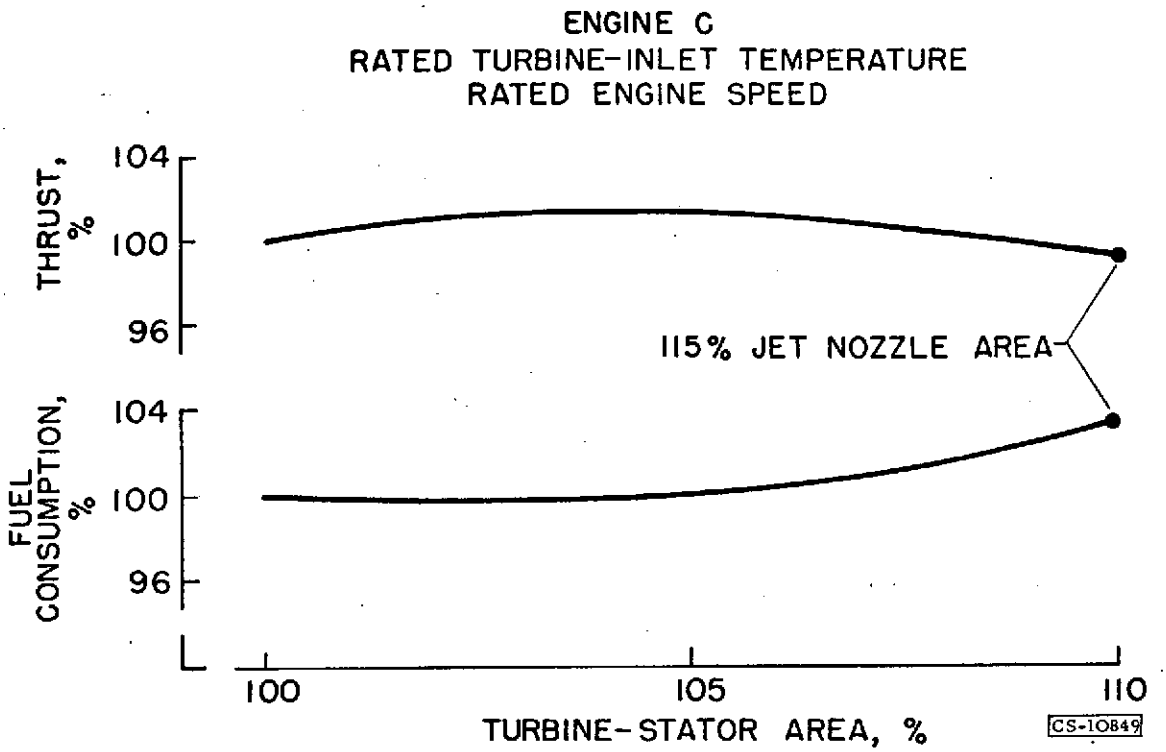

Figure 5. - Effect of turbine nozzle area on thrust and fuel consumption.

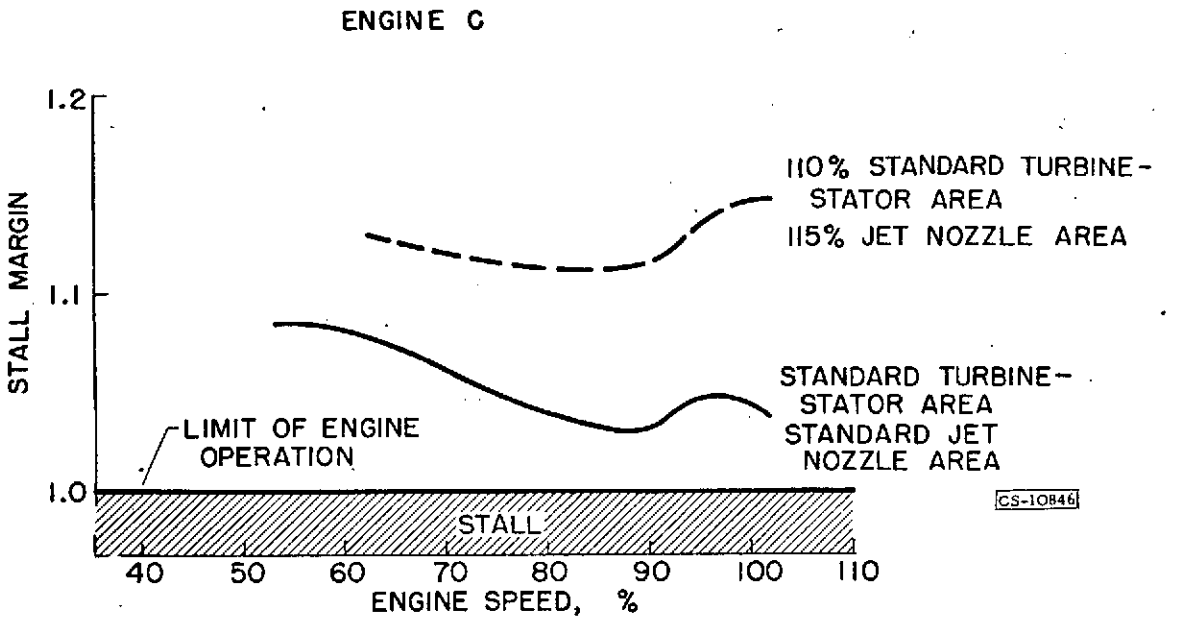

Figure 6. - Effect of increasing turbine-stator area on stall margin.

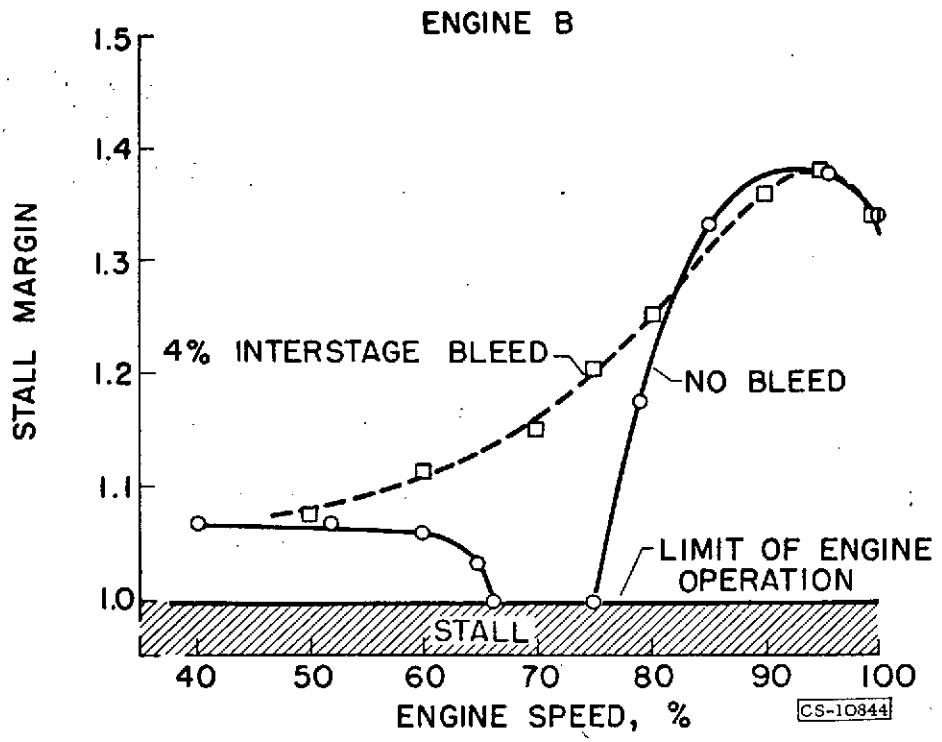

Figure 7. - Effect of compressor interstage bleed on stall margin.

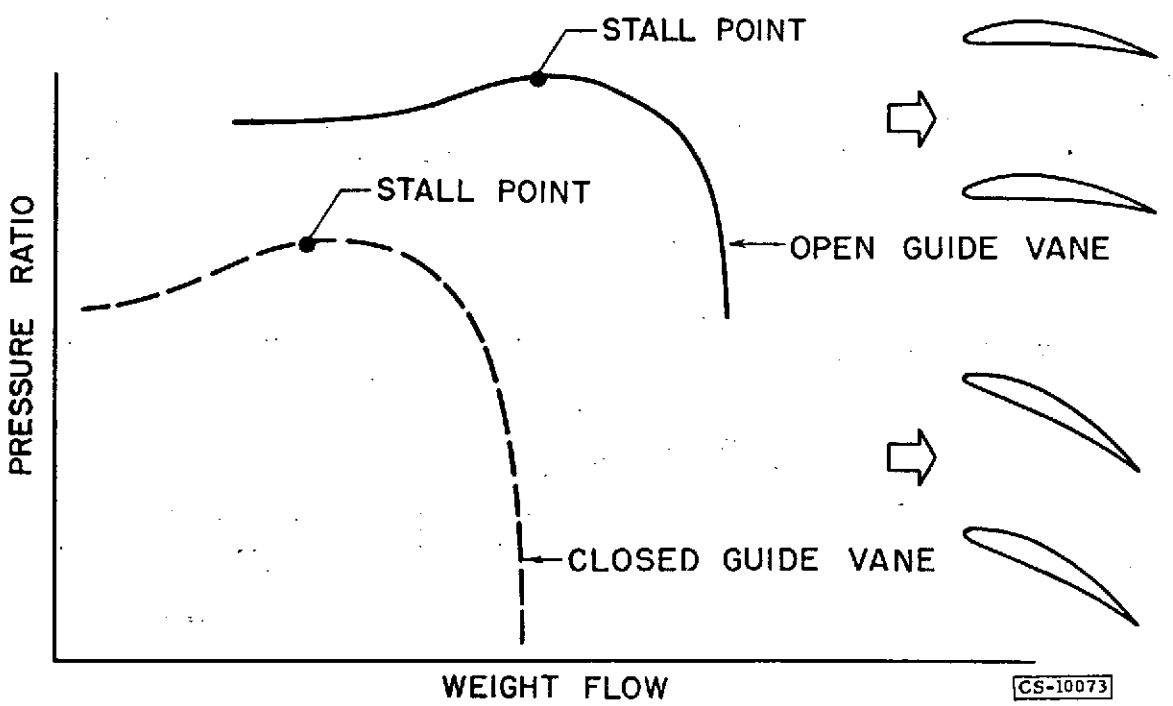

Figure 8. - Effect of guide-vane position on first-stage performance.

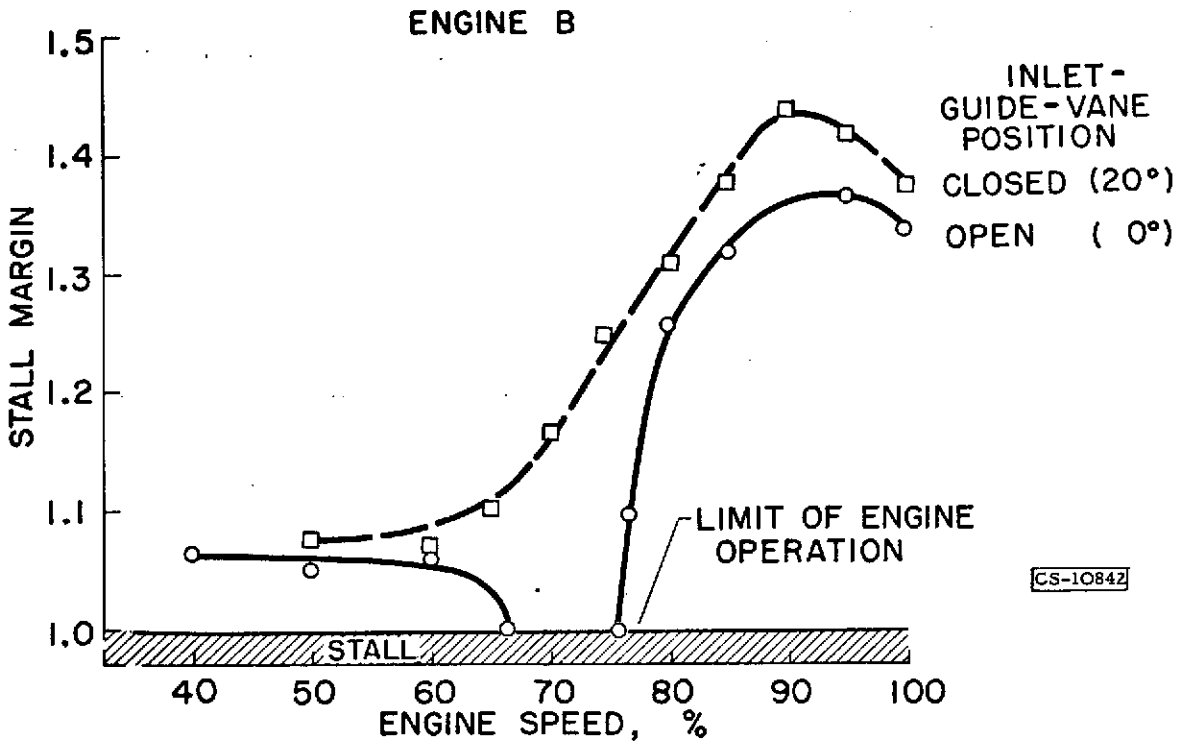

Figure 9. - Effect of inlet-guide-vane position on stall margin.

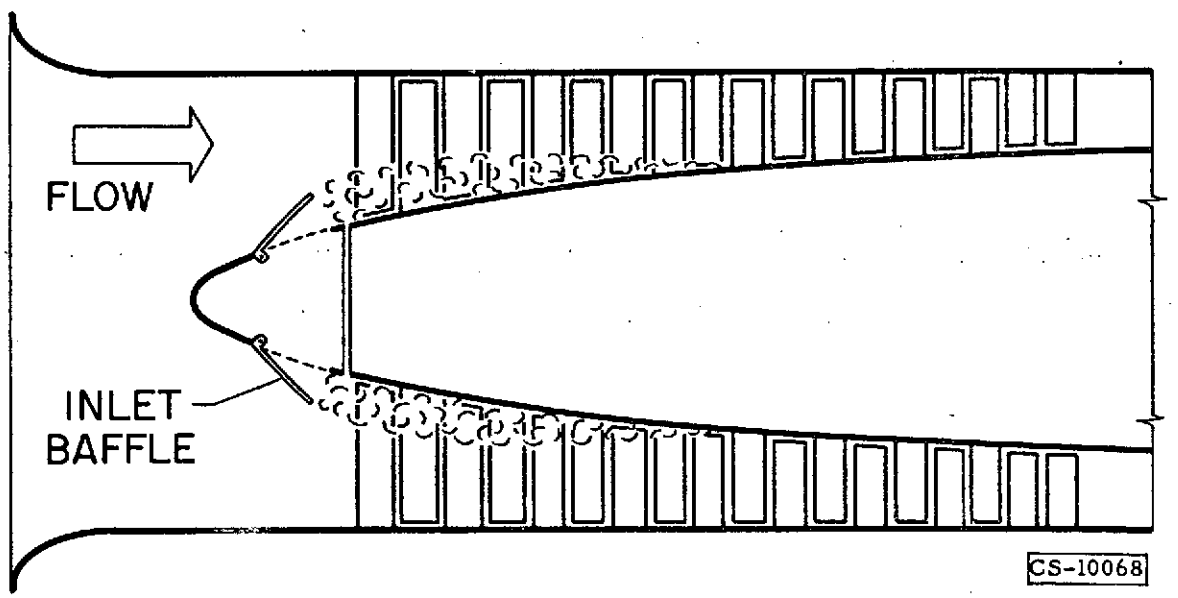

Figure 10. - Inlet-air baffle.

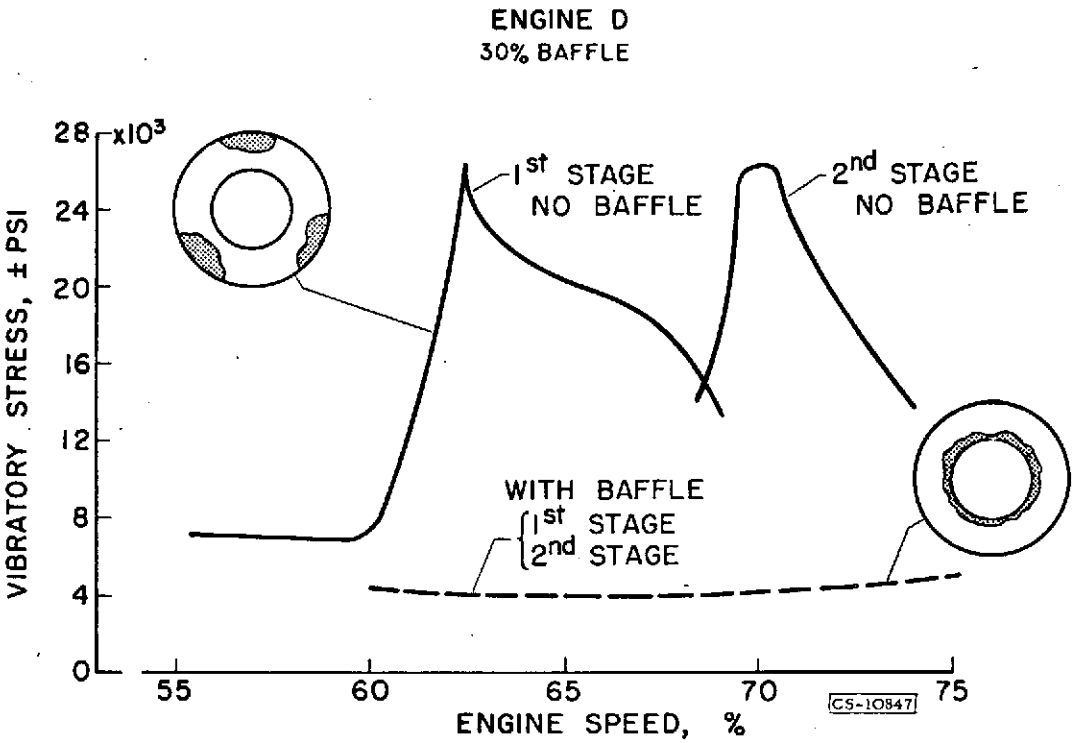

Figure 11. - Effect of inlet-air baffle on blade vibratory stress.

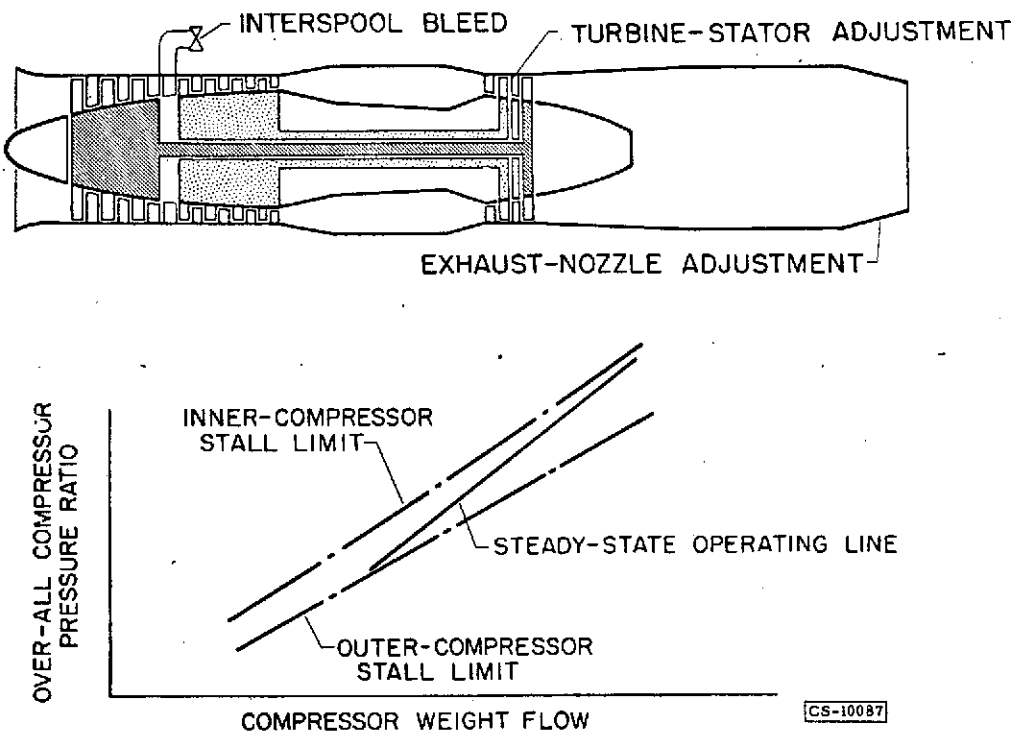

Figure 12. - Two-spool-engine modifications.

VI

STALL AND FLAME-OUT RESULTING FROM FIRING OF ARMAMENT

by

J. H. Childs, F. D. Kochendorfer, R. J. Lubick, R. Friedman

VI - STALL AND FLAME-OUT RESULTING FROM FIRING OF ARMAMENT

By J. H. Childs, F. D. Kochendorfer, R. J. Lubick
and R. Friedman

SUMMARY

An analysis is presented of the causes of compressor stall and flame-out when armament is fired during flight at high altitudes. Experimental data are also presented on this subject.

The increase in compressor-inlet temperature during armament firing is probably the most important single factor affecting engine performance. This increase in temperature is sufficient by itself to account for the observed occurrences of compressor stall and flame-out.

The changed compressor-inlet pressure, inlet-flow distortions, and combustibles in the compressor, for the most part, increase the likelihood of compressor stall beyond that for an inlet-temperature increase alone.

If the combustible materials entering the engine inlet do not burn until they reach the combustor, their effect will be very small. Also, the reduction in oxygen concentration is not sufficient to affect combustor performance appreciably.

The principal change occurring in the combustor during armament firing is the great increase in fuel-air ratio due to the reduced compressor air flow. In some engines, this increase in fuel-air ratio may be enough to cause a flame-out before compressor stall occurs. However, for the particular engine analyzed in this report, it appears that compressor stall precedes flame-out.

Measures to alleviate these engine difficulties during armament firing include all the features of variable engine geometry that increase the margin between the compressor operating point and the stall limit. A reduction in fuel flow during armament firing will also decrease the likelihood of compressor stall and should prevent combustor flame-out as long as stall does not occur. However, the best solution to the problem is to move the armament away from the engine inlets so that the hot gases never enter the engine.

INTRODUCTION

Compressor stall and flame-out in turbojet engines have occurred on numerous occasions when rocket missiles and cannon were fired at high altitudes. The U.S. Air Force has reported stall and flame-out in the F-86 and the F-94C, and the U.S. Navy in the Cutlass and the Fury. In addition, the British have encountered this problem in their Swift and Hunter airplanes. Obviously, then, the problem is rather general in nature and is not one that is peculiar to any one aircraft or to any one engine.

One factor that obviously contributes to these engine difficulties is the ingestion of rocket and cannon-shell exhaust gases into the engines. The extent to which rocket exhaust can enter the engine air intakes is illustrated in figure 1, which shows a photograph of an F-94C aircraft approximately 0.7 second after firing rockets. The exhaust smoke and vapor trails from the rockets envelop a large part of the airplane and can enter the air intakes in appreciable quantities.

The following engine-inlet effects will occur during the firing of armament:

(1) Increased inlet temperature

(2) Changed inlet pressure

(3) Distorted inlet-pressure and temperature profiles

(4) Entry of combustibles into engine

(5) Reduced oxygen content in gases entering engine

The object of this paper is to examine each of these things that occur when armament is fired and to show by analysis and by experimental data which of these items are important and how each affects engine performance. Deductions are made of the causes of the compressor stall and flame-out that have been encountered in flight. Finally, some remedial measures are suggested.

EFFECTS AT ENGINE INLET

Rocket Firing

Analysis. - The magnitude of the temperature and pressure effects at the engine inlet cannot be obtained directly from existing data. Several sets of data on jet spreading and mixing must be considered together.

For the 2.75-inch air-to-air rocket (fig. 2), the combustion-chamber pressure is 1100 pounds per square inch and the temperature is 4500° R. The design exit Mach number is 2.7 and the exit static pressure is 42 pounds per square inch. Since this pressure is considerably above ambient pressure at altitude, the jet will expand greatly upon leaving the nozzle. The amount of initial expansion can be obtained directly from existing data (ref. 1), but the amount of mixing farther downstream cannot. Experimental data on jet mixing are presented in reference 2. These mixing data were obtained with low velocities for both the jet and the stream; in addition, the two streams had equal temperatures and static pressures. These conditions are in marked contrast to the high velocities and the temperature and pressure differences noted for the rocket. Nevertheless, an estimate of rocket-jet spreading can be obtained by adding the results of reference 2 to the supersonic expansion, as indicated by the diagram in figure 2.

Results of a typical calculation are shown in figure 3. The stream Mach number relative to the launching station is taken to be 0.9 and the altitude 45,000 feet. At the time shown (about 0.3 sec after firing), the rocket is 60 feet from the launcher and is moving away at a speed of 400 feet per second. Contours of temperature are shown for the exhaust from a single rocket; these temperatures are expressed as the difference between the temperature at various locations and the ambient temperature.

If the position of the inlet relative to the launcher is known, temperature increments at the engine inlet can be estimated. For example, consider an inlet 1 foot in diameter whose centerline is spaced 1.5 feet from that of the rocket. If the inlet is in the plane of the launcher, the average temperature of the entering stream would be about 200° F above ambient. The temperature increment will vary from 260° F at the inner face to 140° F at the outer, as indicated by the inset in figure 3.

If the calculations represented in figure 3 are repeated for other lengths of time after firing, the temperature profiles at any station can be obtained as a function of time. Temperature variations at the launcher station are shown in figure 4. Variations in total pressure are also shown in figure 4, and these pressures are expressed as the difference between the local pressure and the free-stream total pressure divided by the free-stream total pressure. For the example cited of an inlet 1 foot in diameter and located 1.5 feet from the rocket centerline, a maximum temperature increase of 400° F is reached at the inner face of the inlet 0.15 second after firing. At this time, there is a variation in temperature across the inlet of 400°. A maximum total-pressure increase of 25 percent above free-stream pressure is experienced at a slightly later time after firing, 0.22 second. At this time, the total-pressure variation across the inlet is 25 percent. Figure 4 also shows the duration of these increases. A temperature increase of 200° at the

inner face, for example, will be reached at 0.09 second and will persist until 0.32 second after firing.

Experiment. - The only available experimental data showing the magnitude of increase in inlet temperature when firing rockets were obtained by Lockheed for the F-94C fighter firing a charge of 24 rockets during a 0.15-second time interval. Figure 5 shows the relative position of the rockets and the engine-inlet ducts in the F-94C. The rocket cluster is located in the nose section, while the fuselage scoop-type air inlets are located just rearward. Because of this positioning, it can be expected that more rocket exhaust will be diverted into the inlet duct and higher temperatures will result than for the sample inlet indicated in figures 3 and 4.

The actual temperature rise measured by Lockheed (ref. 3) is presented in figure 6, which shows the variation in temperature measured at the engine inlet as a function of time elapsed after firing the rockets. Three curves represent the minimum, average, and maximum temperature rise where peak temperatures are approximately 300°, 600°, and 900° F, respectively. One reason for the wide variation in temperature rise lies in the large difference in burning characteristics of the individual rockets. Ignition lag may vary from 0.025 to 0.035 second and total burning time from 1.4 to 2.0 seconds. For a burst of 24 rockets, these variations can result in a large range of possible temperatures in the wake of the rockets.

The approximate time during which these hot gases pass into the engine (fig. 6) agrees quite well with the calculations presented earlier. The hot gases start to pass into the engine about 0.1 second after the beginning of rocket firing and continue to enter the engine until about 0.4 second after the beginning of firing. The values of temperature increase are higher than would be predicted from figure 4, because a large number of rockets were fired and because the nose section tends to divert the exhaust gases into the inlets.

Cannon Firing

The effects of cannon fire are different in certain respects from those for rockets. Figure 7 shows an aircraft in the process of firing cannon. As the muzzle gases move out ahead of the inlet, they mix with the incoming air and the inlet temperature is increased. In certain cases, the gun chambers are vented into the inlet; this permits a considerable blast of hot gases directly into the engine. An additional factor is muzzle flash, a sudden burning or explosion of the gases ahead of the guns. If this occurs, the hot gases can expand ahead of the aircraft and enter the engine at greater than normal rates.

In addition to the temperature effects, cannon firing can alter inlet pressures. Pressure effects for cannon should be in a direction opposite to that noted for rockets, because the momentum of the muzzle gases opposes that of the incoming air. Mixing effects are even more difficult to evaluate than those for the rocket. However, it has been estimated that, at a Mach number of 0.9 and an altitude of 45,000 feet, firing four 20-millimeter guns at the rate of 1500 rounds per minute could reduce inlet pressures by as much as 9 percent if the guns were located close beside the inlet.

EFFECTS ON COMPRESSOR

Analysis

Increased inlet temperature. - Figure 8 is a compressor operating map for a typical single-spool axial-flow turbojet engine. The map shows the variation of compressor pressure ratio with corrected air flow for lines of constant corrected engine speed. Also shown are the steady-state operating line and the stall line for no inlet-flow distortion. Calculations of the point of compressor operation have been made for an increase in inlet temperature. The initial point of operation (point A) was taken at rated mechanical engine speed at an altitude of 45,000 feet and a flight Mach number of 0.9. For these calculations, fuel flow and engine speed were assumed to remain constant while the inlet temperature increased. This is a valid assumption, since, during the short time (approximately 0.3 sec for an actual rocket-firing case), the engine control would not have time to adjust fuel flow nor would engine speed have time to change.

To completely analyze compressor operation during an inlet-temperature increase would necessitate calculating the history of the compressor operating point as the armament gases pass through the engine. However, with only the operating map for the complete compressor, this calculation is impossible. The discussion must therefore be limited to the operating point that is reached after the armament gases reach the turbine station (point B, fig. 8). The location of point B depends on two factors: (1) The compressor equivalent speed $N/\sqrt{\theta}$ must be corrected for the increased value of θ; and (2) the reduced equivalent speed produces a reduced air-flow rate, and, since fuel flow remains constant during the short time involved, the turbine-inlet temperature rises. Point B is therefore located on a line of lower equivalent speed and is shifted upward from the steady-state operating line. (Symbols are defined in the appendix.)

Since the path followed in the transient from points A to B cannot be calculated, the dashed curve in figure 8 serves only as an indication of one possible path. The obvious question as to what happens if the

path enters the stall region cannot be answered at present. Since time is required for stall to set in, it is possible that some stages of the compressor could momentarily operate above their steady-state stall limit. On the other hand, if the path crosses the stall-limit line and stall does occur, then operation at point B will not be realized.

Compressor operating points calculated by this procedure for several values of inlet-temperature increase are presented in figure 9. A 300° increase results in an operating point just at the stall line. For this particular engine, an inlet-temperature increase of slightly over 300° F would certainly cause compressor stall.

Changed inlet pressure. - If a pressure change accompanies the temperature change, the stall tendency can be affected. Three paths between points A and B are shown in figure 10. Assume that the center path would be followed for a temperature change alone. Now, if the inlet pressure is reduced as a result of cannon fire, the reduction in compressor-inlet pressure effectively increases the compressor pressure ratio. The path will therefore be shifted upward toward the stall limit. The amount of shift will, of course, depend on the magnitude and duration of both the temperature and pressure change. The pressure effects of cannon fire should, in general, increase the probability of stall.

For rockets, the inlet pressure is increased and the compressor pressure ratio is momentarily decreased. This moves the path downward away from stall.

Inlet-flow distortions. - As shown in the jet-spreading analysis, both temperature gradients and pressure distortions may be expected after armament firing. Pressure distortions effectively lower the stall limit. Temperature distortions may also have a similar effect. The reduction in stall margin due to these changes is indicated in figure 11. In many instances, armament firing takes place while the aircraft is at high angle of attack. The inlet-flow distortions caused by angle of attack also affect the stall margin as indicated in figure 11.

Combustibles in compressor. - Numerous instances of afterburning from rockets and muzzle flash from guns serve to show that the armament gases can undergo further burning. If burning occurs while these gases are in the compressor, then the pressure will rise where the burning takes place. This means that the pressure ratio across the compressor stages upstream of this location will be greatly increased. The resultant effect cannot be shown on the compressor map, but the probability of encountering stall is increased.

Experiment

Lockheed (ref. 3) reports that a 300° increase in inlet temperature is the critical value in the F-94C, which uses a J48 engine. They state that a temperature increase of less than 300° can be tolerated, while a temperature increase in excess of this value causes engine difficulties. These temperature effects were probably accompanied by inlet-flow distortion and pressure changes; consequently, the 300° value is probably unique for the F-94C configuration.

Experimental data showing the effect of an increase in inlet temperature on a modern turbojet engine are presented in figure 12 which shows that surge was produced by inlet-temperature increases of 70° F or more. These data were obtained in the Lewis altitude wind tunnel by deflecting hot air into the engine inlet. A time interval of 1 to 2 seconds was required for the complete temperature rise to be felt at the compressor inlet during these tests; consequently, these data are not strictly analogous to the more rapid temperature increase accompanying armament firing.

EFFECTS ON COMBUSTOR

Before considering the effects of armament on the combustor, the factors that affect combustor performance will be reviewed briefly. A combustor performance map is shown in figure 13. Combustion efficiency is plotted as a function of the combustion parameter $\alpha \frac{P_3 T_3}{V_r} \varphi(\alpha)$, where α is the oxygen concentration in the inlet gases, P_3 and T_3 are the total pressure and temperature at the combustor inlet, V_r is the combustor reference velocity and is equal to the inlet volume flow rate divided by the maximum cross-sectional area of the combustor, and $\varphi(\alpha)$ is an exponential function that depends primarily on the oxygen concentration. The combustion parameter was derived from theory by assuming that chemical reaction kinetics control the rate of burning in the combustor (refs. 4 and 5). For most combustors, a reasonable correlation of data can be obtained with the parameter.

A typical family of experimental curves is shown in figure 13 for several fuel-air ratios. For lower values of the combustion parameter, efficiency decreases sharply. The solid points at the ends of the curves denote flame-out. The value of the combustion parameter at which flame-out occurs is a function of fuel-air ratio, as shown in figure 14. Each of the solid points indicates an experimental flame-out for a typical turbojet combustor. Since flame-outs are not exactly reproducible, a shaded band is used to indicate the flame-out region. Above this band, combustion is stable; below, no burning is possible.

To facilitate estimation of flame-out margin for this combustor, operating points are indicated at several altitudes. These points correspond to rated engine speed and a flight Mach number of 0.9. This combustor obviously has ample steady-state flame-out limits.

The combustor operating map can now be used to analyze the effect of armament firing on combustor performance in a hypothetical turbojet engine that uses the combustor of figure 14 and the compressor of figure 9. Consider an initial operating point at an altitude of 45,000 feet, rated mechanical speed, and a flight Mach number of 0.9; this is point A on the combustor map (fig. 15). If the armament firing causes a 300° F increase in compressor-inlet temperature, then the combustor operating conditions become those of point B (fig. 15). The location of point B depends on both the change in inlet temperature and gas composition and the change in compressor operating point. On the compressor map (fig. 9), it was shown that a 300° F increase in compressor-inlet temperature causes a marked decrease in both compressor pressure ratio and mass-flow rate. The decreases in oxygen content and in combustor-inlet pressure adversely affect the combustor; however, these effects are largely offset by the increase in inlet temperature and the decrease in air-flow rate. Thus, the change in the combustion parameter between points A and B is slight. However, the fuel-air ratio increases considerably from point A to point B, since fuel flow remains constant and air flow decreases. For the combustor map illustrated in figure 15, point B lies in the stable burning region, and flame-out does not occur.

As indicated by figure 9, the operating point corresponding to a 300° F increase in inlet temperature lies just underneath the compressor stall line. If the compressor stalls at this condition, then the combustor operating point changes to the values indicated by the two points labeled C in figure 15. The upper point corresponds to the highest and the lower point to the lowest of the oscillating pressures that have been measured in a similar turbojet engine operating in a stalled condition at this particular value of equivalent speed (ref. 6). Since these operating points for the combustor during stall lie outside the stable burning region, combustor flame-out will follow the occurrence of compressor stall.

The foregoing discussion does not mean that in all engines compressor stall must precede combustor flame-out. Obviously, if this same sequence of events occurred in some engine for which the combustor did not have as wide a fuel-air-ratio range for stable operation, combustor flame-out could occur at point B, because the fuel-air ratio would be too high even though the compressor did not stall.

The possibility of the entry of some combustible material into the engine due to incomplete combustion in the armament exhaust gases has been mentioned. The effect of these materials passing through the compressor without burning and then burning in the combustor, is shown in figure 16.

For a combustion efficiency in the armament gases of 85 percent, and the remaining 15 percent of their chemical heat release assumed to occur in the combustor, point B would be moved over to the location indicated by point D. The effect is quite small.

EFFECT ON SUPERSONIC AIRCRAFT

At supersonic speeds, an additional component, the air inlet, must be considered. If reduced air flow accompanies the temperature increase, a supersonic inlet can be forced into its subcritical operating range, and the inlet then becomes an additional source for pressure and flow pulsations. The effects of firing rocket exhaust into an inlet-engine combination operating at a Mach number of 1.9 have been briefly investigated in the Lewis 8- by 6-foot supersonic wind tunnel. Although quantitative data are not available as yet, it is known that large pressure fluctuations existed at both the compressor inlet and outlet stations. Because of compressor surge or inlet instability, a quasi-steady operating condition was never reached.

REMEDIAL MEASURES

Possible remedial measures are as follows:

Transient adjustments:
- Close inlet guide vanes
- Open compressor bleeds
- Reduce fuel flow
- Inject water at compressor inlet
- Open engine exhaust nozzle

Design changes to avoid intake of exhaust gases:
- Move armament away from inlet
- Vent gun chambers away from inlet
- Deflect muzzle gas away from inlet

The first course of action is the use of transient adjustments, such as closing the inlet guide vanes, opening the compressor bleeds, reducing fuel flow, and injecting water at the compressor inlet. These are all measures that can be put into effect an instant before armament is fired and maintained during the critical period. The length of time the hot gases are passing into the engine is approximately 0.3 second, so that the use of these adjustments may be limited by the speed of actuation. Unfortunately, all these items (except water injection) also appreciably decrease the engine thrust level, and this effect on performance must be considered. F. A. Holm stated that reducing fuel flow during rocket firing on the F-94C was effective (I. A. S. meeting, Cleveland, Ohio, March 11, 1955).

The compressor operating margin between the steady-state line and the stall limit decreases as altitude is increased. The gains resulting from design changes to increase this stall margin will be largely taken up by future increases in flight altitude. In addition, angle-of-attack operation decreases the stall margin, and the size and firing rate of armament are being steadily increased. From these considerations it would appear that the use of transient adjustments to increase the stall margin may prove to be only a temporary solution to the problem of armament firing.

The best course of action, and the most obvious, is to avoid completely the intake of exhaust gases. Moving the armament, venting the gun chambers, and deflecting muzzle gas away from the inlet are all possible solutions. The problem for the F-86F has been greatly alleviated by installing blast deflectors on the nose-mounted cannon. It is noteworthy that the F-89, which has wing-tip-mounted rocket pods, has encountered no engine problems due to rocket firing, according to Holm.

CONCLUSIONS

The increase in compressor-inlet temperature during armament firing is probably the most important single factor affecting engine performance. This increase in temperature is sufficient by itself to account for the observed occurrences of compressor stall and flame-out.

The changed compressor-inlet pressure, the inlet-flow distortions, and the combustibles in the compressor, for the most part, increase the likelihood of compressor stall beyond that for an inlet-temperature increase alone.

If the combustible materials entering the engine inlet do not burn until they reach the combustor, their effect will be very small. Also, the reduction in oxygen concentration is not sufficient to affect combustor performance appreciably.

The principal change occurring in the combustor during armament firing is the greatly increased fuel-air ratio due to the reduced compressor air flow. In some engines, this increase in fuel-air ratio may be enough to cause a flame-out before compressor stall occurs. However, for the particular engine analyzed here, it appears that compressor stall precedes flame-out.

Measures to alleviate these engine difficulties during armament firing include all the features of variable engine geometry that increase the margin between the compressor operating point and the stall limit. A

reduction in fuel flow during armament firing will also decrease the likelihood of compressor stall and should prevent combustor flame-out as long as stall does not occur. However, the best solution to the problem is to move the armament away from the engine inlets so that the hot gases never enter the engine.

Lewis Flight Propulsion Laboratory
National Advisory Committee for Aeronautics
Cleveland, Ohio, June 1, 1955

APPENDIX - SYMBOLS

The following symbols are used in this report:

M	Mach number
N	engine rotational speed
P	total pressure
T	total temperature
V_r	combustor reference velocity
W_a	air flow
α	oxygen concentration in inlet gases
δ	ratio of total pressure to absolute pressure of NACA standard sea-level conditions
θ	ratio of total temperature to absolute temperature of NACA standard sea-level conditions
$\Phi(\alpha)$	exponential function depending primarily on oxygen concentration

Subscripts:

c	rocket combustion chamber
e	rocket-nozzle outlet
0	free stream
2	compressor inlet
3	compressor outlet

REFERENCES

1. Love, Eugene S., and Grigsby, Carl E.: Some Studies of Axisymmetric Free Jets Exhausting from Sonic and Supersonic Nozzles into Still Air and into Supersonic Streams. NACA RM L54L31, 1955.

2. Forstall, Walton, Jr., and Shapiro, Ascher H.: Momentum and Mass Transfer in Coaxial Gas Jets. Meteor Rep. No. 39, Dept. Mech. Eng., M.I.T., July 1949. (Bur. Ord. Contract NOrd 9661.)

3. Anon.: Engine Performance During Rocket Firing at High Altitude with the F-94C Starfire. Rep. PN/459808, Addendum A, Lockheed Aircraft Corp., Mar. 1, 1954.

4. Childs, J. Howard: Preliminary Correlation of Efficiency of Aircraft Gas-Turbine Combustors for Different Operating Conditions. NACA RM E50F15, 1950.

5. Graves, Charles C.: Effect of Oxygen Concentration of the Inlet Oxygen-Nitrogen Mixture on the Combustion Efficiency of a Single J33 Turbojet Combustor. NACA RM E52F13, 1952.

6. Delio, G. J., and Stiglic, P. M.: Experimental Investigation of Control Signals and the Nature of Stall and Surge Behavior in a Turbojet Engine. NACA RM E54I15, 1954.

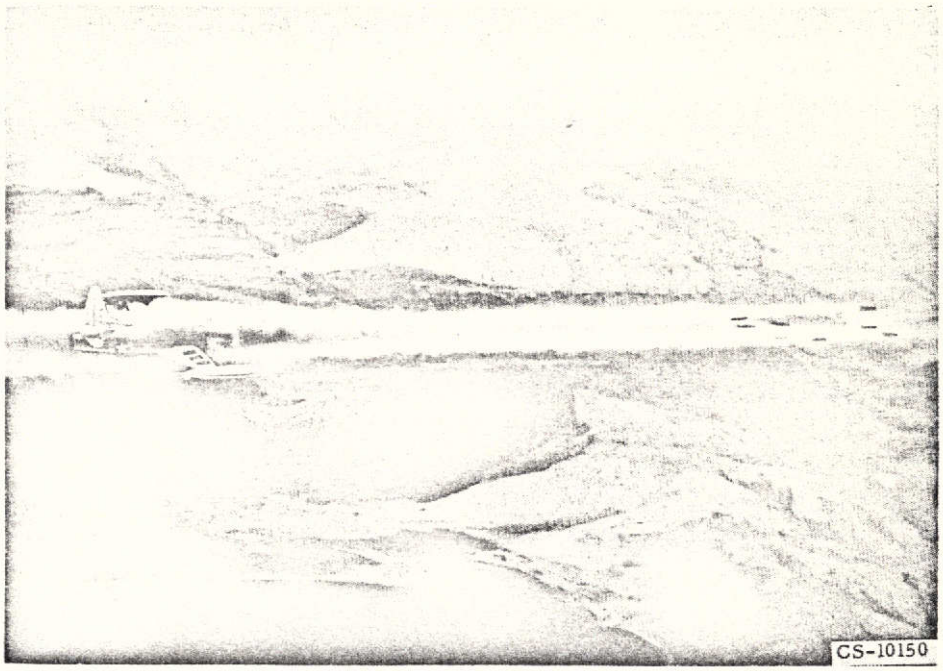

Figure 1. - F-94C firing rockets. (Obtained from Lockheed Aircraft Corp.)

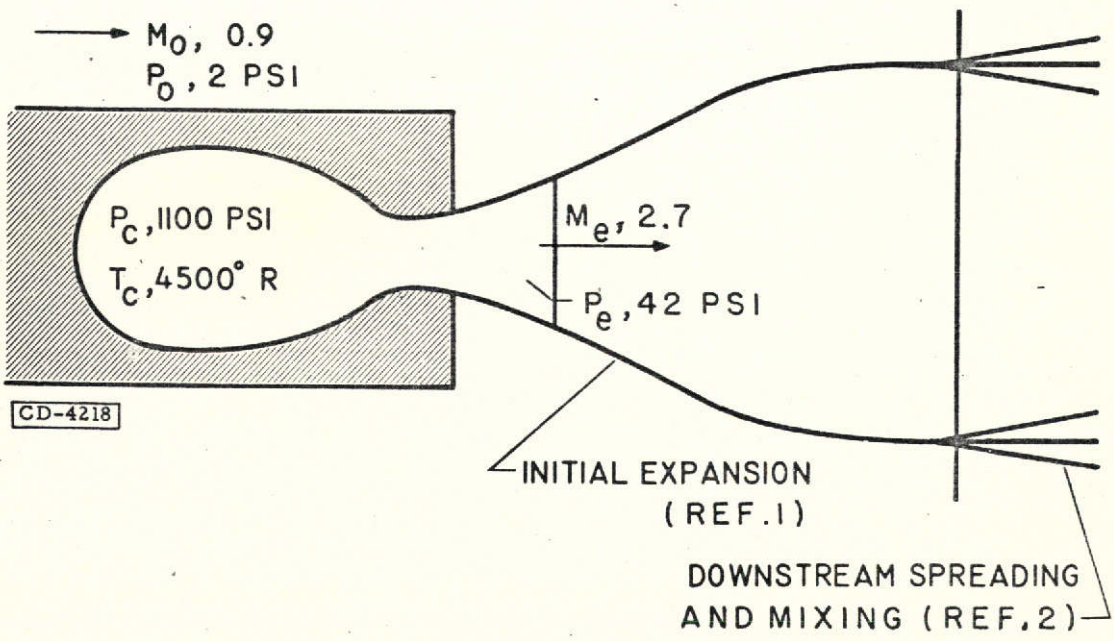

Figure 2. - Jet spreading from 2.75-inch rocket. Altitude, 45,000 feet.

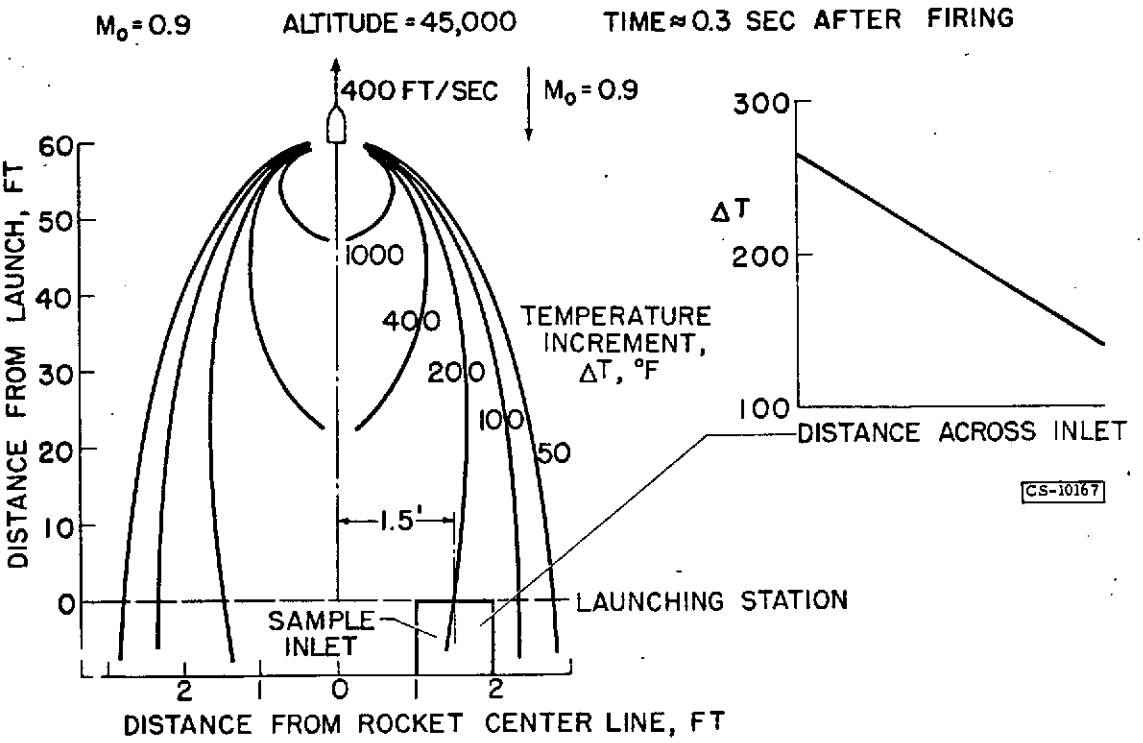

Figure 3. - Temperature contours for 2.75-inch rocket. Altitude 45,000 feet; time after firing, 0.3 second.

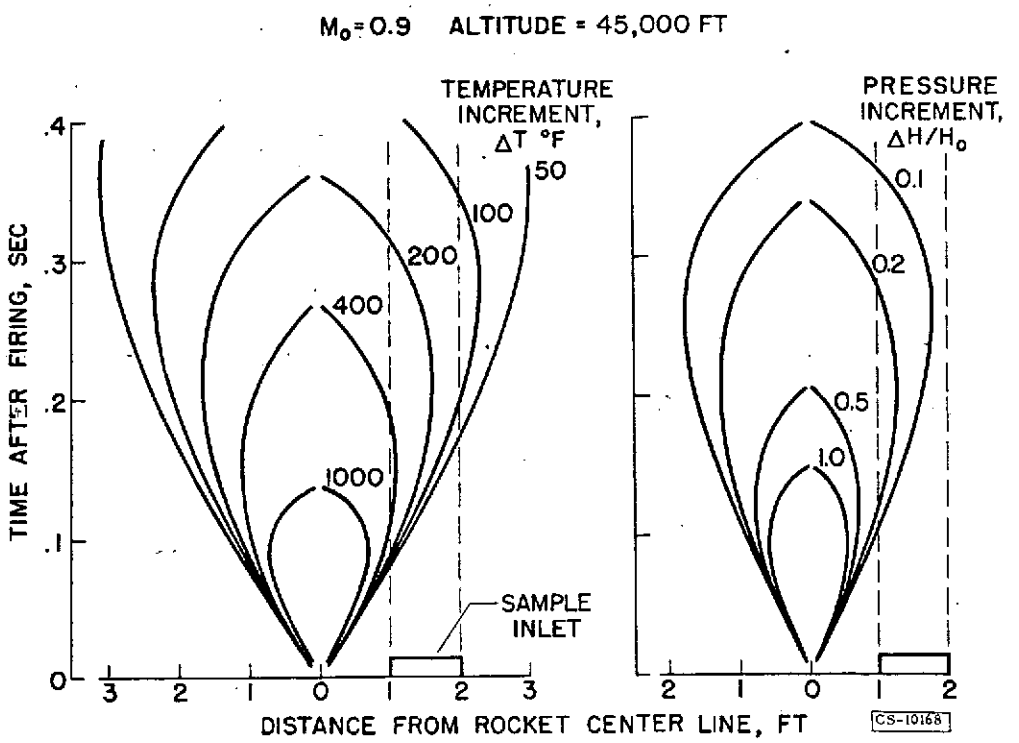

Figure 4. - Pressure and temperature increments for 2.75-inch rocket. Free-stream Mach number, 0.9; altitude, 45,000 feet.

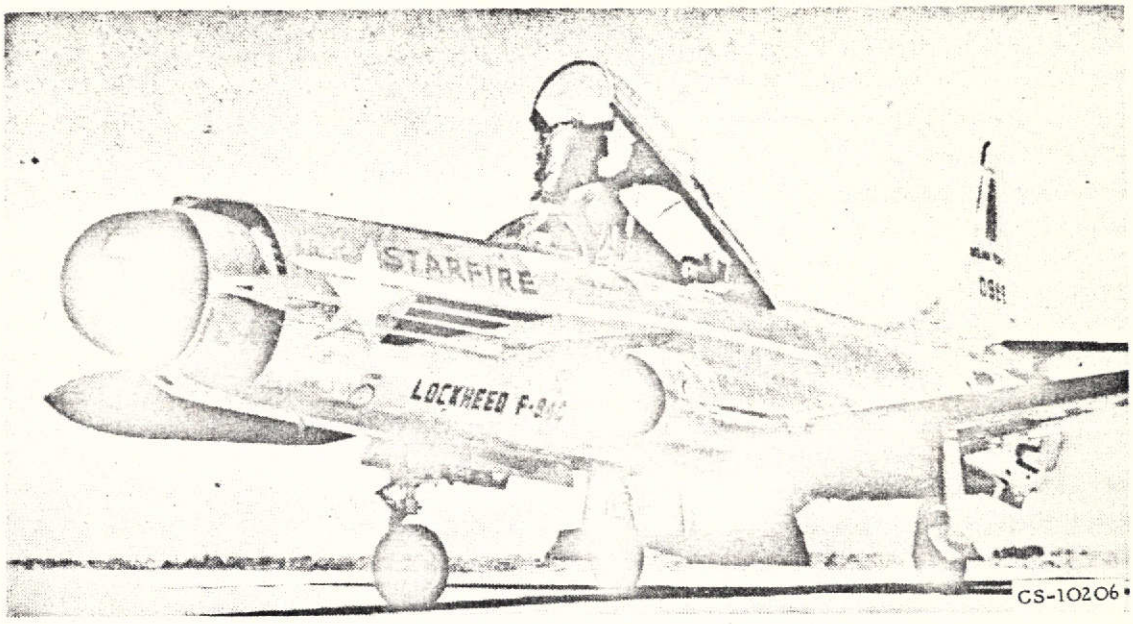

Figure 5. - Rocket installation for F-94C.

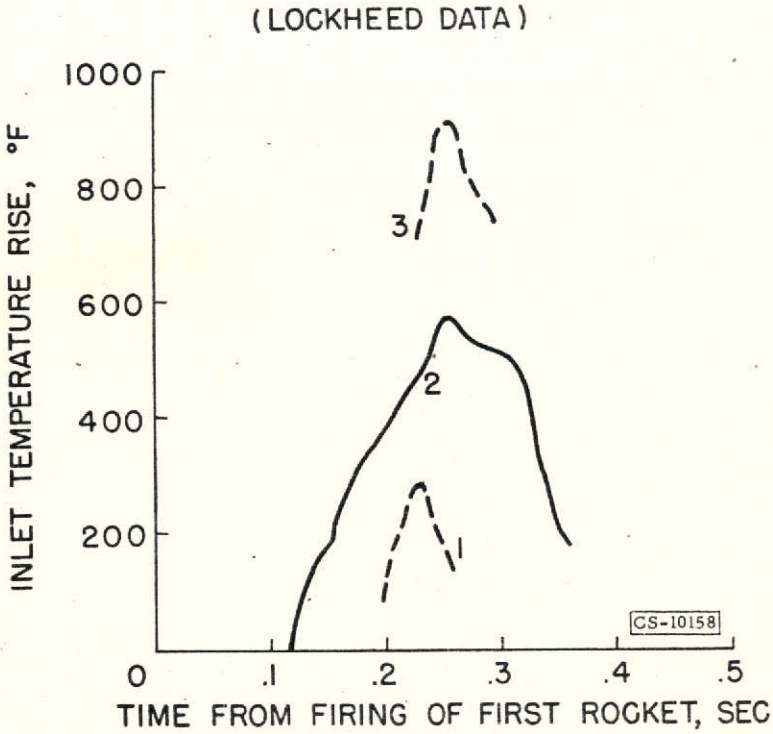

Figure 6. - Inlet temperatures for F-94C after firing rockets. (Data from ref. 3).

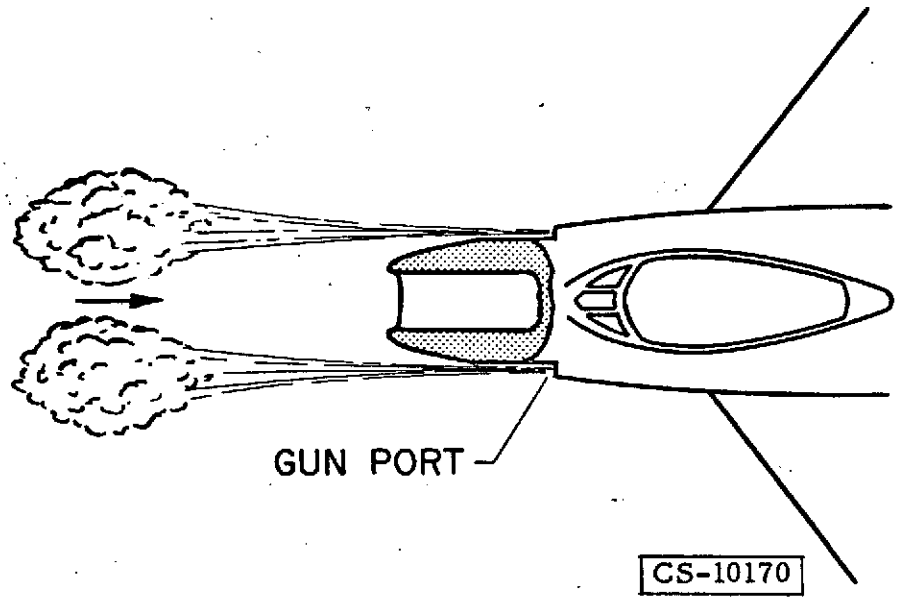

Figure 7. - Cannon blast effect.

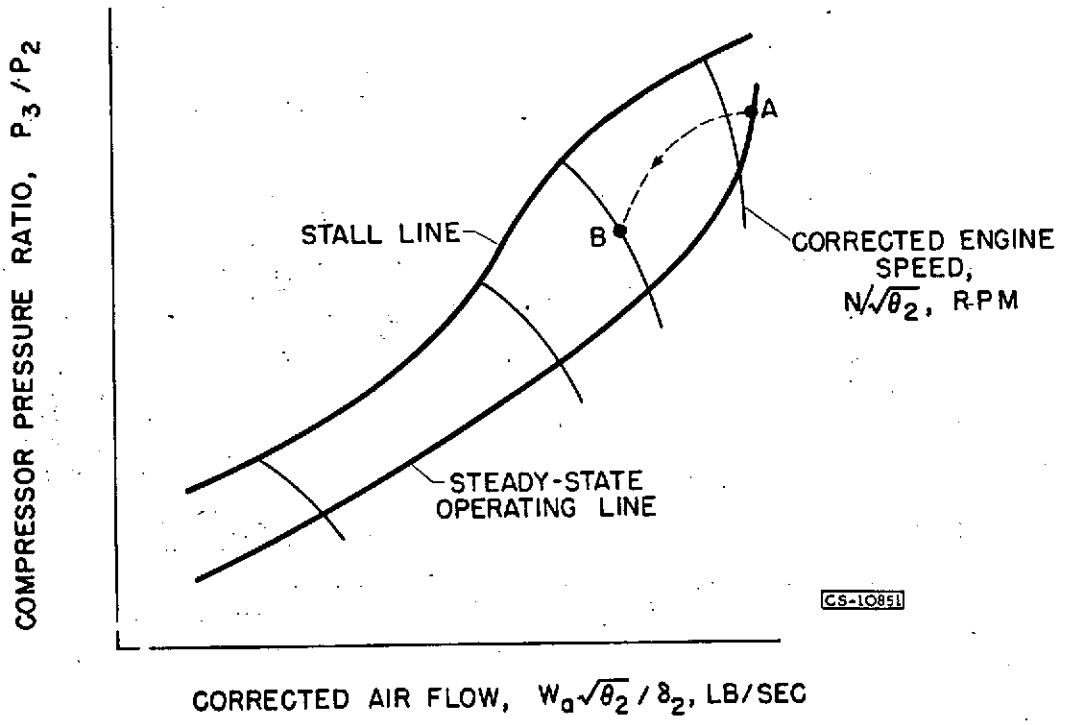

Figure 8. - Theoretical compressor operation for instantaneous inlet-temperature increase.

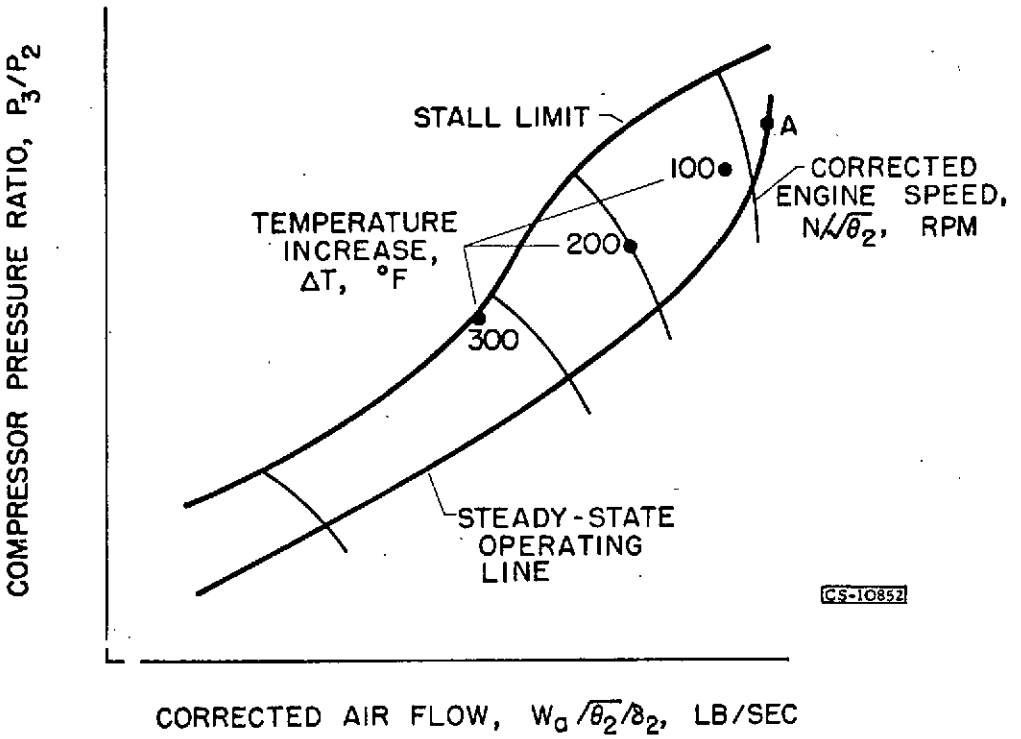

Figure 9. - Calculated effect of various inlet-temperature increases.

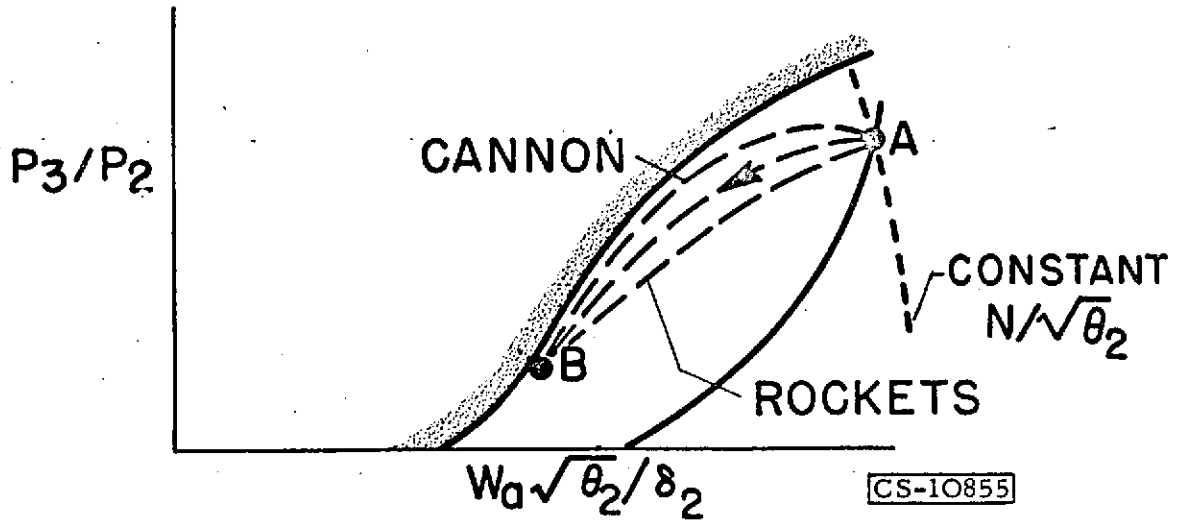

Figure 10. - Effect of changed inlet pressure.

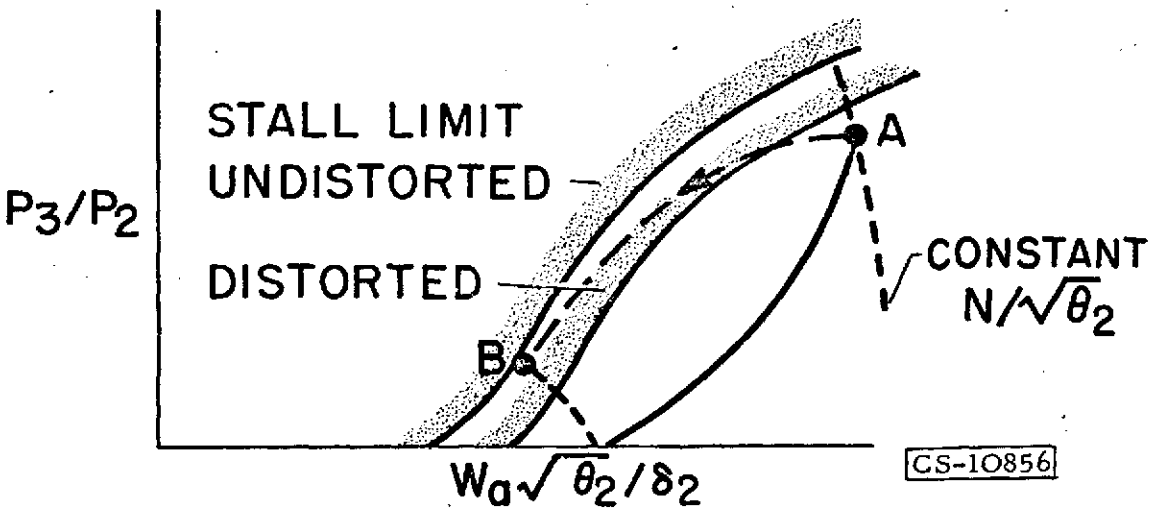

Figure 11. - Effect of inlet distortions.

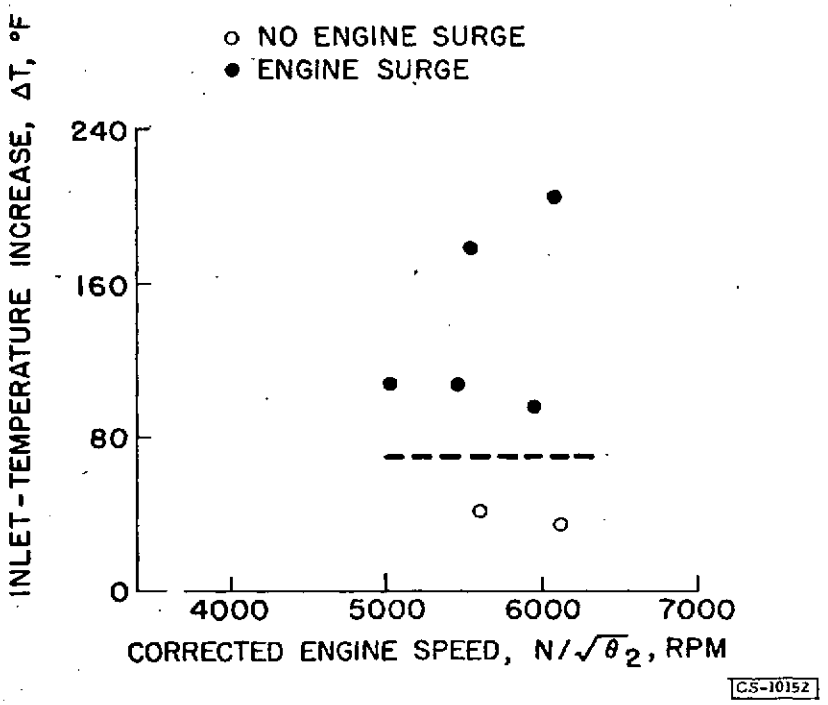

Figure 12. - Experimental effect of various inlet-temperature increases.

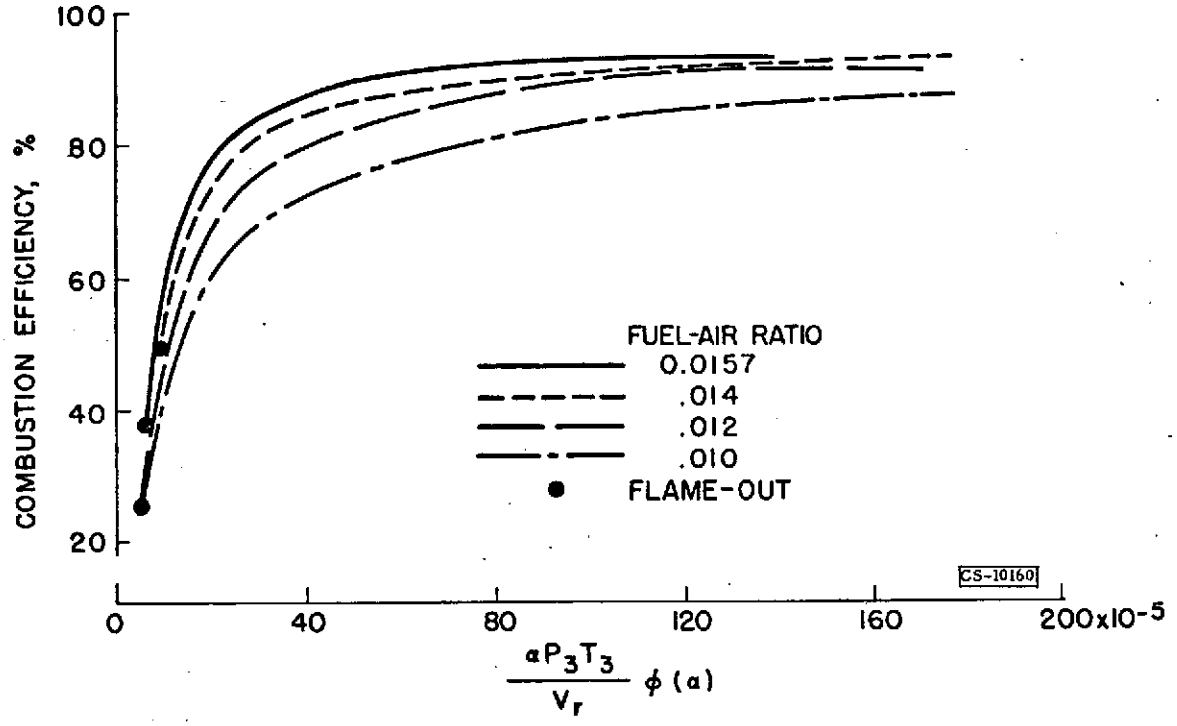

Figure 13. - Combustor operating lines for several fuel-air ratios.

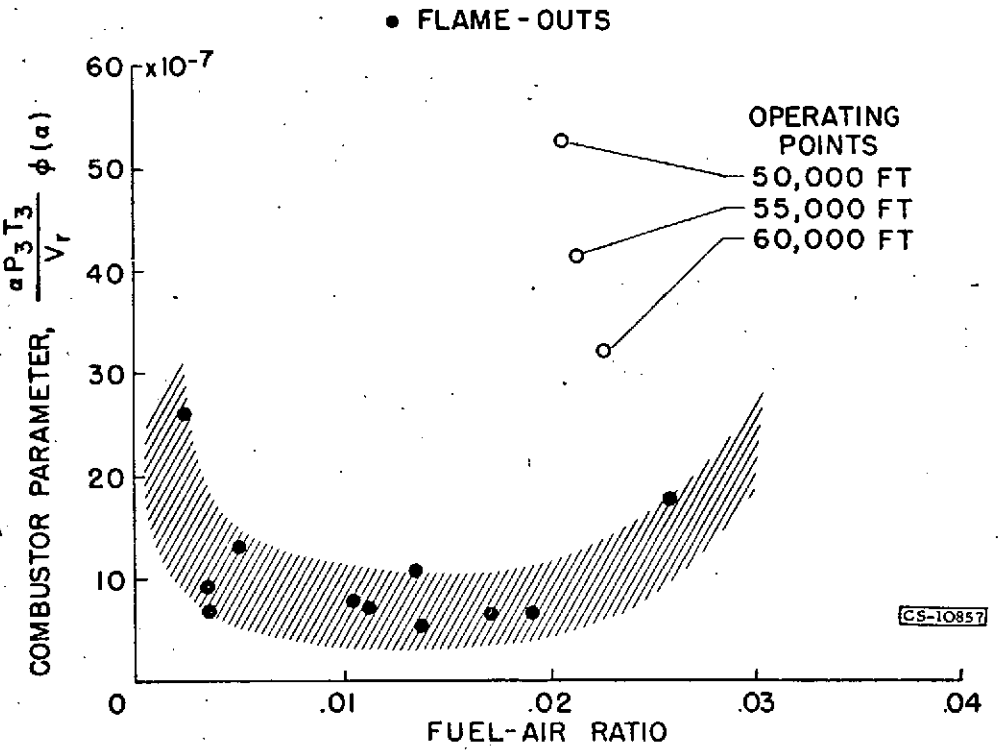

Figure 14. - Combustor flame-outs.

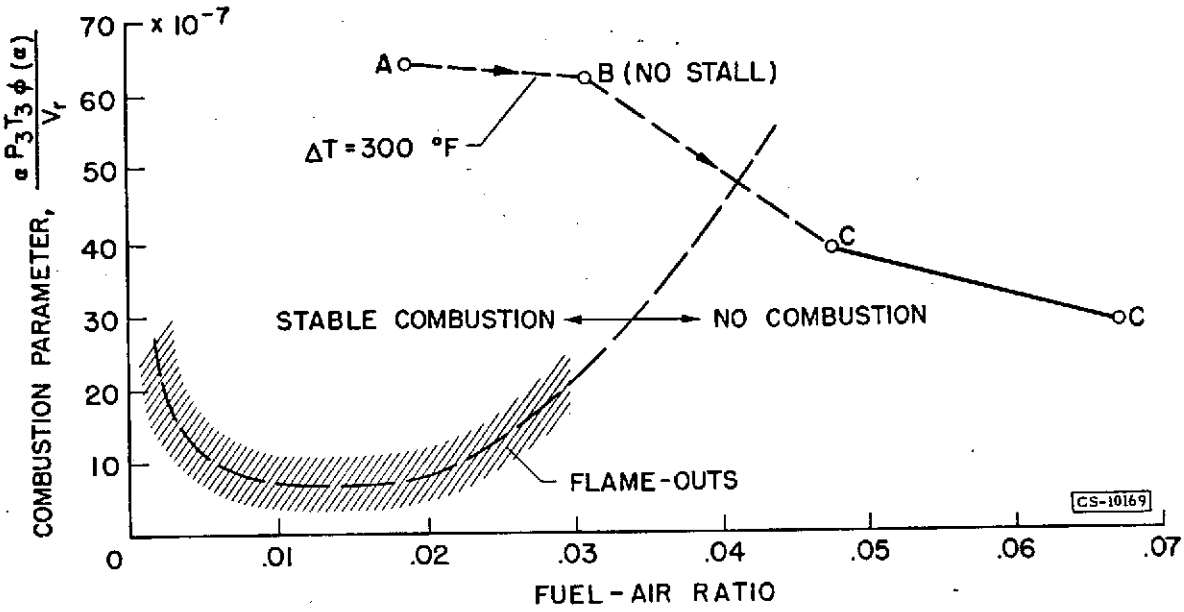

Figure 15. - Combustor conditions during rocket firing.

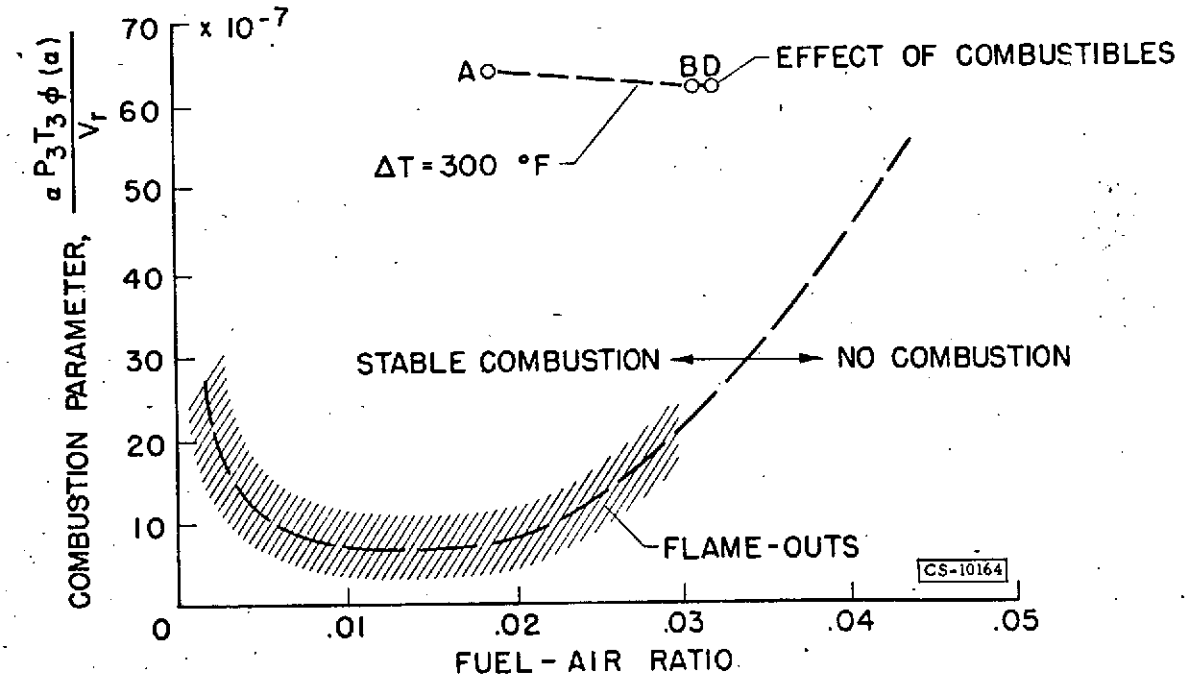

Figure 16. - Effect of armament gases burning within combustor.